uOttawa

L'Université canadienne
Canada's university

FACULTÉ DES ÉTUDES SUPÉRIEURES ET POSTOCTORALES

uOttawa

L'Université canadienne
Canada's university

FACULTY OF GRADUATE AND POSDOCTORAL STUDIES

Denis Lacelle

AUTEUR DE LA THÈSE / AUTHOR OF THESIS

Ph.D. (Earth Sciences)

GRADE / DEGREE

Department of Earth Sciences

FACULTÉ, ÉCOLE, DÉPARTEMENT / FACULTY, SCHOOL, DEPARTMENT

Carbonate Deposits in Polar Regions- Origin, Age and Paleoclimatology: A Geochemical and Isotopic Approach

TITRE DE LA THÈSE / TITLE OF THESIS

Ian Clark

DIRECTEUR (DIRECTRICE) DE LA THÈSE / THESIS SUPERVISOR

Bernard Lauriol

CO-DIRECTEUR (CO-DIRECTRICE) DE LA THÈSE / THESIS CO-SUPERVISOR

EXAMINATEURS (EXAMINATRICES) DE LA THÈSE / THESIS EXAMINERS

John Blenkinsop

Christian Zdanowicz

André Desrochers

Henry Schwarz

Gary W. Slater

Le Doyen de la Faculté des études supérieures et postdoctorales / Dean of the Faculty of Graduate and Postdoctoral Studies

CARBONATE DEPOSITS IN POLAR REGIONS

Origin, age and paleoclimatology:
a geochemical and isotopic approach

Denis Lacelle

Thesis submitted to the
Faculty of Graduate and Postdoctoral Studies
in partial fulfillment of the requirements
for the PhD degree in Earth Sciences

Department of Earth Sciences
Faculty of Science
University of Ottawa

Your file Votre référence
ISBN: 978-0-494-25879-8
Our file Notre référence
ISBN: 978-0-494-25879-8

CARBONATE DEPOSITS IN POLAR REGIONS

Origin, age and paleoclimatology:
a geochemical and isotopic approach.

Denis Lacelle

Ottawa-Carleton Geosciences Center
Department of Earth Sciences
University of Ottawa
Ottawa, Ontario, Canada

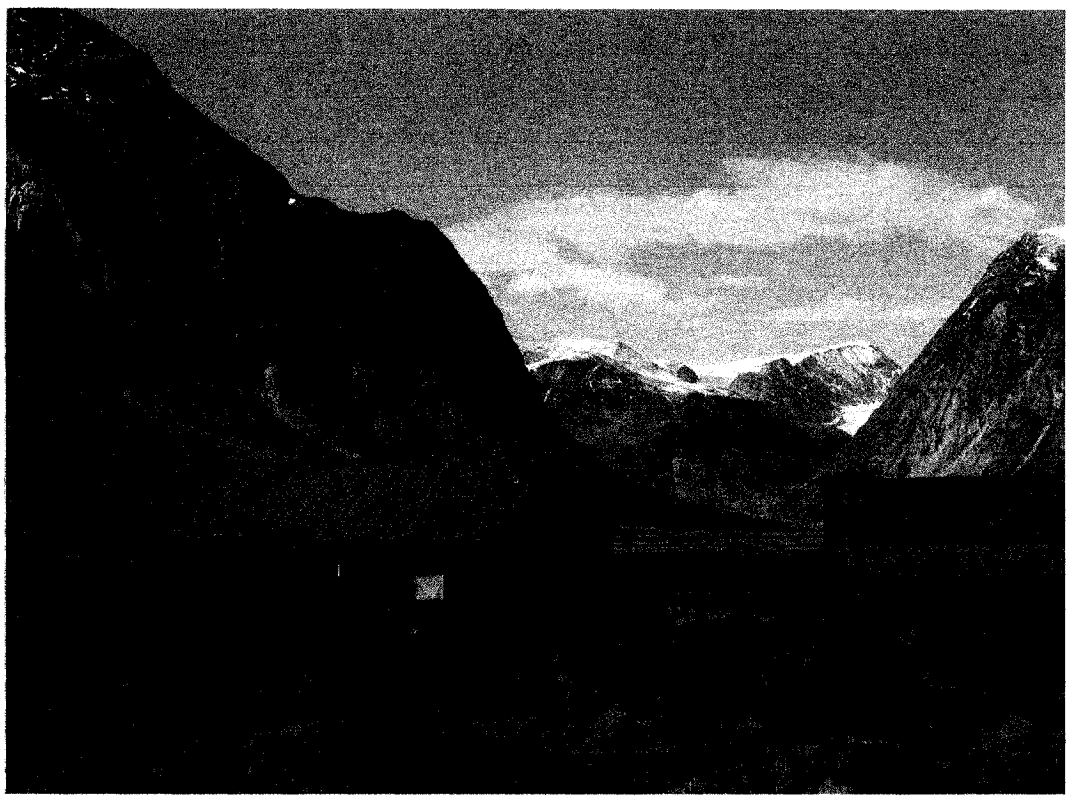

Abstract

Given the growing interest in secondary carbonate deposits from polar regions as paleoclimatic proxies, this thesis evaluated if they could be effectively be used in paleoclimatic reconstructions. To facilitate comparison between studies, the cold-climate carbonate precipitates were classified into three categories: *powders, crusts* and *speleothems*. The carbonate powders include those that precipitated in relation to aufeis aggradation (cryogenic aufeis calcite) and in relation to the growth of annual and perennial ice formations in caves (cryogenic cave calcite). The carbonate crusts were further subdivided according to their lithic environment; those that precipitated on the upper surface of bedrock/clasts (i.e. subglacially precipitated calcite and evaporative calcite crusts); those that are located on the underside of clasts (i.e. active layer carbonates); and those that precipitated in rock outcrop fissures (i.e. endostromatolites). The speleothems consist of a group on their own because they are not restricted to polar regions and most are currently inactive due to the presence of permafrost.

To determine if the secondary carbonates in polar regions can be used as reliable paleoclimatic proxies, the chemical and isotopic ($^{18}O/^{16}O$; $^{13}C/^{12}C$) partitioning that is occurring prior to and during the precipitation of carbonates and the water from which they precipitated was examined. The cold-climate carbonate precipitates, which were collected in distinct geological settings (carbonated vs. non-carbonated), have a $\delta^{18}O$ composition between –6.5 and 36‰ and $\delta^{13}C$ values in the –5 to 17‰ range. The measurement of the difference (Δ) in stable C-O isotope composition of actively forming carbonate deposits and of the water from which they precipitated provided valuable insights into the formative mechanism that led to their precipitation. It was found that carbonates that precipitated under equilibrium physico-chemical conditions (i.e. cryogenic aufeis calcite powders, cryogenic cave calcite pearls, subglacially precipitated calcite) had a $\delta^{13}C$ value that is in equilibrium with that of the parent water, while their $\delta^{18}O$ compositions were more variable, as it is in part controlled by the temperature of reaction, by the $\delta^{18}O$ and calcite saturation state of the parent water and formative mechanism. By contrast, carbonate deposits that precipitated under non-equilibrium physico-chemical conditions (i.e. cryogenic cave calcite powders, evaporative calcite crusts), their $\delta^{18}O$ and $\delta^{13}C$

values are highly enriched relative to that of the parent water due to the faster rate of reactions which precludes isotopic equilibrium to be reached. In the case of biologically precipitated carbonate deposits (i.e. endostromatolites), their $\delta^{18}O$ composition reflects that of the parent water, while its $\delta^{13}C$ composition was enriched over that of the parent water because bacteria prefer to metabolize the light C (^{12}C) in the DIC pool. These findings have significant implications regarding the use of cold-climate carbonate precipitates in paleoclimate studies as the $\delta^{18}O$ signature preserved in most carbonates have been modified by freezing or other processes prior to their precipitation, which will modify $\delta^{18}O$ composition of the carbonates.

Résumé

Suite à l'intérêt croissant pour l'utilisation des dépôts secondaires de carbonates provenant de régions nordiques en tant que traceurs paléoclimatiques, cette thèse évalue le réel potentiel des dépôts secondaires de carbonates en tant que indicateur paléoclimatiques. Pour facilité les comparaisons entre études, les dépôts secondaire de carbonates en climat froid ont été classifiées en trois catégories : les *poudres*, les *croûtes* et les *spéléothèmes*. Les poudres de carbonate inclus les poudres précipitées pendant l'agradation des aufeis (calcite cryogénique d'aufeis) et à la croissance annuelle et pérennale de la formation de glace dans les cavernes (calcite cryogénique de cavernes). Les croûtes de carbonate ont été subdivisées en fonction de leur environnement lithique; celles précipitées sur la surface supérieure du substratum rocheux/claste (ex. précipité de calcite sous-glaciaire et croûtes de calcite évaporée) ; celles qui sont situées sur la surface inférieure des clastes (ex. carbonates de couche active) ; et celles qui sont précipitées dans les fissures des affleurements rocheux (ex. endostromatolites). Parce qu'ils ne sont pas restreint aux régions polaires et qu'ils sont présentement majoritairement inactifs dû à la présence de pergélisol, les spéléothèmes constituent un groupe à eux seuls.

Pour déterminer si les dépôts de carbonates secondaires dans les régions polaires peuvent être des traceurs paléoclimatiques valables, le fractionnement chimique et isotopique ($^{18}O/^{16}O$; $^{13}C/^{12}C$) qui survient avant et pendant la précipitation des carbonates ainsi que de l'eau desquels ils sont précipités ont été étudiés. Les carbonates précipités dans les climats froids, qui ont été collectés dans des environnements géologiques distincts (carbonatés vs. non-carbonatés), ont une composition de $\delta^{18}O$ entre –6.5 et 36‰ ainsi que des valeurs de $\delta^{13}C$ de –5 à 17‰. Les mesures de la différence (Δ) entre la composition des isotopes stables C-O des dépôts de carbonate formés activement et de l'eau desquels ils ont été précipités fournissent des informations utiles sur les mécanismes de formation qui mènent à leur précipitation. Les carbonates précipités sous des conditions d'équilibre physio-chimique (ex. poudre de calcite cryogénique d'aufeis, perle de calcite cryogénique de cavernes, précipité de calcite sous-glaciaire) présentent des valeur de $\delta^{13}C$ en équilibre avec celles de l'eau apparentée, alors que leurs compositions de $\delta^{18}O$ sont plus variables parce qu'ils sont en partie contrôlées par la température de la réaction, le $\delta^{18}O$ et le stade de saturation en calcite de l'eau apparentée et des mécanismes de formation.

Différemment, les dépôts de carbonate précipités sous des conditions physico-chimiques en non-équilibre (ex. poudre de calcite cryogénique de cavernes, croûtes de calcite évaporée) ont des valeurs de $\delta^{18}O$ et de $\delta^{13}C$ hautement enrichies comparativement à celles de l'eau apparentée dues au taux rapide des réactions qui empêche l'atteinte de l'équilibre isotopique. En présence de dépôts de carbonate précipités biologiquement, la composition de $\delta^{18}O$ reflète celle de l'eau apparentée, alors que la composition de $\delta^{13}C$ est enrichie au-dessus de celle de l'eau apparentée du aux bactéries qui préfèrent métaboliser le carbone léger (^{12}C) dans l'ensemble du carbone inorganique dissous. Ces découvertes ont un impact significatif en regard à l'utilisation des précipités de carbonate des climats froids dans les études paléoclimatiques, car la signature de $\delta^{18}O$ préservée dans la plupart des carbonates a été modifiée lors de la glaciation ou d'autres processus survenus avant leur précipitation, lesquels modifient la composition de $\delta^{18}O$ des carbonates.

Acknowledgements

The research fort this thesis was conducted at the Department of Earth Sciences, University of Ottawa from September 2002 to March 2006. I am most grateful to my supervisors Ian D. Clark and Bernard Lauriol for sharing their expertise in the fields of low-temperature stable isotope geochemistry and periglacial geomorphology, as well as for their enthusiasm during our field seasons together in the Canadian Arctic.

I would like to thank W. Abdi and P. Middlestead (G.G. Hatch Laboratory, University of Ottawa), L. Ling (SEM Laboratory, Carleton University), B. Cousens (strontium isotope analyses, Carleton University) and M. Alewany for their technical assistance in the laboratory. J. Clark, J.F. Dion and A. Doucet provided valuable field assistance. Special thanks to B. Etooangat and P. Smiley (Parks Canada) for providing logistical support during our stay in Auyuittuq National Park in 2002-2004. R. Zalatan provided helpful editorial comments and P. Bertrand kindly drafted some of the illustrations.

I thank the reviewers of this thesis, J. Blenkinshop, A. Desrochers, H. Schwartz and C. Zdanowicz and also those who reviewed the chapters published in scientific journals (I. Fairchild, R. Léveillé, T. Waragai) for their constructive comments.

This thesis was funded by Natural Sciences and Engineering Research Council of Canada (NSERC) discovery grants to B. Lauriol and I.D. Clark, by an Ontario Graduate Scholarship (OGS) and Northern Scientific Training Program (NSTP) grant to D. Lacelle.

Foreword

The work in this thesis is presented as a series of manuscripts. Manuscript I and III evaluates the geochemical and isotopic partitioning that occurs prior to and during the precipitation of modern cold-climate carbonates in order to determine if they can be used as reliable paleoclimatic proxies. Manuscript II determines the origin and age of calcite crusts precipitated in an area of granitc bedrock, which are poorly understood features and quite rare in Arctic regions, in order to derive a chronology of Holocene alpine glaciers fluctuations.

Even though the thesis is presented as a series of manuscripts with many authors, the first author (DL) accomplished most of the experimental and analytical work. The only exception is the strontium isotope analyses presented in Manuscript I and II that were kindly performed by B. Cousens at Carleton University. The interpretations of the results and writing of the manuscripts were done by the DL with editorial reviews from BL and IDC.

CARBONATE DEPOSITS IN POLAR REGIONS

Origin, age and paleoclimatology:
a geochemical and isotopic approach.

Denis Lacelle

Department of Earth Sciences
University of Ottawa, Ottawa, Canada

This thesis has three appendant manuscripts referenced by their listed roman numerals.

Table of Content

Introductory chapter

Manuscript I

Effect of chemical composition of water on the oxygen-18 and carbon-13 signature preserved in cryogenic carbonates, Arctic Canada: implications in paleoclimatic studies.

Manuscript II

Origin, age and paleo-environmental significance of carbonate precipitates from a granitic environment, Akshayuk Pass, southern Baffin Island, Canada.

Manuscript III

Cold-climate carbonate precipitates: a review of their stable C-O isotope composition and evaluation of their potential as paleoclimatic proxies.

Conclusions

General Introduction

1. Introduction

1.1 Overview

During the last century, the global mean annual air temperature has increased by 0.6°C (IPCC 2002). In polar regions, the consequence of the warming is already causing a decrease in snow cover, thawing of permafrost, melting of ice caps and sea ice. To recognize the amplitude of the ongoing climate change, past climatic and environmental conditions are essential to be known. As instrumental records do not go far back in time, quantitative reconstructions of paleotemperatures are based on the $\delta^{18}O$ composition of glacier ice, such as the Greenland ice cores (GRIP; GISP2), Canadian Arctic ice cores (Fisher et al. 1998; Zdanowicz et al. 2002) and Antarctic ice cores (Epica Community Members 2004). Ice cores can provide high temporal resolution where annual layer-counting provides yearly resolution of a few thousand years (Yiou et al. 1997).

In regions where glacier ice is not available, paleotemperatures have been retrieved from speleothems (i.e. speleothem $\delta^{18}O$ record from Devil's Hole; Winograd et al., 1992; 1997). The use of speleothems as paleoclimatic proxies relies, just like ice cores, on the $\delta^{18}O$ record preserved in the speleothem and the Dansgaard's global $\delta^{18}O$-T°C relation ($\delta^{18}O = 0.69$ T°C – 13.6; Dansgaard 1964), providing that the water from which the carbonate formed reflects the local mean annual air temperature. Although the paleoclimatic signal retrieved from speleothems may not be as long and continuous as the one obtained in ice cores, the recent development of micro-milling techniques has improved the resolution of sampling to a few micrometers (25 μm) and consequently improved the temporal resolution of these climatic proxies.

To date, few studies have explored the potential of secondary carbonate deposits in polar regions as paleoclimatic proxies. Ford et al. (1970) and Hallet et al. (1978) suggested that subglacially-precipitated carbonate deposits in the Canadian Rockies may be used as paleoclimatic proxies because they recorded information about the $\delta^{18}O$ composition of glacier ice at the time of precipitation. Hillaire-Marcel et al. (1979) also came to the same conclusion while studying subglacial carbonate deposits in the Ottawa Valley region. However, based on a present-day study of the isotopic composition of water, ice and calcite coatings from the Tsanfleuron glacier (Switzerland), Souchez and Lemmens (1985) and Sharp et al. (1990) concluded that glacier ice is not necessarily at the origin of the meltwater that gives rise to the

subglacially-precipitated calcite deposits, but rather the melting of basal ice layers, which is usually slightly enriched in ^{18}O over glacier ice. Recently, Clark et al. (2004) extracted a valuable $\delta^{18}O$ paleoclimatic record from endostromatolites formed in fissures in bedrock outcrops in the northern Yukon Territory. The $\delta^{18}O$ record was constrained by U/Th and ^{14}C methods and showed that summer air temperatures during the early Holocene were up to 7 °C warmer than present-day. This increase in air temperatures in the northern Yukon Territory is corroborated by other regional climate proxies (Ritchie et al. 1983; Burn 1997).

1.2 Cold-climate carbonate precipitates

In polar regions, carbonate precipitates have been observed in various environments, such as in freezing caves (Clark and Lauriol 1992; Zak et al. 2004), on the surface of aufeis along riverbeds (Hall 1980; Pollard 1983; Lauriol et al. 1991; Clark and Lauriol 1997), in lakebeds of the Dry Valleys of Antarctica (Nakai et al. 1975), on the underside of clasts in soil profiles (Washburn 1969; Sweet 1974; Bunting and Christensen 1978; Forman and Miller 1984; Courty et al. 1994), on the upper surface of clasts and bedrock (Ford et al. 1970; Hillaire-Marcel et al. 1979; Souchez and Lemmens 1985; Sharp et al. 1990; Fairchild et al. 1993; Blake 2005), and in fissures in bedrock outcrops (Lauriol and Clark 1999; Clark et al. 2004). Various mechanisms have been advanced to explain the formation of these carbonate deposits. Cailleux (1964) first suggested that the formation of carbonate deposits in cold environments was related to cryogenic processes, where the solution would reach calcite supersaturation during the freezing of a calcium bicarbonate-rich solution. Experimental work (Adolphe 1972; Hallet 1976; Killawee et al. 1998) and stable isotope analysis of carbon and oxygen (Hillaire-Marcel et al. 1979; Souchez and Lemmens 1985; Lauriol et al. 1991; Clark and Lauriol 1992; Fairchild et al. 1993; Courty et al. 1994; Manuscript II) have since confirmed the effectiveness of freezing to precipitate carbonates. However, other physico-chemical processes operating in polar regions, such as cryodessication (Marlin et al. 1993) and intense evaporation (Bunting and Christensen 1978; Manuscript I) of calcium bicarbonate solutions have also been suggested as possible mechanisms to precipitate carbonate deposits. Recently, Clark et al. (2004) suggested that endostromatolites, a finely laminated calcite deposit developed within the fissures of limestone outcrops, have a biogenic origin.

Based on the extensive literature on cold-climate carbonate precipitates in polar regions, the various types of carbonate deposits encountered can be grouped according to the mechanisms that led to their formation (Fig. 1). The most common process that explains the formation of cold-climate carbonate precipitates is the freezing of a calcium bicarbonate solution. In this thesis, the term *cryogenic* is used to describe all types of carbonate that formed by freezing of a calcium bicarbonate solution. Cryogenic carbonate deposits include the calcite powders found in freezing caves (cryogenic cave calcite), on the surface of aufeis along riverbeds (cryogenic aufeis calcite) and the subglacially-precipitated carbonate crusts. Carbonate deposits precipitated by cryodessication or evaporation include the evaporative calcite crusts found on the upper surface of clasts. Carbonate deposits associated with a biogenic origin are currently restricted to the endostromatolites discovered in the northern Yukon Territory and in / around the Haughton Impact Structure on Devon Island. Some carbonate deposits, such as the calcareous crusts/pendants located on the lower surface of clasts within the active layer, have been shown to be related to either freezing or evaporation. A final process that can lead to the formation of carbonate deposits is associated with degassing, which produces the speleothems (stalagmites, stalagtites, flowstones) in caves. However, this process will not be examined in great detail since the growth of speleothems is generally inactive, where in polar settings, the presence of permafrost restricts groundwater circulation in caves.

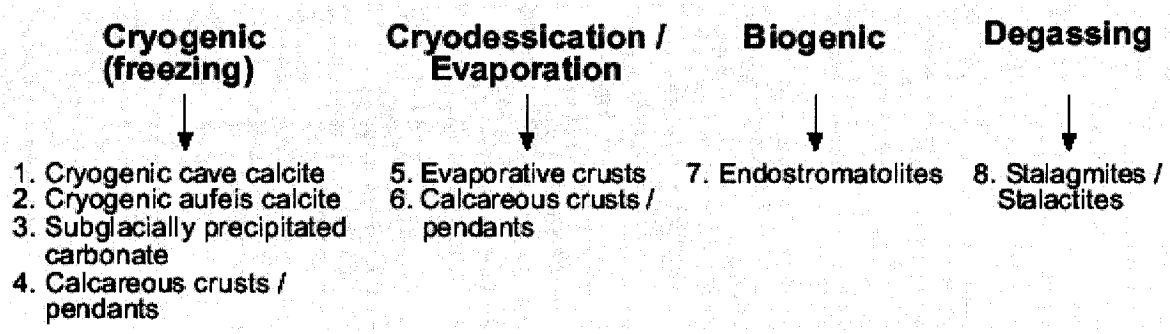

Fig. 1: Classification of the carbonate deposits encountered in polar regions according to the dominant process(es) leading to their formation.

1.3 Segregation of solutes and isotopic partitioning during freezing

Most freshwaters have a chemistry dominated by Ca^{2+} and HCO_3^- that originates from the preferential dissolution of calcareous components of the bedrock. Even in crystalline bedrock environments, where the bedrock can comprise less than 1% carbonate, calcite dissolution will dominate over silicate weathering given the lower solubility of calcite (White et al. 1999). Therefore during freezing, evaporation, CO_2 degassing or other processes operating in polar regions, the precipitation of calcite is expected, irrespective of the local geology.

The suggestion that freezing could cause the precipitation of calcite was first made by Cailleux (1964) in his studies of authigenic mineralization in soils that underwent occasional freezing. The first known study to experimentally verify the effect of freezing on the solute concentration was made by Ek and Pissart (1965). However, they used a high initial CO_2 pressure and therefore could not isolate the role of freezing on carbonate precipitation given that precipitation could have occurred because of a decrease in CO_2 pressure during degassing. Later, Hallet (1976) carried out a careful experiment on the role of freezing Ca^{2+} - HCO_3^- waters in equilibrium with the atmosphere. It was found that freezing caused a progressive enrichment in Ca^{2+} and HCO_3^-, to a point where their ion activity product reached and exceeded the calcite saturation point, causing calcite to precipitate (Fig. 2). Therefore, freezing induces a concentration of solutes in the residual water and also leads to a progressive increase in the calcite saturation state. Recently, Killawee et al. (1998) verified the consequence of calcite precipitation on the distribution of solutes among the ice, water and gas phases under steady-state freezing. Their results complement those of Hallet (1976), but Killawee et al. (1998) indicated that ice growth led to a slight solute concentration at the ice-water boundary. However, none of these studies examined the effect of freezing different geochemical solutions on the stable isotope composition of the resulting carbonate deposits ($^{18}O/^{16}O$ and $^{13}C/^{12}C$).

Stable isotopes are useful in helping to understand the conditions under which the secondary carbonate deposits have formed. Stable isotopes are normally measured as the ratio of the two most abundant isotopes of a given element. In calcium carbonate deposits ($CaCO_3$), it is the $^{18}O/^{16}O$ and $^{13}C/^{12}C$ ratios that are of interest. During the formation of calcite minerals, the heavy isotopes (^{18}O and ^{13}C) are preferential incorporated from the aqueous phase into the minerals in proportion governed by their fractionation factor, which is inversely proportional to

the temperature under which the precipitation occurs. The following general equation describes this process:

$$[1] \quad R_S = R_W + \varepsilon_{S\text{-}W}$$

where R is the relative abundance of the isotopes ($^{18}O/^{16}O$; $^{13}C/^{12}C$), the subscript S represents the solid carbonate phase, the subscript W stands for water and ε is the fractionation factor. This equation is valid only for calcite formed under equilibrium conditions. Under such conditions, the $\delta^{18}O$ and $\delta^{13}C$ composition of the calcite minerals, which is the normalized difference between the sample and a standard, i.e. $\delta^{18}O = [(^{18}O/^{16}O)_{spl} / (^{18}O/^{16}O)_{std} - 1] \cdot 1000‰$, is controlled by the $\delta^{18}O$ and $\delta^{13}C_{DIC}$ composition of the parent water and temperature at which precipitation occurs. However, the $\delta^{13}C_{DIC}$ is determined by the pH of the solution and will be affected by chemical reactions (i.e. carbonate dissolution) prior to carbonate precipitation.

In nature, a sudden change in temperature or the removal/addition of reactants from the solution can create conditions of kinetic fractionation. One possible process that affects the $\delta^{18}O$ composition of calcium carbonate deposits is freezing the aqueous phase prior to calcite precipitating. The effect of freezing on the stable isotope composition ($^{18}O/^{16}O$) of water is well known and freezing can also cause calcite deposits to precipitate by increasing the calcite saturation state of the parent water. During freezing, the stable isotope composition of water evolves according to a Rayleigh-type distillation ($\delta = \delta_0 + \varepsilon \cdot \ln f$) where δ_0, δ are the initial and final δ (‰) values respectively, $\varepsilon = (\alpha - 1) \cdot 1000$ *where* α is the fractionation factor, and *f* is the fraction of water remaining in solution. The first ice to be formed during freezing will be enriched in $\delta^{18}O$ by about 3‰, with a corresponding depletion on the $\delta^{18}O$ of the water. As freezing continues, the $\delta^{18}O$ of the residual water fraction becomes progressively lower. Therefore, if freezing is the cause of calcite precipitation, its $\delta^{18}O$ composition might not reflect the initial $\delta^{18}O$ value of the water from which it precipitated. The greatest $\delta^{18}O$ deviation that of the parent water would be expected to occur in calcite deposits whose parent water has a low calcite saturation index since calcite precipitation would be expected to occur in the late stage of freezing. However, little is known about evolution of $\delta^{13}C_{DIC}$ during freezing. The only known

study that examined the effect of freezing on the $\delta^{13}C$ of carbonate was the one done by Clark and Lauriol (1992) on kinetically-precipitated calcite powders.

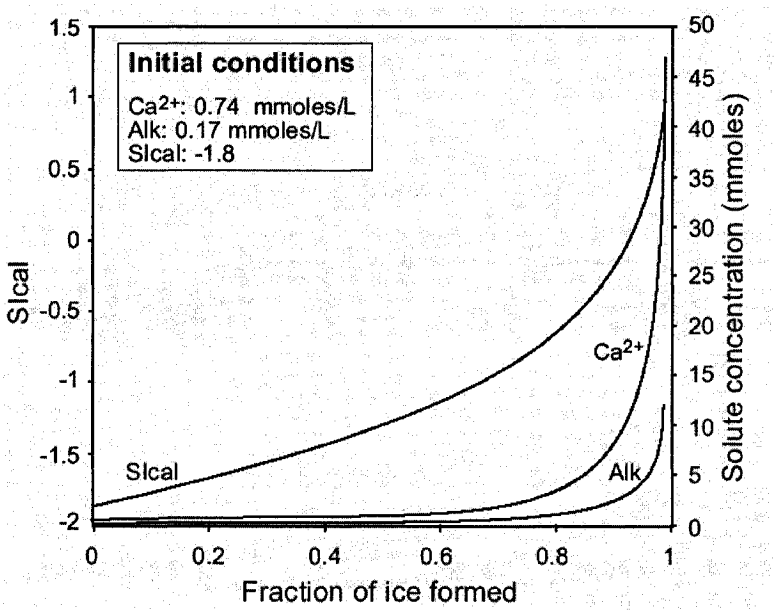

Fig. 2: Evolution of log SIcal and solution concentration during the freezing of water.

2. Objectives and region of study

The main objective of this thesis is to determine if the stable C-O isotope composition preserved in cold-climate carbonate precipitates is a reliable paleoclimatic and paleoenvironmental proxy. The secondary objective of this thesis are to provide insights into the principal formative mechanism by which the cold-climate carbonates precipitated and to determine the origin of carbonate deposits found in a granitic environment, since they are still poorly understood features in this type of environment. To facilitate a comparison between studies, a morphological classification of the numerous types of carbonate precipitates encountered in polar regions is also presented. The study area of this thesis (Fig. 3) includes the limestone terrain of the northern Yukon Territory and the granitic environment of southern Baffin Island, Nunavut.

More specifically, the objectives of the thesis will be reached by analyzing stable C-O isotope composition of actively forming secondary carbonate deposits and the geochemical composition of the water from which the carbonates precipitated in order to investigate the geochemical and isotopic partitioning that is occurring prior to and during the precipitation of the

carbonate deposits. To verify the extent of the effect of the geochemical and isotopic composition of the waters from which they precipitated, samples of secondary carbonate precipitates and the associated water were collected in distinct geological settings (i.e. limestone terrain versus granitic environment). Both of these regions are located within the zone of continuous permafrost, which facilitates a comparison of the operating processes.

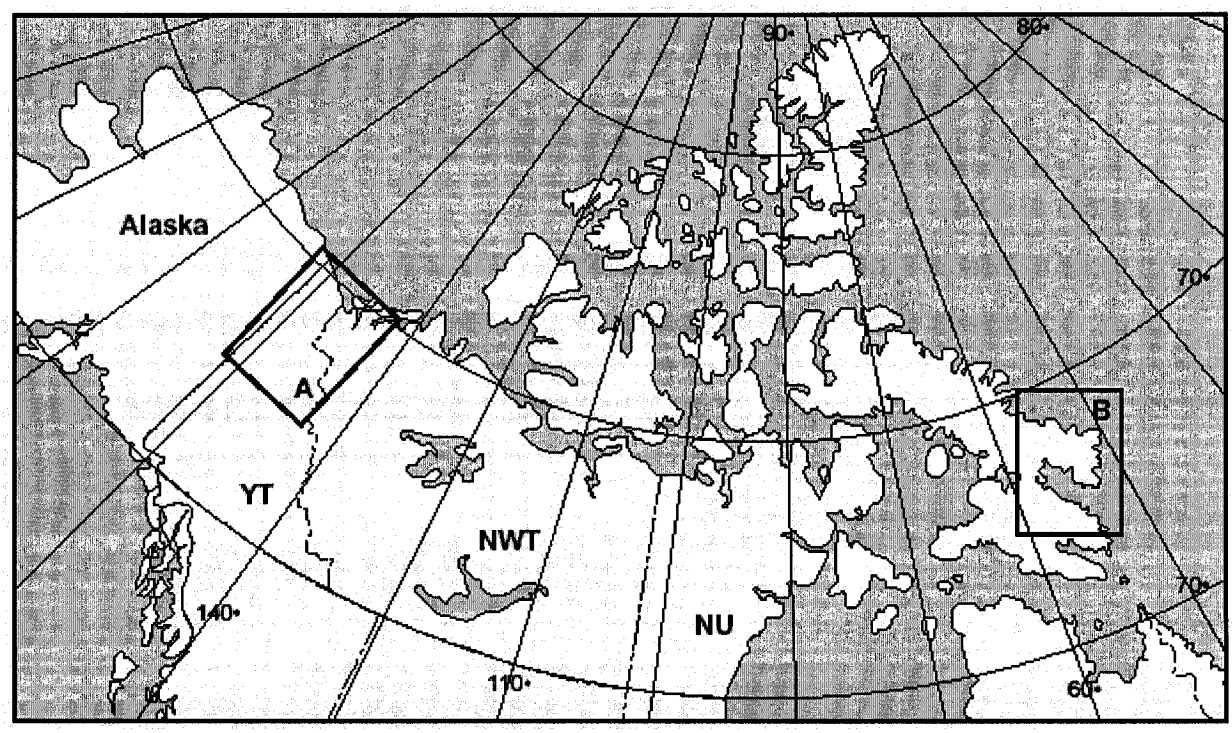

Fig. 3: Map showing location of areas studied in this thesis. A) northern Yukon Territory; B) southern Baffin Island, Nunavut.

References

Adolphe, J.P. 1972. Obtention d'encroûtements carbonates par gel experimental. Comptes Rendues Académies des Sciences 274, 1139-1142.

Blake, W. Jr. 2005. Holocene carbonate precipitates on Precambrian bedrock in the High Arctic: age and potential for paleoclimatic information. Geografiska Annaler 87A, 175-192.

Bunting, B.T. and Christensen L. 1978. Micromorphology of calcareous crusts from the Canadian High Arctic. Geologiska Foreningens Forhandlinger 100, 361-367.

Burn, C.R. 1997. Cryostratigraphy, paleogeography and climate change during the early Holocene warm interval, western Arctic coast, Canada. Canadian Journal of Earth Sciences 34, 912-925.

Cailleux, A. 1964. Genèse possible de dépôts chimiques par congélation. Compte Rendus de la Société Géologique de France 1, 11-12.

Clark, I.D. and Lauriol, B. 1992. Kinetic enrichment of stable isotopes in cryogenic calcites. Chemical Geology 102, 217-228.

Clark, I.D. and Lauriol, B. 1997. Aufeis of the Firth River basin: insights into permafrost hydrology and karst. Arctic and Alpine Research 29, 240-252.

Clark, I.D., Lauriol, B., Marschner, M., Sabourin, N., Chauret, Y. and Desrochers, A. 2004. Endostromatolites from permafrost karst, Yukon Canada: paleoclimatic proxies for the Holocene thermal hypsithermal. Canadian Journal of Earth Sciences 41, 387-399.

Courty, M.A., Marlin, C., Dever, L., Tremblay, P. and Vachier, P. 1994. The properties, genesis and environmental significance of calcitic pendants from the high Arctic (Spitsbergen). Geoderma 61, 71-102.

Dansgaard, W. 1964. Stable isotopes in precipitation. Tellus 16, 436-468.

Ek, C. and Pissart, A. 1965. Dépôt de carbonate de calcium par congélation et teneur en bicarbonate des eaux résiduelles. Compte Rendus Académie de Science Paris 260, 929-932.

Epica Community Members. 2004. Eight glacial cycles from an Antarctic ice core. Nature 429, 623–628.

Fairchild, I., Bradly, L. and Spiro, B. 1993. Carbonate diagenesis in ice. Geology 21, 901-904.

Fisher, D.A., Koerner, R.M., Bourgeois, J.C., Zielinski, G., Wake,C., Hammer, C.U., Clausen, H.B., Gundestrup, N., Johnsen, S., Goto-Azuma, K., Hondoh, T., Blake, E. and Gerasimoff,

M. 1998. Penny Ice Cap cores, Baffin Island, Canada, and the Wisconsinan Foxe dome connection: Two states of Hudson Bay ice cover. Science 279, 692-695.

Ford, D.C., Fuller, P.G. and Drake, J.J. 1970. Calcite precipitates at the sole of temperate glaciers. Nature 226, 441-442.

Forman, S.L. and Miller, G. 1984. Time-dependent soil morphologies and pedogenic processes on raised beaches. Broggerhalwoya, Spitsbergen, Svalbard archipelago. Arctic and Alpine Research 16, 381-393.

Hall, D.K. 1980. Mineral precipitation in North Slope river icings. Arctic 33, 343-348.

Hallet, B. 1976. Deposits formed by subglacial precipitation of $CaCO_3$. Geological Society of America Bulletin 87, 1003-1015.

Hallet B., Lorrain R. and Souchez R. 1978. The composition of basal ice from a glacier sliding over limestones. Geological Society of America Bulletin 89, 3142320.

Hillaire-Marcel, C., Soucy, J.M. and Cailleux, A. 1979. Analyse isotopique de concrétions sous-glaciaire de l'inlandsis laurentidiens et teneur en oxygène 18 de la glace. Canadian Journal of Earth Sciences 16, 1494-1498.

IPCC. 2002. The third assessment. http://www.ipcc.ch/. Intergovernmental panel on climate change.

Killawee , J.A., Fairchild, I.J., Tison, J.L., Janssens, L. and Lorrain, R. 1998.. Segregation of solutes and gases in experimental freezing of dilute solutions: implication for natural glacier systems. Geochimica Cosmochimica Acta 62, 3637-3655.

Lauriol, B., Cinq-Mars, J. and Clark, I.D. 1991. Localisation, genèse et fonte de quelques naleds du nord Yukon (Canada). Permafrost and Periglacial Processes 2, 225-236.

Lauriol, B. and Clark, I.D. 1999. Fissure calcretes in the arctic: a paleohydrologic indicator. Applied Geochemistry 14, 775-785.

Nakai, N., Wada, H., Kiyosu, Y. and Takimoto, M. 1975. Stable isotope studies on the origin and geological history of water and salts in the Lake Vanda area, Antarctica. Geochemical Journal 9, 7-24.

Pollard, W. 1983. A study of seasonal frost mounds, North Fork Pass, northern interior Yukon Territory. Unpublished PhD Thesis, University of Ottawa.

Ritchie, J.C., Cwynar, L.C. and Spear, R.W. 1983. Evidence from northwest Canada for an early Holocene Milankovitch thermal maximum. Nature 305, 126-128.

Sharp, M., Tison, J.L. and Fierens, G. 1990. Geochemistry of subglacial calcites: implications for the hydrology of the basal water film. Arctic and Alpine Research 22, 141-152.

Souchez, R.A. and Lemmens, M. 1985. Subglacial carbonate deposition – an isotopic study of present-day case. Palaeogeography, Palaeoclimatology and Palaeoecology 51, 357-364.

Swett, K. 1974. Calcrete crusts in an arctic permafrost environment. American Journal of Science 274, 1059-1063.

Washburn, A.L. 1969. Weathering, frost action, and patterned ground in the Mesters Vig district, Northeast Greenland. Medelelser om Gronland 176, 303p.

Winograd, I.J., Coplen, T.B., Landwehr, J.M.., Riggs. A.C., Ludwig, K.R., Szabo, B.J., Kolesar, P.T. and Revesz, K.M. 1992. Continuous 500 000 year climate record from vein calcite in Devil's Hole, Nevada. Science 258, 255-260.

Winograd, I.J., Landwehr, J.M., Ludwig, K.R., Coplan, T.B. and Riggs, A.C. 1997. Duration and structure of the past four interglaciations. Quaternary Research 48, 141-154.

Yiou, P., Fuhrer, K., Meeker, L.D., Jouzel, J., Johnsen, S. and Mayewski, P.A. 1997. Paleoclimatic variability inferred from the spectral analysis of Greenland and Antarctic ice-core data. Journal of Geophysical Research 102, :26411-26454.

Zak, K., Urban, J., Cilek, V. and Hercman, H. 2004. Cryogenic cave calcite from several Central European caves: age, carbon and oxygen isotopes and a genetic model. Chemical Geology 206, 119-136.

Zdanowicz, C., Fisher, D., Clark, I.D. and Lacelle, D. 2002. An ice-marginal $\delta^{18}O$ record from Barnes Ice Cap, Baffin Island, Canada. Annals of Glaciology 35, 145-149.

Manuscript 1

Effect of chemical composition of water on the oxygen-18 and carbon-13 signature preserved in cryogenic carbonates, Arctic Canada: implications in paleoclimatic studies

Lacelle, D., Lauriol, B. and Clark, I.D.

Chemical Geology vol. 234 p. 1-16

Abstract

This study examines the $\delta^{18}O$ and $\delta^{13}C$ composition of cryogenic carbonate deposits in relation to the initial $\delta^{18}O$, $\delta^{13}C_{DIC}$ and chemical composition of the water from which it precipitated. This study focuses on cryogenic calcites precipitated in relation to aufeis aggradation since it offers the possibility of examining the chemical and isotopic partitioning that occurs during freezing. The studied aufeis are located in the western Canadian Arctic (YT and NWT), a region underlain mostly by limestone bedrock, and southern Baffin Island (NU), an area of crystalline bedrock. The results indicate that the $\delta^{18}O$ composition of cryogenic calcite from a carbonated environment are slightly depleted over that of the initial $\delta^{18}O$ of the parent water, while those from a non-carbonated environment are strongly depleted over the initial $\delta^{18}O$ of the parent water as a result of the lower calcite saturation state of the parent water. This suggest that the $\delta^{18}O$ of cryogenic carbonates not only depends on the initial $\delta^{18}O$ composition of the parent water and the temperature at which the carbonate precipitated, but also on the calcite saturation state of the parent water and kinetic inhibitions during calcite precipitation. Given that the aggradation of aufeis occurs under closed-system freezing, the residual water will become progressively depleted in $\delta^{18}O$ as a result of the removal of heavier isotopes in the ice. In addition, freezing imparts a concentration of solutes in the residual water, which leads to an increase in calcite saturation index. Therefore, carbonate precipitated in equilibrium from water that has a low calcite saturation index will have a highly depleted $\delta^{18}O$ composition over that of the initial $\delta^{18}O$ values of the parent water since the calcite saturation state will only be exceeded in the late stage of freezing. By contrast, solute and isotopic partitioning during freezing has little effect on the $\delta^{13}C$ of the cryogenic carbonates as it tends to reflect that of the initial $\delta^{13}C_{DIC}$ value of the parent water. These findings have significant implications in the use of cryogenic carbonates in paleoclimate studies. Care must be taken when interpreting the $\delta^{18}O$ signature preserved in cryogenic carbonates since their signature might be modified by freezing prior to their precipitation, which will lead to a lighter $\delta^{18}O$ composition of the cryogenic carbonates. Therefore, it would be difficult to use the $\delta^{18}O$ composition of cryogenic carbonates as a direct proxy in paleoclimatic reconstruction unless details about the chemical composition of parent waters are known. Nevertheless, the $\delta^{13}C$ composition of the cryogenic carbonates that precipitated under close-system conditions can allow insights into the different water sources contributing to carbonate precipitation.

1. Introduction

Currently, with the exception of ice cores (Dansgaard 1982; Fisher et al. 1998; Epica Community Members 2004), freshwater endostromatolites (Clark et al. 2004) and Tertiary speleothems (Lauriol et al. 1997), direct climate proxies in polar regions are rare. As a consequence, cryogenic carbonate deposits, which form by CO_2 degassing during the freezing of water containing calcium and bicarbonate, have been receiving growing interest as paleoclimatic proxies due to the sensitivity of polar regions to the recent changes in climate. In polar regions, cryogenic carbonates have been reported from various environments, including in freezing caves (Clark and Lauriol 1992; Zak et al. 2004), on the surface of aufeis along riverbeds (Hall 1980; Pollard 1983; Lauriol et al. 1991; Clark and Lauriol 1997), in lakebeds of the Dry Valleys of Antarctica (Nakai et al. 1975), on the upper surface of clasts in deglaciated regions (Hallet 1976; Hillaire-Marcel et al. 1979; Souchez and Lemmens 1985; Sharp et al. 1990; Fairchild et al. 1993; Blake 2005) and on the lower surface of clasts within the active layer (Swett 1974; Bunting and Christensen 1978; Forman and Miller 1984; Marlin et al. 1993; Courty et al. 1994).

Generally, quantitative reconstructions of paleotemperatures rely on the analysis of the stable isotope ratio of oxygen ($^{18}O/^{16}O$) preserved in the carbonates and the global $\delta^{18}O$-T°C relation developed by Dansgaard (1964), providing that the waters from which the carbonate precipitated reflect the local mean annual air temperature. Carbon isotopes ($^{13}C/^{12}C$) are also included whenever they contribute significant paleoclimatic information. However, before cryogenic carbonates can be regarded as reliable archives of past climatic conditions, two key issues relating to the interpretation of the $^{18}O/^{16}O$ and $^{13}C/^{12}C$ ratios preserved in the cryogenic carbonate must be addressed. The first is to verify if the $^{18}O/^{16}O$ ratio preserved in cryogenic carbonate deposits reflects that of the local mean annual air temperature, since freezing is a fractionating process that imparts a progressive depletion on the initial $^{18}O/^{16}O$ ratio of the parent water. The second issue is related to the effect of freezing on the $^{13}C/^{12}C$ ratio in cryogenic carbonate. According to Clark and Lauriol (1992), Socki et al. (2001) and Zak et al. (2004), the $^{13}C/^{12}C$ ratio in cryogenic carbonate is dependant on the rate of reaction at which the carbonate precipitates, which can lead to severe kinetic fractionation of ^{13}C between the cryogenic carbonate and the escaping CO_2. If the cryogenic carbonate precipitated from waters that were modified by such secondary processes, their $^{18}O/^{16}O$ and $^{13}C/^{12}C$ ratio might not be useful in quantitative paleoclimatic studies.

In this study, the chemical and isotopic ($^{18}O/^{16}O$; $^{13}C/^{12}C$) partitioning that is occurring between the water feeding aufeis in distinct geological settings (carbonated vs. non-carbonated) and their associated mineral precipitates are examined to evaluate the potential of the cryogenic aufeis carbonate as direct paleoclimatic proxies. The studied aufeis are located in the western Canadian Arctic, a region dominantly underlain by limestone bedrock, and southern Baffin Island (NU), an area of crystalline bedrock (Fig. 1). The objective of this study will be reached by *i*) determining the chemical composition and stable isotope ratios of O, H and C of the waters feeding the aufeis; *ii*) determining the stable isotope ratios of O and H of the ice-layers composing the aufeis; and *iii*) determining the stable isotope ratios of O and C of the cryogenic aufeis calcite deposits associated with aufeis growth. This should provide insights into the concurrent segregation of solutes and stable isotope partitioning that occurs during freezing between water and the precipitating carbonate in areas of limestone and granitic bedrock. This study will also evaluate whether cryogenic aufeis carbonates precipitated in isotopic equilibrium with the parent water, or if kinetic conditions controlled their formation.

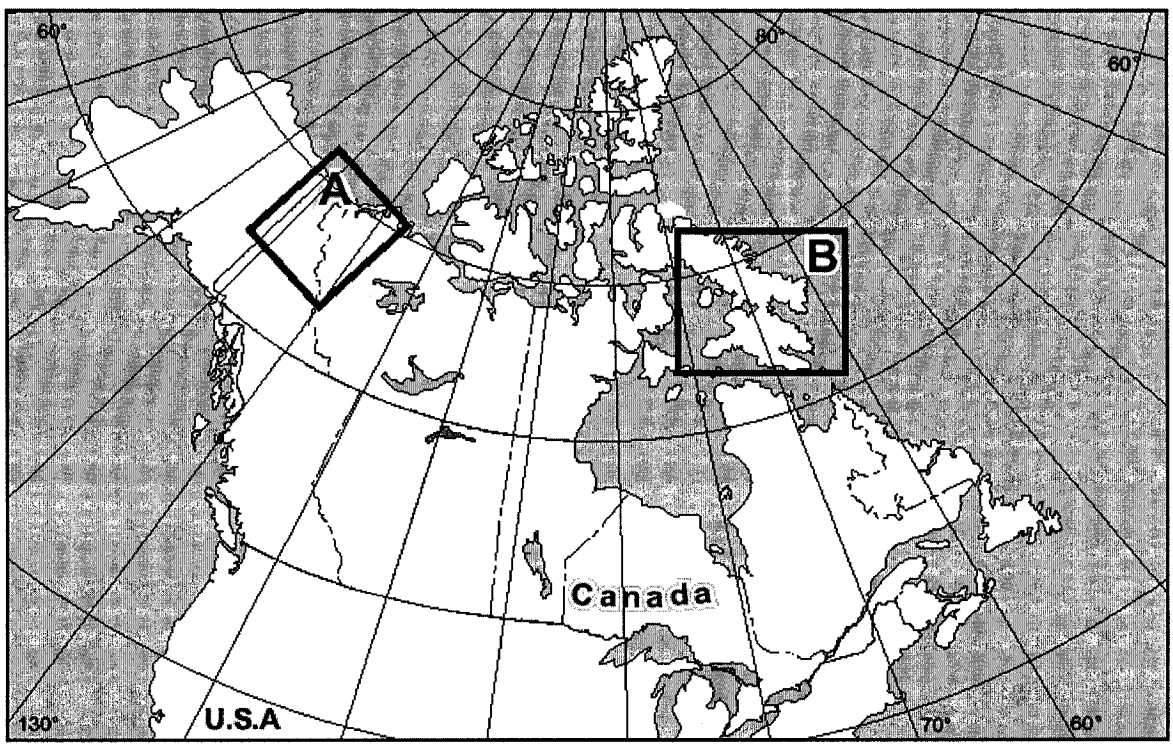

Fig. 1: Location of the regions studied in the Canadian Arctic. The boxes A and B identifiy the areas mapped in Figs. 2 and 4 respectively.

2. Background on aufeis and their associated mineral precipitates

Aufeis (icings) are sheet-like masses of layered ice that accumulate on river channels by the freezing of successive overflows of perennial groundwater-fed springs upon exposure to cold air (Van Everdingen 1974; Tolsikhin and Tolsikhin 1976). Most aufeis are located in permafrosted limestone environments (Akerman 1982; Van Everdingen and Allen 1983; Pollard 1983; Van Everdingen 1988; Lauriol et al. 1991; Clark and Lauriol 1997; Pollard 2005) as they offers the greatest possibility to host perennial groundwater discharge through the development of open fractures and fissures, which facilitate the circulation of groundwater through taliks (Clark and Lauriol 1997; Clark et al. 2001). As a result, the groundwaters feeding aufeis are typically characterized by a Ca-HCO_3 facies. The geochemical signature of the groundwaters feeding the aufeis is important since the process of aufeis aggradation is associated with the production of mineral precipitates within the ice-layers by solute expulsion during freezing (Hall 1980; Pollard 1983; Clark and Lauriol 1997). The most common mineral precipitated during aufeis growth are calcite ($CaCO_3$), gypsum ($CaSO_4 \cdot 2H_2O$), halite (NaCl) and ikaite ($CaCO_3 \cdot 6H_2O$) (Hall 1980; Clark and Lauriol 1997; Pollard 2005). The mineral precipitates are released from the aufeis onto its surface and surroundings during the thaw season. Residual accumulations of calcite powders of up to 18,000 m^3 were reported by Hall (1980) on the surface of aufeis located along the north slopes of Alaska.

3. Site descriptions

3.1 Carbonated environment: western Canadian Arctic (YT and NWT)

Numerous aufeis can be found along the beds of rivers in the western Canadian Arctic, and three were examined in this study: the Babbage River, Fish Hole Creek and Little Fish Creek aufeis (Fig. 2). The Babbage River and Fish Hole Creek aufeis (68°48'N; 138°47'W) are located at the southern footslope of the Barn's Range in the British Mountains, an area underlain by Jurassic-Lower Cretaceous marine shale and siltstone of the Kingak Formation (Norris 1977). Little Fish Creek aufeis (67°45'N; 136°19'W) is located in the White Mountains near McDougall Pass. The White Mountains are part of the Richardson Mountains and consist of a circular limestone and dolomite massif from the Carboniferous Lisburne group flanked by highly folded and faulted Mesozoic shales and sandstones (Norris 1975). These aufeis cover an approximate surface area of a few km^2 or less, which is far less than the Firth River aufeis (31.5

km^2), the largest aufeis located in the British Mountains, northern Yukon Territory (Clark and Lauriol 1997).

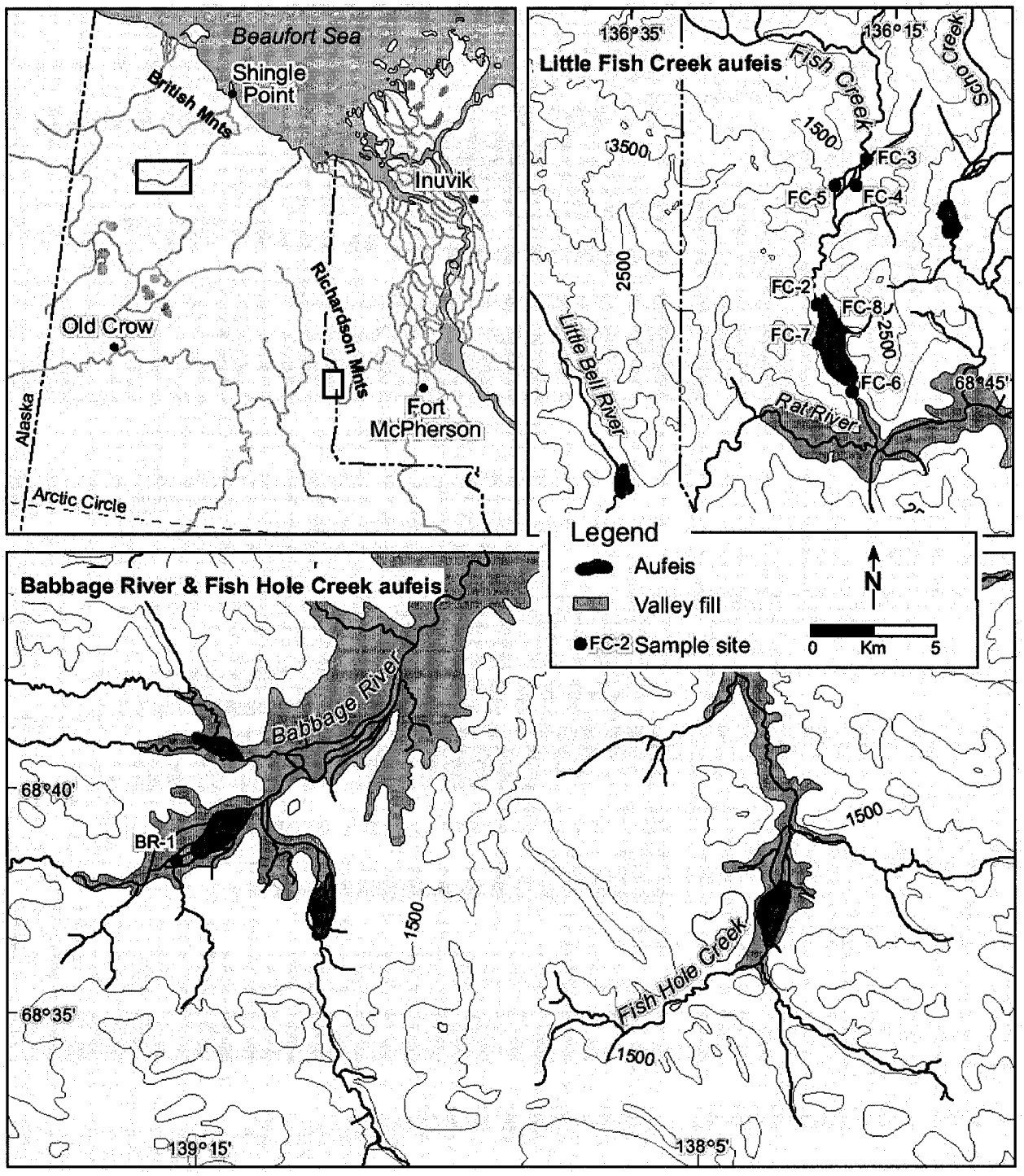

Fig. 2: Maps showing the location of the Babbage, Fish Hole and Little Fish Creek aufeis in the western Canadian Arctic along with the water sample sites.

The studied aufeis in the western Canadian Arctic are associated with fault zones in carbonated bedrock. The Babbage River and Fish Hole Creek aufeis are located downstream from a regional strike that intersects the riverbeds on which the aufeis are located. Little Fish Creek aufeis is also located in a region with geological structures (Fig. 3). An orthogonal fault crosses an anticlinal structure formed by Permian and Jurassic sediments in an SW-NE direction, perpendicular to the Fish Creek valley. Consequently, the presence of faults and strikes probably enhances groundwater discharge from the carbonate terrain, which promotes the growth of aufeis.

The climate in the western Canadian Arctic is part of the polar continental regime. The climate recorded at Shingle Point, located along the coastline of the Beaufort Sea, reports a mean annual air temperature of -10°C (January *T*°C -25°C; July *T*°C 11°C; Environment Canada 2004), while the mean annual air temperature at Fort McPherson, located 100 km east of the Richardson Mountains, is -8.8°C (January *T*°C -30°C; July *T*°C 15°C; Environment Canada 2004). Precipitation in the western Canadian Arctic is generally light. The total annual precipitation along the coastline averages between 125 to 185 mm yr^{-1} but increases to 366 mm yr^{-1} at Fort McPherson due to orographic effects (Environment Canada 2004). Vegetation is largely arctic tundra with forest-tundra ecotone along the valleys, grading into alpine tundra with increasing elevation. Barren limestone outcrop dominates at higher elevations.

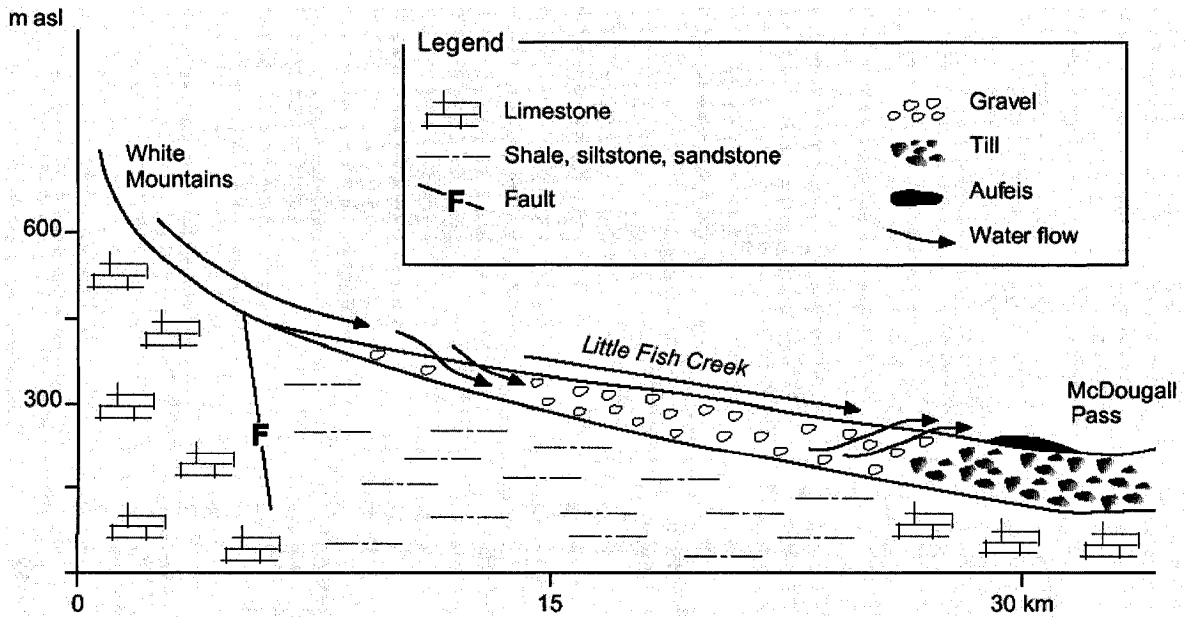

Fig. 3: Schematic diagram of a cross-section from the White Mountains to McDougall Pass showing recharge and circulation of groundwater feeding the Little Fish Creek aufeis, NWT.

3.2 Non-carbonated environment: southern Baffin Island (NU)

Aufeis in a non-carbonated environment are rare, but a few were found in Akshayuk Pass (66°44'N; 65°00'W), a 98 km long U-shaped glacial valley incised into the Penny highlands on southern Cumberland Peninsula, Baffin Island, Nunavut. The most impressive and largest aufeis in Akshayuk Pass is Highway Glacier aufeis, which accumulates near the terminus of Highway Glacier, a tributary glacier of the 6000 km^2 Penny Ice Cap (Fig. 4). An examination of historical aerial photographs (1948) and field observations (2004) revealed that Highway Glacier aufeis underwent a geographical shift that is likely related to the receding Highway Glacier (Fig. 4). It is suggested that the aufeis is fed by subglacial meltwaters circulating through a proglacial talik, and the presence of permafrost in the proglacial zone forces the groundwater to the surface. In early summer 2004, Highway Glacier aufeis measured 1 km long, up to 400 m wide and 3-4 m thick, giving it an approximate surface area of 0.5 km^2. Other aufeis in Akshayuk Pass are located at the foothill of Turnweather Glacier and along the Weasel River near Thor shelter. These aufeis cover a surface area of less than 0.5 km^2.

Bedrock in Akshayuk Pass consists primarily of granitic rocks of the Precambrian Canadian Shield, medium to coarse-grained gneiss and quartz monzonites (Dyke et al. 1982). Carbonate bedrock is absent from the area, but fracture-filling calcite provides a carbon source that can assist in the precipitation of cryogenic carbonates.

The climate in Akshayuk Pass is part of the polar maritime regime and is highly variable due to the presence of the Penny Ice Cap in the highlands. The climate recorded at the nearest meteorological station, the hamlet of Pangnirtung, reports a mean annual air temperature of -10.4°C (January T°C -28°C; July T°C 7°C) and total annual precipitation of nearly 400 mm (Environment Canada 2004). Vegetation in Akshayuk Pass ranges from very patchy and open on the slopes, to lush tundra meadows near the flood plain. Arctic shrubs such as dwarf birch, willow, heather, and blueberry form a continuous carpet in sheltered valleys, while tussocks of grasses and sedges grow in less favourable areas.

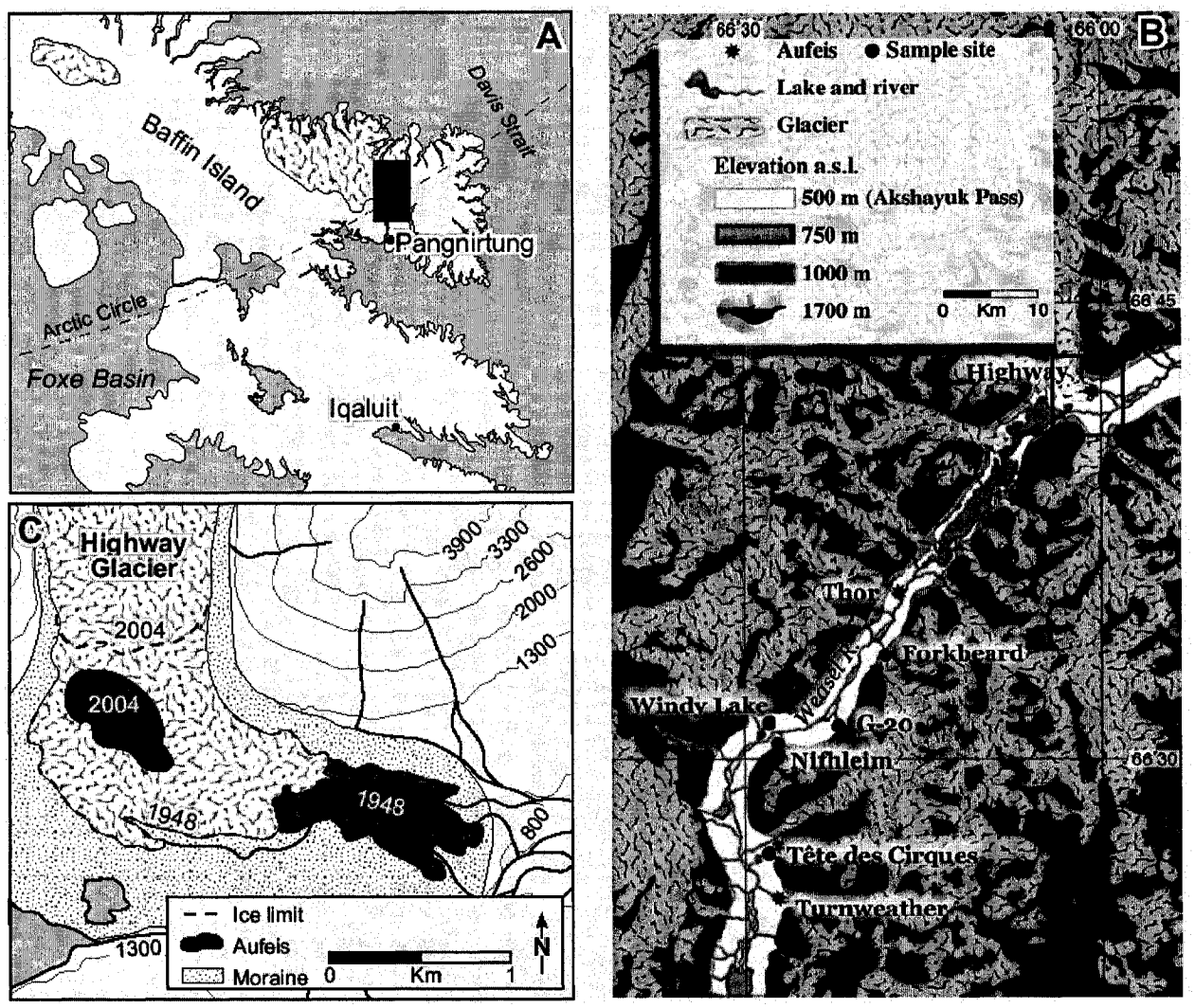

Fig. 4: A) Map showing the location of Akshayuk Pass, a 98 km long glacial valley on southern Cumberland Peninsula, Nunavut. B) Map showing the location of Highway Glacier aufeis in Akshayuk Pass along with the water sample sites. C) Map showing the geographical shifting of Highway Glacier aufeis between 1948 (aerial photograph T214-L59) and 2004 (field observations).

4. Methodologies

4.1 Sampling techniques

The Babbage River, Fish Hole Creek and Little Fish Creek aufeis, located in the western Canadian Arctic, were sampled in July 1996 and 1997. Highway Glacier aufeis, located in southern Baffin Island, was sampled in July 2004. At all sites, water samples for cations analysis were field filtered (0.45μm pore diameter) and collected in 20 ml pre-rinsed polyethylene bottles, with subsequent acidification using ultra-pure nitric acid. Filtered, unacidified samples were collected for anions analysis in 20 ml pre-rinsed polyethylene bottles. Water samples for the measurement of the stable isotope ratios of oxygen ($^{18}O/^{16}O$) and hydrogen (D/H) were collected unfiltered in 20 ml polyethylene bottles. Filtered water samples were collected unpreserved in 40 ml glass amber bottles for the determination of dissolved inorganic carbon (DIC) and its stable isotope ratio ($^{13}C/^{12}C$). In addition, individual ice-layers of the aufeis were collected using a ice axe. The ice was melted in the field and then poured unfiltered in polyethylene bottles for the analysis of the stable isotope ratios of oxygen and hydrogen. Mineral precipitates found on the surface of the aufeis were collected in sterile roll-top bags.

4.2 Analytical procedures

Field measurements included temperature and pH of the water. Alkalinity was measured in the field during our visits to the western Canadian Arctic aufeis only, and in the laboratory for the southern Baffin Island water samples.

Major cations were analyzed by Inductively Coupled Plasma Atomic Emission Spectroscopy. The anions were analyzed using a Dionex DX-100 ion chromatograph. All samples were run in duplicate and the analytical reproducibility was ± 5% for the cations and ± 10% for the anions.

The $^{18}O/^{16}O$ ratio of the water samples was determined on CO_2 isotopically equilibrated with the water at 25°C (analytical reproducibility of ± 0.1‰). The D/H ratio was measured on H_2 isotopically equilibrated with the water at 25°C using a Pt based catalyst (analytical reproducibility of ± 1.5‰). Both stable isotope measurements were made on the same sample using a Gas Bench II interfaced with a Finnigan Mat Delta$^+$ XP isotope mass spectrometer at the G.G. Hatch Laboratory (University of Ottawa). Results are presented using the δ-notation, where δ represents the parts per thousand difference of $^{18}O/^{16}O$ or D/H in a sample with respect to Vienna Standard Mean Ocean Water (VSMOW).

The $^{13}C/^{12}C$ ratio of the dissolved inorganic carbon (DIC) in the water samples from the northern Yukon Territory was determined upon return from the field by acidification under vacuum and cryogenic purification of the CO_2, which was then analyzed on a VG SIRA-12 mass spectrometer. The DIC concentrations and $^{13}C/^{12}C$ of the DIC in the water samples from southern Cumberland Peninsula were determined on a TIC-TOC analyser model OI-1010 interfaced to a Finnigan Mat Delta$^+$ isotope ratio mass spectrometer at the G.G. Hatch Laboratory following the wet oxidation technique described by St-Jean (2003). The DIC concentrations were normalized using internal standards and the analytical precision is ± 0.002 ppm. The $^{13}C/^{12}C$ ratios of the DIC are expressed in δ-notation, where δ represents the parts per thousand difference of $^{13}C/^{12}C$ in a sample with respect to the Vienna Pee-Dee Belemnite (VPDB) standard. Analytical precision is ± 0.2‰.

The $^{18}O/^{16}O$ and $^{13}C/^{12}C$ ratios of the calcite deposits were determined on CO_2 gas produced by reacting the powdered calcite with 100% phosphoric acid (H_3PO_4) in glass septum vials for 24 hours at 25°C. The evolved CO_2 gas was analyzed in continuous flow using a Gas Bench II interfaced to a Finnigan Mat Delta$^+$ XP isotope mass spectrometer at the G.G. Hatch Laboratory. Stable isotope data for C and O are expressed in δ-notation, where δ represents the parts per thousand difference of $^{18}O/^{16}O$ and $^{13}C/^{12}C$ in a sample with respect to the Vienna Pee-Dee Belemnite standard (VPDB). Analytical reproducibility is ± 0.15‰ for both isotopes.

4.3 Data analysis

The temperature, pH and geochemical composition of the waters were entered into PHREEQC, an hydrogeochemical program (Parkhurst and Appelo 1999), to calculate the partial pressure of CO_2 (log pCO_2) and saturation state of the water with respect to calcite (SIcal). The partial pressure of CO_2 is determined from pH and HCO_3^- measurements from the following equation:

$$[1] \quad \log pCO_2 = -pH + \log ([aHCO_3^-] / K_{CO2} K_1)$$

where $aHCO_3^-$ is the ion activity, K_{CO2} is the equilibrium constant for CO_2 and K_1 is the first dissociation constant of H_2CO_3. This equation assumes that HCO_3^- is the main contributor to alkalinity, which is the case given the pH range of the surface and spring waters.

In PHREEQC, the saturation state of the water with respect to calcite is calculated by the following equation:

[2] $SIcal = \log aCa^{2+} + \log aCO_3^{2-} - KCaCO_3$

Where SIcal is the saturation index of calcite, aCa^{2+} and aCO_3^{2-} are the respective ion activities and $KCaCO_3$ is the equilibrium solubility product for calcite. The solution is undersaturated if SIcal is < 0, at equilibrium if SIcal = 0, or supersaturated if SIcal > 0.

5. Results

5.1 Water chemistry

Based on the ternary diagram of the geochemical composition of the waters sampled in the western Canadian Arctic and in Akshayuk Pass, three principal geochemical facies are identified. The geochemical facies can be distinguished according to the local bedrock lithology and groundwater recharge circulation pathways (Fig. 5).

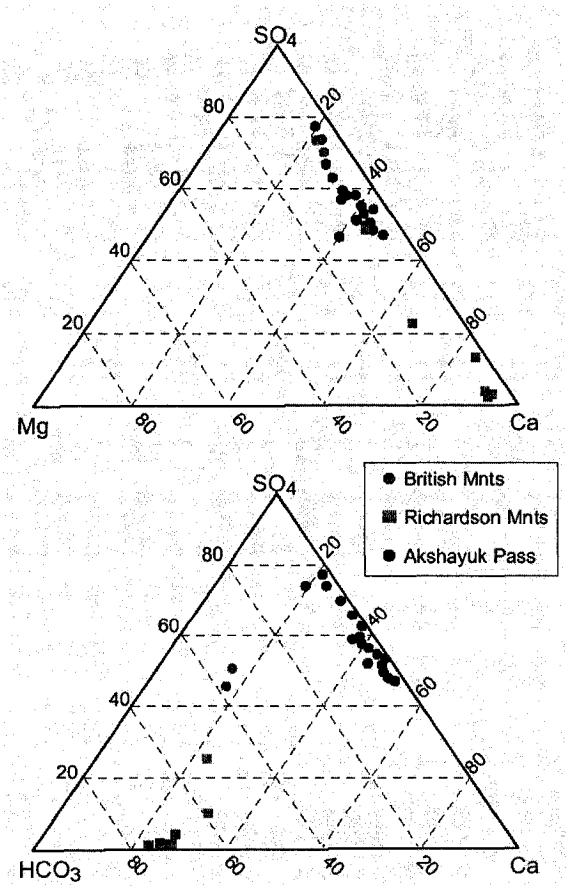

Fig. 5: Ternary diagrams of the geochemical composition of the waters feeding the Babbage River and Fish Hole Creek aufeis (British Mountains), Little Fish Creek aufeis (Richardson Mountains) and Highway Glacier aufeis (Akshayuk Pass).

The first group is associated with the surface and spring waters feeding the Babbage River and Fish Hole Creek aufeis, which are located in the British Mountains. These waters are highly mineralized (specific conductivity in the 1372 to 3723 μS/cm range), are characterized by a Ca-HCO_3-SO_4 facies and have pH values around 8 (Table 1). For comparison, the waters feeding the Firth River aufeis (Clark and Lauriol 1997) have a similar geochemical composition (Table 1). This suggests that the Ca-HCO_3-SO_4 facies might be characteristic of groundwater circulating through the limestone bedrock of the Lisburne Group, which is the dominant lithological group in the British Mountains. The calcite saturation indices of the surface and spring waters circulating in this region are also close to saturation due to carbonate dissolution. The surface waters in the area have $\delta^{18}O$ values averaging -22.4 ± 0.7‰.

The second group is associated with waters feeding the Little Fish Creek aufeis, located in an area underlain by Carboniferous limestone and Mesozoic shale and sandstone in the Richardson Mountains. The surface waters feeding Little Fish Creek aufeis have a low mineralization (specific conductivity = 410 μS/cm), a Ca-HCO_3 facies and pH values in the 4.9 to 7.6 range (Table 1). The waters feeding Little Fish Creek aufeis probably circulated through the highly faulted Mesozoic shale and sandstone overlying the marine limestone, as indicated by the lower pH values and salinity compared to those feeding the Babbage River and Fish Hole Creek aufeis located in the British Mountains. The calcite saturation indices of the waters feeding the Little Fish Creek aufes, which averages -2.0 ± 1.9, is further supportive of a shallow groundwater circulating through the Mesozoic shale and sandstone. The surface waters feeding Little Fish Creek aufeis have invariant $\delta^{18}O$ values (-21.4 ± 0.5‰; n = 7).

The third group is associated with waters feeding Highway Glacier aufeis, located in an area underlain by granitic, gneiss and quartz monzonite bedrock in southern Cumberland Peninsula, Baffin Island. The glacial meltwaters have a very low solute concentration (< 7 mg/L), are characterized by a Ca-Mg-SO_4 facies and a pH in the 5.4 to 6.6 range (Table 2). The glacial meltwaters are also highly undersatured with respect to calcite mineral (SIcal < -5) due to the local bedrock lithology. The glacial meltwaters have $\delta^{18}O$ values averaging -22.5 ± 1.8‰ (n = 31), which reflects that of the average $\delta^{18}O$ of precipitation in the area (Fisher et al. 1998).

Carbon isotope measurement of the dissolved inorganic carbon ($\delta^{13}C_{DIC}$) of surface waters feeding Little Fish Creek and Highway Glacier aufeis are shown in Table 1 and Table 2. The surface waters feeding the Little Fish Creek aufeis have $\delta^{13}C_{DIC}$ values in the –10.6 to -0.1‰ range. The glacial meltwaters in Akshayuk Pass have similar $\delta^{13}C_{DIC}$ values, ranging from -

11.3‰ to -3.1‰. The $\delta^{13}C_{DIC}$ values surface and spring waters feeding the Firth River aufeis are also similar as they range between -8.9 to -3.3‰ (Clark and Lauriol 1997). This range in $\delta^{13}C_{DIC}$ values is attributed to varying degree of exchange with atmospheric CO_2 during surface flow.

The $\delta^{18}O$ and δD compositions of the individual ice-layers from the Babbage River, Fish Hole Creek, Little Fish Creek and Highway Glacier aufeis are illustrated in Fig. 6. Since an isotopic mass-balance must be preserved during freezing, the $\delta^{18}O$ values of the individual ice-layers represent the average $\delta^{18}O$ composition of the waters feeding the aufeis. The $\delta^{18}O$ composition of the studied aufeis ranges between -23.5 to -19.4‰ and show no significant differences among the different geological regions (limestone and granitic). They are also very similar to the $\delta^{18}O$ composition of surface and spring waters feeding the aufeis (Table 1 and 2).

Table 1: Geochemical (mg/L) and isotopic (‰) data from surface waters and springs in the northern Yukon Territory and Northwest Territories.

Sample ID	T°C	pH	Ca	Mg	Na	K	Cl	ALK	SO_4	SIcal	log pCO_2	$\delta^{18}O$	$\delta^{13}C_{DIC}$
British Mountains													
Surface waters – Babbage River													
BR-1	4.0	8.4	43.8	10.8	198.0	7.0	185.9	98.8	148.3	0.2	-3.5	*n.d.*	*n.d.*
Firth River[1]													
AVERAGE	*4.3*	*7.7*	*48.4*	*3.1*	*0.3*	*0.2*	*n.d.*	*151.0*	*10.0*	*-0.3*	*-2.6*	*-22.4*	*-7.2*
STDEV	*1.5*	*0.2*	*15.1*	*0.9*	*0.1*	*0.1*	*n.d.*	*26.0*	*6.0*	*0.4*	*0.2*	*0.7*	*1.4*
Springs - Firth River[1]													
AVERAGE	*2.4*	*7.6*	*62.8*	*5.3*	*0.2*	*0.3*	*0.8*	*153.4*	*55.5*	*-0.2*	*-2.5*	*n.d.*	*-5.6*
STDEV	*1.7*	*0.2*	*28.1*	*2.7*	*0.1*	*0.3*	*0.2*	*29.3*	*72.9*	*0.3*	*0.2*	*n.d.*	*1.8*
Richardson Mountains													
Surface waters - Little Fish Creek													
FC-2	5.4	7.0	34.0	1.9	0.3	0.3	0.3	100.0	1.2	-1.1	-2.0	-22.0	-7.8
FC-3	1.2	5.0	5.7	0.9	0.3	0.1	0.4	11.0	1.9	-4.8	-4.1	-21.5	-0.8
FC-4	3.5	6.5	30.6	0.9	0.3	0.1	0.6	79.0	4.6	-1.8	-3.1	-21.8	-0.9
FC-5	1.8	4.9	6.6	1.0	0.3	0.3	0.1	15.0	7.4	-4.8	-3.4	-20.8	-0.1
FC-6	2.3	7.4	46.0	2.6	0.4	0.8	0.6	119.0	1.2	-0.6	-2.5	-21.6	-0.2
FC-7	0.6	7.6	44.1	2.4	0.4	1.4	0.4	145.0	0.9	-0.3	-2.6	-20.8	-0.2
FC-8	0.4	7.3	43.2	2.1	0.3	0.7	0.4	124.0	1.0	-0.8	-2.3	-21.1	-10.6
AVERAGE	*2.2*	*6.5*	*30.0*	*1.7*	*0.3*	*0.5*	*0.4*	*84.7*	*2.6*	*-2.0*	*-2.9*	*-21.4*	*-2.9*
STDEV	*1.8*	*1.1*	*17.2*	*0.7*	*0.1*	*0.5*	*0.2*	*53.1*	*2.5*	*1.9*	*0.7*	*0.5*	*4.4*
Springs - Little Fish Creek													
	1.5	8.6	72.3	13.3	4.7	0.6	2.1	160.7	96.6	0.8	-3.5	*n.d.*	*n.d.*

[1]Data from Clark and Lauriol (1997)
n.d. : no data

Table 2: Geochemical (mg/L) and isotopic (‰) data from glacial meltwaters in Akshayuk Pass, southern Cumberland Peninsula (NU).

Sample ID	T°C	pH	Ca	Mg	Na	K	ALK	SO_4	SIcal	log pCO_2	$\delta^{18}O$	$\delta^{13}C_{DIC}$
Akshayuk Pass												
HG-03-04	*n.d.*	*n.d.*	4.45	0.40	1.13	0.59	*n.d.*	*n.d.*	*n.d.*	*n.d.*	-21.6	*n.d.*
HG-04-04	*n.d.*	*n.d.*	3.12	b.d.	0.21	b.d.	*n.d.*	*n.d.*	*n.d.*	*n.d.*	-21.0	*n.d.*
HG-05-04	*n.d.*	*n.d.*	2.94	0.32	0.48	0.59	*n.d.*	*n.d.*	*n.d.*	*n.d.*	-22.7	*n.d.*
HG-06-04	*n.d.*	*n.d.*	2.95	0.33	0.44	0.56	*n.d.*	*n.d.*	*n.d.*	*n.d.*	-22.7	*n.d.*
HG-08-04	*n.d.*	*n.d.*	1.03	0.12	1.63	0.76	*n.d.*	*n.d.*	*n.d.*	*n.d.*	-21.0	*n.d.*
HG-10-04	*n.d.*	*n.d.*	1.22	0.12	0.25	b.d.	*n.d.*	*n.d.*	*n.d.*	*n.d.*	-22.2	*n.d.*
HG-11-04	*n.d.*	*n.d.*	2.11	0.10	2.68	1.62	*n.d.*	*n.d.*	*n.d.*	*n.d.*	-21.0	*n.d.*
HG-12-04	*n.d.*	*n.d.*	2.64	b.d.	1.57	0.69	*n.d.*	*n.d.*	*n.d.*	*n.d.*	-22.9	*n.d.*
HG-13-04	*n.d.*	*n.d.*	2.67	0.32	0.54	0.70	*n.d.*	*n.d.*	*n.d.*	*n.d.*	-22.8	*n.d.*
HG-14-04	*n.d.*	*n.d.*	0.83	b.d.	0.10	b.d.	*n.d.*	*n.d.*	*n.d.*	*n.d.*	-22.6	*n.d.*
HG-15-04	*n.d.*	*n.d.*	0.83	b.d.	2.51	1.18	*n.d.*	*n.d.*	*n.d.*	*n.d.*	-22.8	*n.d.*
HG-21-04	*n.d.*	*n.d.*	1.18	b.d.	0.17	b.d.	*n.d.*	*n.d.*	*n.d.*	*n.d.*	-22.4	*n.d.*
FG-101-03	7.8	5.7	0.22	0.04	b.d.	b.d.	0.02	0.73	-7.3	-4.4	-22.0	-9.6
FG-110-03	9.2	5.7	0.24	0.04	b.d.	b.d.	0.02	0.94	-7.3	-4.4	-22.0	-11.3
G20-61-03	4.3	6.5	1.72	0.22	b.d.	b.d.	0.11	2.42	-5.7	-4.5	-22.0	-4.1
G20-71-03	4.3	6.5	1.48	0.19	b.d.	b.d.	0.12	2.26	-5.7	-4.5	-21.9	-6.5
G20-81-03	4.1	6.1	1.38	0.18	b.d.	b.d.	0.06	1.76	-6.3	-4.4	-22.0	-6.6
NG-41-03	5.6	5.9	1.71	0.39	0.94	b.d.	0.04	3.55	-6.3	-4.4	-22.0	-6.7
NG-42-03	1.3	6	2.58	0.89	1.31	b.d.	0.04	3.07	-6.2	-4.5	-22.1	-5.3
NG-51-03	5.5	6.4	1.36	0.31	0.65	b.d.	0.09	2.19	-5.9	-4.5	-21.9	-4.2
NG-52-03	4.8	6.1	1.60	0.38	0.94	b.d.	0.07	4.00	-6.2	-4.4	-22.0	-5.9
SG-82-03	3.6	6.5	2.11	0.19	0.46	b.d.	0.10	2.08	-5.7	-4.6	-21.8	-4.5
SG-86-03	4.7	6.1	1.94	0.17	0.34	b.d.	0.06	1.87	-6.1	-4.4	-21.9	-4.5
SG-90-03	4.1	6.5	2.01	0.14	0.31	b.d.	0.10	2.54	-5.7	-4.6	-22.0	-6.3
SG-91-03	9.5	6.6	0.31	0.05	b.d.	b.d.	0.11	1.23	-6.3	-4.6	-22.0	-9.9
TCG-09-04	5.0	5.6	1.27	0.29	0.40	b.d.	0.14	b.d.	-6.4	-3.5	-22.7	-9.9
TCG-27-03	4.0	6.3	0.81	0.16	b.d.	b.d.	0.09	1.00	-6.3	-4.4	-22.5	-10.8
TCG-28-03	5.0	6.4	0.94	0.18	b.d.	b.d.	0.11	1.52	-6.0	-4.4	-22.5	-9.2
TCG-30-03	4.8	5.4	1.01	0.20	0.32	b.d.	0.02	1.73	-6.7	-4.2	-22.5	-8.6
WG-119-03	6.0	6.5	1.82	0.24	b.d.	b.d.	0.11	1.92	-5.7	-4.5	-22.0	-3.7
WG-125-03	8.6	6.4	1.90	0.26	0.33	b.d.	0.09	2.16	-5.8	-4.5	-22.0	-3.1
AVERAGE	*5.3*	*6.2*	*2.09*	*0.29*	*0.88*	*1.11*	*0.08*	*2.06*	*-6.2*	*-4.4*	*-22.5*	*-6.9*
STDEV	*1.9*	*0.3*	*2.54*	*0.28*	*0.94*	*1.07*	*0.04*	*0.80*	*0.5*	*0.2*	*1.8*	*2.6*

Sample code: HG = Highway Glacier; FG = Forkbeard Glacier; G20 = G20 Glacier; NG = Nifhleim Glacier; SG = Sivingavuk Glacier; TCG = Tête des Cirques Glacier; WG = Windy Lake Glacier

n.d. : no data

b.d. : below detection limit

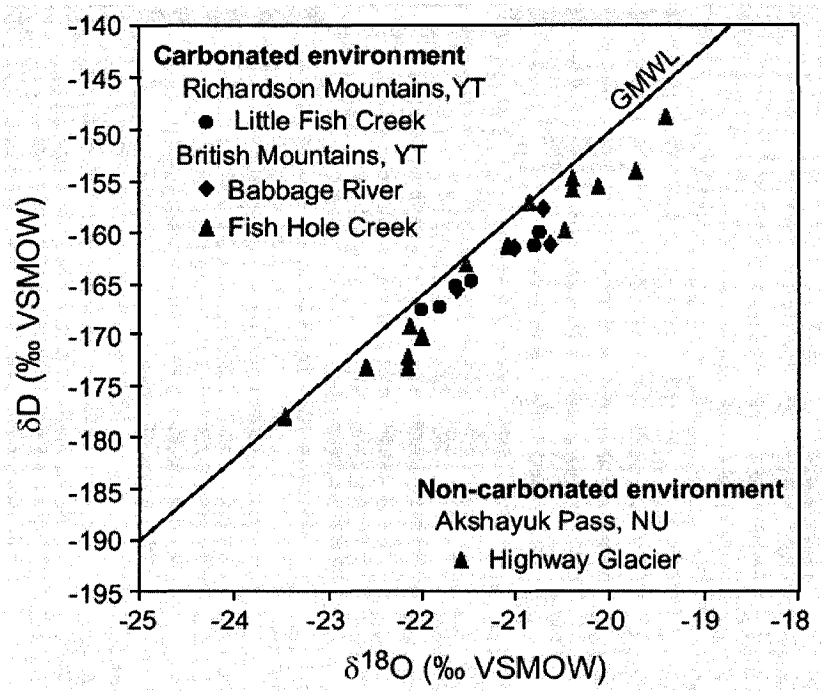

Fig. 6: $\delta^{18}O$ and δD composition of individual ice-layers from the Babbage River, Fish Hole Creek, Little Fish Creek and Highway Glacier aufeis. The global meteoric water line (GMWL) is shown for comparison purposes.

5.2 Mineral precipitates

Mineral precipitates in the form of loose powders were present on the surface of all studied aufeis. The mineralogy of the precipitates collected from the Babbage River, Fish Hole Creek and Little Fish Creek aufeis was determined by powdered X-ray diffraction and calcite was the only mineral present. By contrast, XRD analysis indicated that the mineral precipitates collected on the surface of Highway Glacier aufeis consisted of a mixture of calcite, quartz and gypsum. Strontium isotope measurements ($^{87}Sr/^{86}Sr$) suggest that the source of silicate in the mineral deposits collected at Highway Glacier aufeis is derived from the crystalline bedrock (Fig. 7). The local granitic bedrock has a radiogenic $^{87}Sr/^{86}Sr$ ratio (0.7885 ± 0.0358; $n = 5$) that is considerably higher than the fracture-filling calcites (0.7261 to 0.7409; $n = 2$). The mineral precipitates have $^{87}Sr/^{86}Sr$ ratios averaging 0.7719 ± 0.003 ($n = 2$), similar to the $^{87}Sr/^{86}Sr$ ratio measured in the local bedrock. This suggests that the cryogenic calcite deposits on the surface of Highway Glacier aufeis incorporated an important fraction of silicate derived from the bedrock by glacial erosion, which released silt-sized particles in the glacial meltwaters, or that the calcium that assisted in their precipitation is derived from silicate weathering (e.g. Jacobson et al. 2002; Hosein et al. 2004).

The $\delta^{13}C$ and $\delta^{18}O$ composition of the cryogenic aufeis calcite deposits are presented in Fig. 8. The $\delta^{13}C$ values of cryogenic calcite collected from the Babbage River, Fish Hole Creek and

Little Fish Creek aufeis average -5.1 ± 1.3‰, -2.6 ± 0.4‰ and -4.5 ± 0.1‰ respectively. Those from Highway Glacier aufeis are slightly more depleted, with $\delta^{13}C$ values between -7.6 and -2.8‰. The $\delta^{18}O$ values of cryogenic calcite from the Babbage River and Fish Hole Creek and Little Fish Creek aufeis average -22.2 ± 2.6‰, -23.5 ± 2.6‰ and -26.5 ± 0.2‰ respectively. By contrast, the calcite component of the mineral precipitates from Highway Glacier aufeis have some of the most depleted $\delta^{18}O$ values reported in the literature for cryogenic aufeis calcite deposits, with $\delta^{18}O$ values ranging from -36.3‰ to -32.6‰.

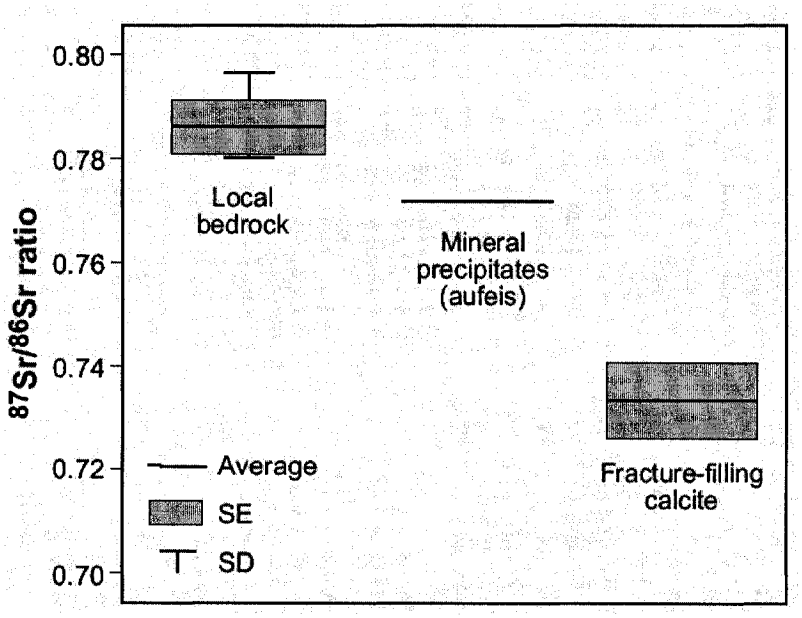

Fig. 7: Radiogenic strontium measurements of the mineral precipitates, local bedrock and fracture-filling calcite sampled in Akshayuk Pass. The $^{87}Sr/^{86}Sr$ ratios were determined by thermal ionization mass spectrometry (TIMS) on a Finnigan Mat Triton at Carleton University. Measured ratios were corrected for mass fractionation using $^{86}Sr/^{88}Sr$ = 0.1194.

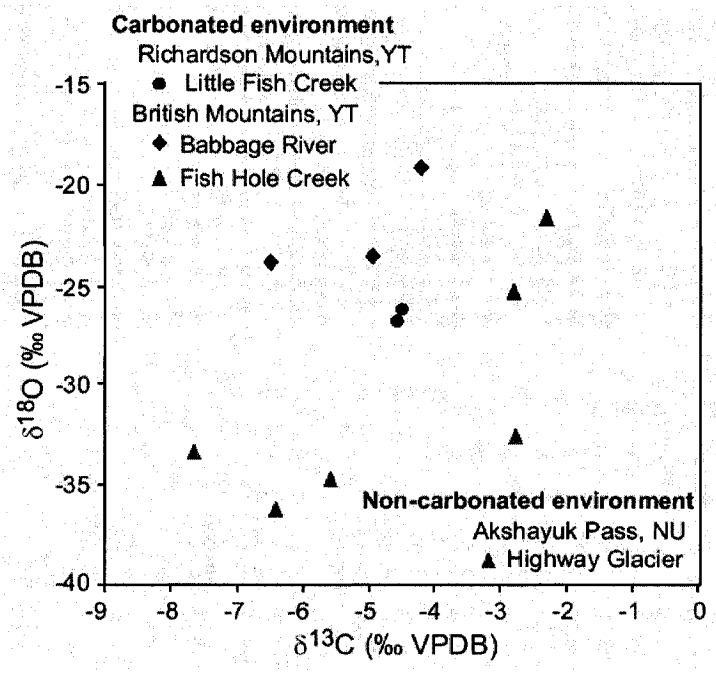

Fig. 8: $\delta^{18}O$ and $\delta^{13}C$ composition of cryogenic calcite collected from the surface of the Babbage River, Fish Hole Creek, Little Fish Creek and Highway Glacier aufeis.

6. Discussion

6.1 Oxygen-18 partitioning and chemical segregation during closed-system freezing

A comparison of the $\delta^{18}O$ composition of cryogenic aufeis calcite collected from carbonated and non-carbonated geological settings in the Canadian Arctic provides some insight into the chemical and isotopic partitioning that occurs during freezing. The $\delta^{18}O$ values of cryogenic aufeis calcite deposits from the Babbage River (-22.2 ± 2.6‰) and Fish Hole Creek (-23.5 ± 2.6‰) aufeis are much more enriched than those from Little Fish Creek aufeis (-26.5 ± 0.2‰) and Highway Glacier aufeis (-34.3 ± 1.6‰). Under most circumstances, the $\delta^{18}O$ of calcite is estimated from the $\delta^{18}O$ of the parent water and temperature at which calcite precipitated. Therefore, the $\delta^{18}O$ composition of the parent water from which the cryogenic aufeis calcite precipitated can be calculated by converting the $\delta^{18}O_{VPDB}$ values of the cryogenic calcite to the VSMOW scale using Coplen's equation:

$$[3]\ \delta^{18}O_{VSMOW} = 1.03091\ \delta^{18}O_{VPDB} + 30.91‰ \quad \text{(Coplen et al. 1983)}$$

and using the fractionation factor for equilibrium exchange of ^{18}O between calcite and water ($\varepsilon^{18}O\ CaCO_3\text{-}H_2O$ at 0°C = 34.4‰ VSMOW; Bottinga 1968). For the Babbage River and Fish Hole Creek aufeis, this gives $\delta^{18}O$ values of -26.3 ± 2.6‰ and -27.7 ± 2.6‰ respectively for the parent water from which the cryogenic calcite precipitated (Fig. 9). However, the cryogenic calcite from Little Fish Creek and Highway Glacier aufeis precipitated from a parent water that had a much more depleted $\delta^{18}O$ composition, -30.8 ± 0.2‰ and -38.8 ± 1.6‰ respectively (Fig. 9). This is quite surprising given that the average $\delta^{18}O$ composition of the individual ice-layers composition the aufeis is much more enriched, with $\delta^{18}O$ values in the -23.5 to -19.4‰ range (Fig. 6).

Figure 10 provides some interesting insights into the possible cause of this discrepancy, where a strong positive relation exists between the average $\delta^{18}O$ composition of the cryogenic aufeis calcite and the average calcite saturation state of the waters feeding the aufeis. This suggests that the $\delta^{18}O$ composition of the cryogenic calcite not only depends on the initial $\delta^{18}O$ composition of the parent water, but that it might also be influenced by the calcite saturation state of the parent water prior to freezing. Based on field observations (Heldmann et al. 2005) and $\delta^{18}O$ stratigraphy of aufeis ice (Clark and Lauriol 1997), which shows a Rayleigh-type

depletion trend within the individual ice layers, the aggradation of aufeis occurs under closed-system conditions. Under such conditions, the freezing of water imparts a progressive depletion in $\delta^{18}O$ in the residual water due to the preferential incorporation of the heavier isotopes in the ice. It should be noted that this progressive ^{18}O depletion trend in the residual water only takes place when freezing is a slow process. In addition to the d18O depletion trend, freezing imparts a concentration of solutes in the residual water, which consequently leads to an increase in the calcite saturation index. Therefore, it can be assumed that the $\delta^{18}O$ composition of calcite precipitating in equilibrium from a water that is highly undersaturated with respect to calcite, such as those from Little Fish Creek and Highway Glacier aufeis, will be depleted over the initial $\delta^{18}O$ composition of its parent water as calcite saturation will only be exceeded in the later stage of freezing.

To verify if the ^{18}O composition of cryogenic calcite is related to the initial calcite saturation state of their parent water, the geochemical partitioning that occurs during freezing was modeled using the PHREEQC computer code (Parkhurst and Appelo 1999). Freezing was simulated by assuming no incorporation of solutes in the ice. During freezing, the solutes concentration and calcite saturation indices progressively increased as the solutes were partitioned in the residual water (Fig. 11). Extreme solutes enrichments (up to 60 times for Ca^{2+}) were found during the late stage of freezing, consistent with the freezing experiments of Hallet (1976) and Killawee et al. (1998). However, once calcite precipitation has occurred, the ionic composition of the solution will deviate from that shown in Fig. 11 as Ca^{2+} and HCO_3^- enrichments will cease. The effect of closed-system freezing on the $\delta^{18}O$ of the residual water was also numerically modeled, but the minor effect of CO_2 and calcite separation on the $\delta^{18}O$ of the residual was neglected. During freezing, the $\delta^{18}O$ composition is progressively depleted due to the Rayleigh fractionation on the residual water. Extreme depletion of up to 12‰ were found when the bulk of the water had frozen.

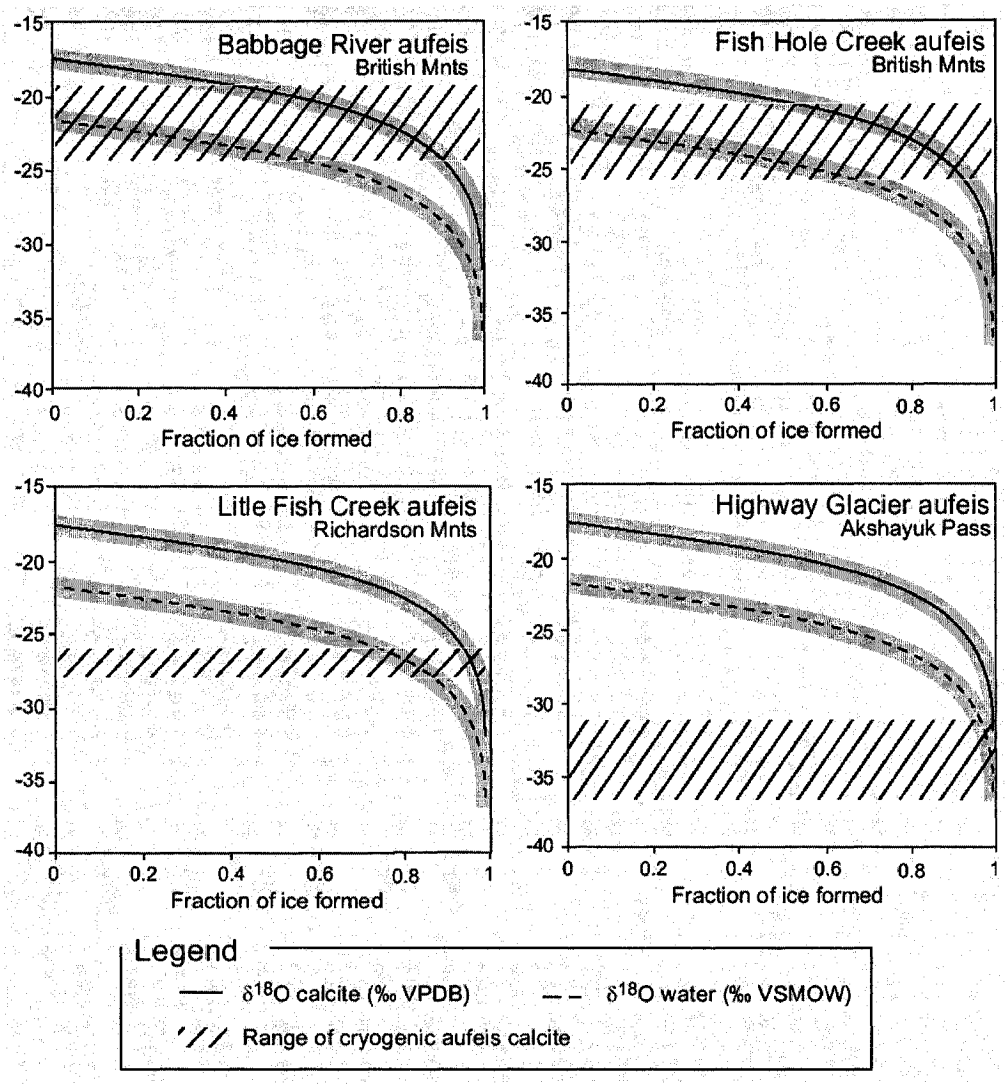

Figure 9: Numerical modeling of the $\delta^{18}O$ evolution of water during closed-system freezing using a Rayleigh-type fractionation. The initial $\delta^{18}O$ value of the water is derived from the average $\delta^{18}O$ composition of the respective aufeis since it represents the average $\delta^{18}O$ composition of the water feeding the individual aufeis. Also shown is the $\delta^{18}O$ composition of calcite precipitating in equilibrium with the evolving water during freezing. The $\delta^{18}O$ composition of calcite was calculated from the $\delta^{18}O$ of the water by correcting for the H_2O-$CaCO_3$ fractionation factor at 0°C (34.4‰; Bottinga 1968) and then converted to the VPDB-scale (Coplen et al. 1983). Dashed area indicates the measured $\delta^{18}O$ range in the cryogenic aufeis calcites.

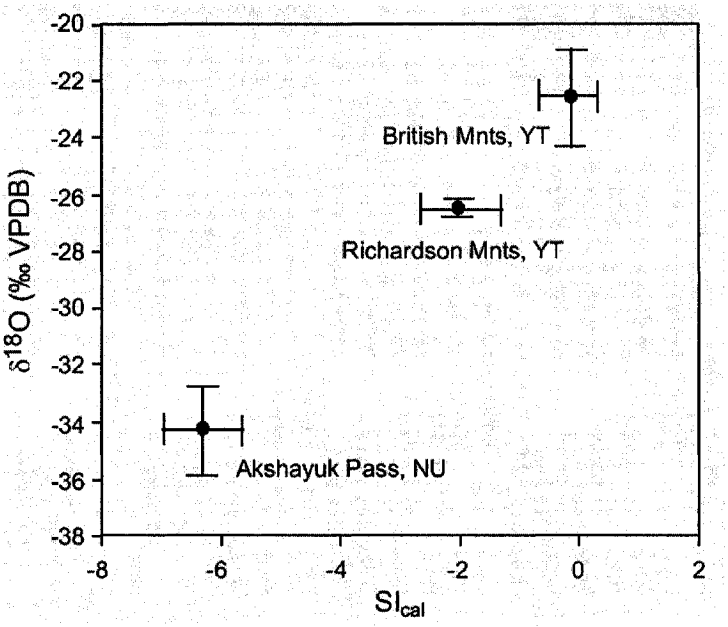

Fig. 10: Diagram showing the relation between the average $\delta^{18}O$ composition of the cryogenic aufeis calcites and the average calcite saturation index of the waters feeding the aufeis.

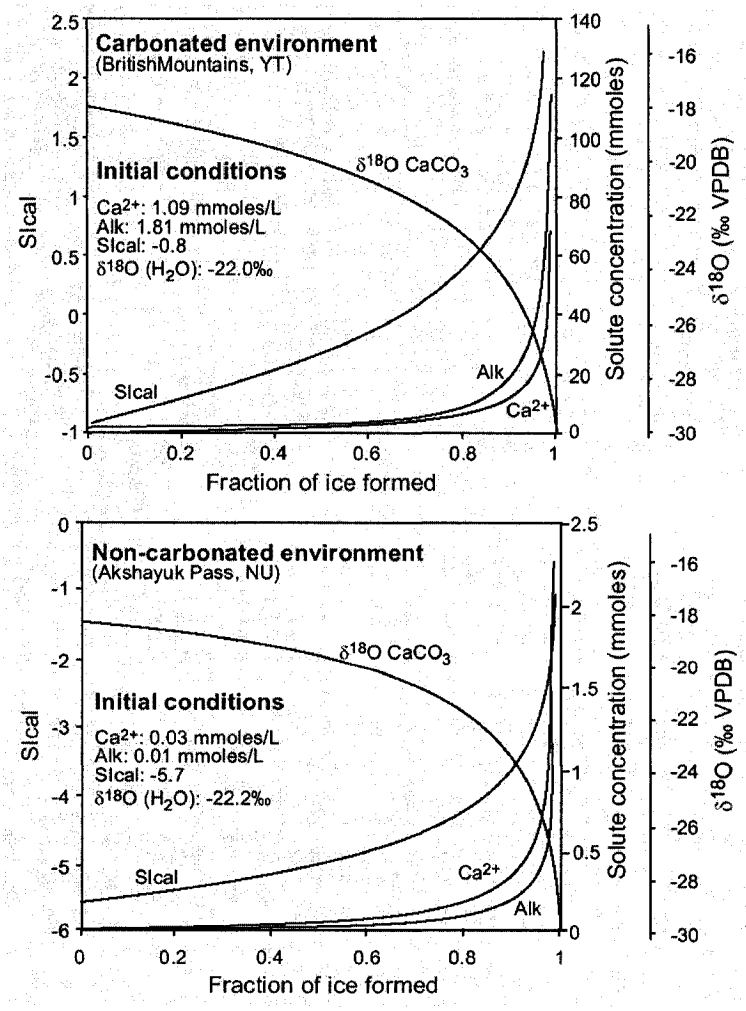

Fig. 11: The evolution of the SIcal and solute concentrations of water collected in the British Mountains (A) and Akshayuk Pass (B) during closed-system freezing as simulated by the PHREECQ hydrogeochemical software (Parkhurst and Appelo 1999). The solubility product of calcite used by PHREECQ at 0°C is $10^{-8.35}$. Also shown is the $\delta^{18}O$ composition of calcite precipitating in equilibrium from these solutions. The $\delta^{18}O$ composition of calcite is derived from the $\delta^{18}O$ of water during freezing under closed-system conditions according to the Rayleigh fractionation and was corrected for the H_2O-$CaCO_3$ fractionation factor at 0°C (34.4‰; Bottinga 1968) and then converted to the VPDB-scale (Coplen et al. 1983).

Based on the PHREEQC hydrogeochemical program, calcite supersaturation (SIcal > 0) is expected to occur in the early to mid stage of freezing for waters that have an initial calcite saturation state close to 0, such as those located in carbonated environments (Fig. 11). This explains why the $\delta^{18}O$ composition of the cryogenic calcite collected from the British Mountains, such as the Babbage River and Fish Hole Creek aufeis, tends to reflect the initial $\delta^{18}O$ composition of their parent water (Fig. 9). But even in carbonated environments, the $\delta^{18}O$ composition of the cryogenic calcite might be slightly depleted with respect to the initial $\delta^{18}O$ composition of the parent water since calcite does not always precipitate instantaneously when supersaturation is reached. Dreybodt et al. (1992) indicated that calcite precipitation tends to occur when the calcite saturation state of the water is in the 0.7 to 1.0 range, due to kinetic inhibition, such as the natural energy barrier preventing calcite nucleation (Berner 1981) or high concentrations of dissolved impurities which might block potential crystal growth sites (Zuddas and Mucci 1994). In non-carbonated environments (i.e. Akshayuk Pass), calcite supersaturation is reached only in the later stage of freezing, which is also when the $\delta^{18}O$ composition of the parent water becomes strongly depleted over its initial $\delta^{18}O$ composition (Fig. 11). Since calcite precipitation does not occur until the calcite saturation state exceeds 0, the $\delta^{18}O$ values of the cryogenic calcite in non-carbonated environments would be highly depleted with respect to the initial $\delta^{18}O$ composition of their parent water due to their low initial calcite saturation index. This was the case for the cryogenic aufeis calcite collected from the surface of Highway Glacier and Little Fish Creek aufeis (Fig. 9).

6.2 Carbon-13 fractionation during closed-system freezing

Previous studies on the $\delta^{13}C$ composition of cryogenic carbonates showed that open system freezing can imparts a severe ^{13}C enrichment in calcite over the bicarbonate-rich solution ($^{13}C_{DIC}$) as a result of either *i*) CO_2 degassing quickly during calcite precipitation which precludes ^{13}C equilibrium between the precipitating carbonate and the escaping CO_2 (Clark and Lauriol 1992); *ii*) continuous escape of CO_2 during calcite precipitation in an open system (Rayleigh-type fractionation; Zak et al. 2004) or *iii*) repeated freeze-thaw events (Socki et al. 2001). However, under closed-system freezing, the ^{13}C fractionation between calcite and the escaping CO_2 is less severe. Zak et al. (2004) numerically modeled the effect of closed-system freezing on the $\delta^{13}C$ composition of cryogenic carbonates based on the assumption that all

evolved CO_2 is kept within the system. The model showed that there was a progressive, but slight increase in the $\delta^{13}C$ composition (up to 4‰) of the cryogenic carbonates over the initial $\delta^{13}C_{DIC}$. Since the aggradation of aufeis occurs under a closed-system condition, the $\delta^{13}C$ of the precipitating cryogenic carbonates should tend to reflect that of the initial $\delta^{13}C_{DIC}$ of the parent water and the temperature at which calcite precipitated.

This was verified by calculating the initial $\delta^{13}C_{DIC}$ value of the parent water from which the cryogenic aufeis calcite precipitated using the following equation:

$$[4]\ \delta^{13}C_{DIC} = \delta^{13}C\ CaCO_3 - \tfrac{1}{2}\ (\varepsilon CO_2\text{-}HCO_3^- + \varepsilon HCO_3^-\text{-}CaCO_3)$$

since carbon is evenly divided between two phases (calcite and CO_2) during calcite precipitation. Using the average $\delta^{13}C$ of the cryogenic aufeis calcite (-4.9 ± 2.1‰), this gives an initial $\delta^{13}C_{DIC}$ value in the -12.5 to -8.4‰ range for the parent water from which the cryogenic aufeis calcite precipitated. These initial $\delta^{13}C_{DIC}$ values are in the same range as the lower end-member of $\delta^{13}C_{DIC}$ measured in the waters feeding the aufeis (-10.6 to -0.1‰; Tables 1 and 2). This indicates that the precipitation of the cryogenic aufeis calcite occurred under closed-system freezing, which precludes an isotopic equilibrium with atmospheric CO_2 (i.e. a $\delta^{13}C_{DIC}$ enrichment of the parent water).

Radiocarbon measurements of cryogenic aufeis calcite collected from Highway Glacier aufeis further supports that they are formed under closed-system conditions. The cryogenic aufeis calcite deposits have ^{14}C activities in the 43.2 to 44.2 pMC range (TO-11968 and TO-11934), while the fracture-filling calcite has a ^{14}C activity of 4.4 pMC (TO-11933), which suggests that it is likely of a hydrothermal origin within the crystalline bedrock (Table 3). However, the ^{14}C activities of the cryogenic calcite deposits should have been near 100 pMC since their production is related to the formation of Highway Glacier aufeis. Aerial photographs and field observations indicate that Highway Glacier aufeis completely melts during the thaw season and rebuilds from subglacial meltwater circulating through a proglacial talik the subsequent winter. Therefore the groundwater that infiltrates in the subglacial environment would have a ^{14}C activity near 100 pMC and will dissolve the near ^{14}C-free fracture-filling calcite. Thus, a stoichiometric dissolution of the fracture-filling calcite with the subglacial meltwater will result in a dilution of the ^{14}C activity of the DIC of the subglacial parent water to

values near 50 pMC. Given that the aggradation of aufeis occurs under closed-system conditions, the ^{14}C activity of the parent water will not re-equilibrate with modern atmospheric CO_2 as was it was observed for the $\delta^{13}C$ of the cryogenic calcites. Therefore, the ^{14}C activity of 43 to 44 pMC measured in the cryogenic calcite deposits suggests that the carbon is derived from a closed-system dissolution of the fracture-filling calcite, followed by closed-system precipitation.

Table 3: Radiocarbon measurements of the cryogenic calcite collected from the surface of Highway Glacier aufeis and fracture-filling calcite.

Location	Type	Latitude	Longitude	^{14}C activity (pMC)	Uncalibrated ^{14}C age	Laboratory number
Highway Glacier	Cryogenic aufeis calcite	66°41.81'N	64°58.67'W	44.2	6560 ± 70	TO-11968
Highway Glacier	Cryogenic aufeis calcite	66°42.13'N	64°59.44'W	43.2	6750 ± 330	TO-11934
Rundell Glacier	Fracture-filling calcite	66°40.34'N	65°01.12'W	4.4	25140 ± 290	TO-11933

Note: The radiocarbon measurements were by accelerator mass spectrometry at IsoTrace Laboratory (University of Toronto). The ^{14}C activities are presented as pMC (percent Modern Carbon) and ^{14}C ages are presented as conventional ^{14}C ages in years BP using Libby's ^{14}C half-life of 5568 years.

7. Conclusion and implications in paleoclimatic studies

In this study the $\delta^{18}O$ and $\delta^{13}C$ composition of cryogenic aufeis calcite in relation to the initial $\delta^{18}O$, $\delta^{13}C_{DIC}$ and chemical composition of the waters feeding aufeis in a carbonated (western Canadian Arctic) and non-carbonated (southern Cumberland Peninsula) environment were examined. Under most circumstances, the $\delta^{18}O$ composition of cryogenic carbonates is estimated from the initial $\delta^{18}O$ composition of the parent water and temperature at which calcite precipitated. However, the $\delta^{18}O$ composition of cryogenic carbonates from a carbonated environment (Babbage River and Fish Hole Creek aufeis) shows a slight depletion over that of the $\delta^{18}O$ of the parent water, while cryogenic carbonates from a non-carbonated environment (Highway Glacier and Little Fish Creek aufeis) show a strong depletion in $\delta^{18}O$ values with respect to that of the initial $\delta^{18}O$ value of the parent water. This discrepancy between the $\delta^{18}O$ of the cryogenic carbonate and that of the parent is attributed to the nature of aufeis growth, the calcite saturation state of the parent water and kinetic inhibitions during carbonate precipitation. Given that the aggradation of aufeis occurs under closed-system freezing of perennial groundwater-fed springs upon exposure to cold air, the freezing of water imparts a progressive depletion in $\delta^{18}O$ in the residual water due to the removal of heavier isotopes into the ice and a

concentration of solutes in the residual water, which leads to an increase in calcite saturation index. Therefore, carbonate that precipitate in equilibrium from water that has a low calcite saturation index will have a highly depleted $\delta^{18}O$ composition over that of the initial $\delta^{18}O$ values of the parent water. By contrast, the $\delta^{13}C$ composition of the cryogenic aufeis calcite is not affected by solute partitioning during closed-system freezing, and tends to reflect that of the initial $\delta^{13}C_{DIC}$ value of the parent water.

These findings can possibly be extended to secondary carbonates in polar regions formed by intense evaporation, such as the calcareous crusts formed on the underside of clasts within the active layer (Bunting and Christensen 1978). In such case, the $\delta^{18}O$ signature of the carbonate in non-carbonated environments would be enriched by several permil over that of the $\delta^{18}O$ composition of the parent water since evaporation is an highly fractionating process that leads to a progressive increase in $\delta^{18}O$ in the residual water.

In light of the evidence presented in this study, care must be taken when interpreting the $\delta^{18}O$ signature preserved in secondary carbonates in polar regions since the $\delta^{18}O$ composition of their parent water might have been modified by secondary processes (i.e. freezing or evaporation) prior to calcite being precipitated. As a result, the $\delta^{18}O$ composition of secondary carbonates cannot easily be used in conjunction with Dansgaard global $\delta^{18}O$ -T°C relation to derive local mean annual air temperatures unless clear details about the chemical and isotopic composition of the parent waters are known. However, the $\delta^{13}C$ composition of secondary carbonates that precipitated under closed-system conditions can allow insights into the different water sources contributing to carbonate precipitation.

Acknowledgments

This work was funded by Natural Science and Engineering Research Council of Canada (NSERC) discovery grants to B. Lauriol and I.D. Clark, by an Ontario Graduate Scholarship (OGS) and Northern Scientific Training Program (NSTP) grant to D. Lacelle. We would like to thank W. Abdi, G. St-Jean, and P. Middlestead (G.G. Hatch Laboratory, University of Ottawa), B. Cousens (strontium analyses, Carleton University) and M. Alewany for their technical assistance. The radiocarbon measurements were made at IsoTrace (University of Toronto). J.F. Dion, J. Clark and C. Duchesne provided valuable field assistance. Special thanks to B. Etooangat and P. Smiley (Parks Canada) for providing logistical support during our stay in

Auyuittuq National Park (research permit number ANP 2004-001). This manuscript benefited from the constructive comments made by Dr. I. Fairchild and an anonymous reviewer.

References

Akerman, H.J., 1982. Studies on naledi (icing) in West Spitsbergen. Fourth Canadian Permafrost Conference, Calgary, Canada. National Research Council of Canada, Ottawa, 189-202.

Berner, R.A., 1981. Kinetics of weathering and diagenesis. In: Lasaga, A.C. and Kirkpartick, R.J. (Eds), Kinetics of Geochemical Processes, Reviews in Mineralogy, vol. 8. Mineralogical Society of America, p. 111-132.

Blake, W. Jr., 2005. Holocene carbonate precipitates on Precambrian bedrock in the High Arctic: age and potential for paleoclimatic information. Geografiska Annaler 87A, 175-192.

Bottinga, Y., 1968. Calculation of fractionation factors for carbon and oxygen in the system calcite–carbon dioxide-water. Journal Physical Chemistry 72, 800-808.

Bunting, B.T., Christensen, L., 1978. Micromorphology of calcareous crusts from the Canadian High Arctic. Geologiska Foreningens Forhandlinger 100, 361-367.

Clark, I.D., Lauriol, B., 1992. Kinetic enrichment of stable isotopes in cryogenic calcites. Chemical Geology 102, 217-228.

Clark, I.D., Lauriol, B., 1997. Aufeis of the Firth River basin, northern Yukon, Canada: Insights into permafrost hydrogeology and karst. Arctic and Alpine Research 29, 240-252.

Clark, I.D., Lauriol, B., Harwood, L., Marschner, M., 2001. Groundwater contributions to discharges in a permafrost setting, Big Fish River, N.W.T., Canada. Arctic, Antarctic and Alpine Research 33, 62-69.

Clark, I.D., Lauriol, B., Marschner, M., Sabourin, N., Chauret, Y., Desrochers, A., 2004. Endostromatolites from permafrost karst, Yukon Canada: paleoclimatic proxies for the Holocene thermal hypsithermal. Canadian Journal of Earth Sciences 41, 387-399.

Coplen, T.B., Kendall, C., Hopple, J., 1983. Comparison of isotope reference samples. Nature 302, 236.

Courty, M.A., Marlin, C., Dever, L., Tremblay, P., Vachier, P., 1994. The properties, genesis and environmental significance of calcitic pendants from the high Arctic (Spitsbergen). Geoderma 61, 71-102.

Dansgaard, W., 1964. Stable isotopes in precipitation. Tellus 16, 436-468.

Dansgaard, W., 1982. A new Greenland deep ice core. Science 218, 1273-1277.

Dreybodt, W., Buhmann, D., Michaelis, J., Usdowski, E., 1992. Geochemically controlled calcite precipitation by CO_2 out-gassing: field measurements of precipitation rates in comparison to theoretical predictions. Chemical Geology 97, 285-294.

Dyke, A.S., Andrews, J.T., Miller, G.H., 1982. Quaternary geology of Cumberland Peninsula, Baffin Island, District of Franklin. Geological Survey of Canada, Memoir 403, 32p.

Environment Canada., 2004. Canadian Climate Normals 1971–2001. Canada Atmospheric Environment Service, Minister of Supply and Services Canada, Ottawa, Ontario, Canada.

Epica Community Members. 2004. Eight glacial cycles from an Antarctic ice core. Nature 429, 623-628.

Fairchild, I., Bradly, L. and Spiro, B., 1993. Carbonate diagenesis in ice. Geology 21, 901-904.

Fisher, D.A., Koerner, R.M., Bourgeois, J.C., Zielinski, G., Wake,C., Hammer, C.U., Clausen, H.B., Gundestrup, N., Johnsen, S., Goto-Azuma, K., Hondoh, T., Blake, E., Gerasimoff, M., 1998. Penny Ice Cap cores, Baffin Island, Canada, and the Wisconsinan Foxe dome connection: Two states of Hudson Bay ice cover. Science 279, 692-695.

Forman, S.L., Miller, G., 1984. Time-dependant soil morphologies and pedogenic processes on raised beaches, Broggerhalwoya, Spitsbergen, Svalbard archipelago. Arctic and Alpine Research 16, 381-393.

Hall, D.K., 1980. Mineral precipitation in North Slope river icings. Arctic 33, 343-348.

Hallet, B., 1976. Deposits formed by subglacial precipitation of $CaCO_3$. Geological Society of America Bulletin 87, 1003-1015.

Heldmann, J.L., Pollard, W.H., McKay, C.P., Andersen, D.T., Toon, O.B., 2005. Annual development cycle of an icing deposit and associated perennial spring activity on Axel Heiberg Island, Canadian High Arctic. Arctic, Antarctic and Alpine Research 37, 127-135.

Hillaire-Marcel, C., Soucy, J.M., Cailleux, A., 1979. Analyse isotopique de concrétions sous-glaciaire de l'inlandsis laurentidiens et teneur en oxygène 18 de la glace. Canadian Journal of Earth Sciences 16, 1494-1498.

Hossein, R., Arn, K., Steinmann, P., Adatte, T., Follmi K.B. 2004. Carbonate and silicate weathering in two presently glaciated, crystalline catchments in the Swiss Alps. Geochemica et Cosmochimica Acta 68, 1021-1033.

Jacobson, A.D., Blum, J.D., Chamberlain, C.P., Poage, M.A., Sloan, V.F. 2002. Ca/Sr and Sr isotope systematics of a Himalayan glacial chronosequence: Carbonate versus silicate weathering rates as a function of landscape surface age. Geochemica et Cosmochimica Acta 66, 13-27.

Killawee, J.A., Fairchild, I.J., Tison, J.L., Janssens, L., Lorrain, R., 1998. Segregation of solutes and gases in experimental freezing of dilute solutions: implication for natural glacier systems. Geochimica Cosmochimica Acta 62, 3637-3655.

Lauriol, B., Cinq-Mars, J., Clark, I.D., 1991. Les naleds du nord Yukon : Localisation, genèse et fonte. Permafrost and Periglacial Processes 2, 225-236.

Lauriol, B., Ford, D.C., Cinq-Mars, J., Morris, W.A., 1997. The chronology of speleothem deposition in northern Yukon and its relationships to permafrost. Canadian Journal of Earth Sciences 34, 902-911.

Marlin, C., Dever, L., Vachier, P., Courty, M-A., 1993. Variations chimiques et isotopiques de l'eau du sol lors de la reprise en gel d'une chouche active sur pergélisol continu (Presqu'ile de Brogger, Svalbard). Canadian Journal of Earth Sciences 30, 806-813.

Nakai, N., Wada, H., Kiyosu, Y., Takimoto, M., 1975. Stable isotope studies on the origin and geological history of water and salts in the Lake Vanda area, Antarctica. Geochemical Journal 9, 7-24.

Norris, D.K., 1975. Geology, Bell River, Yukon Territory and Northwest Territories. Map 1519A, scale 1 :250,000. Geological Survey of Canada, Energy Mines and Resources, Ottawa, Canada.

Norris, D.K., 1977. Geology, Blow River and Davidson Mountains, Yukon Territory, District of Mackenzie. Map 1516A, scale 1 :250,000. Geological Survey of Canada, Energy Mines and Resources, Ottawa, Canada.

Parkhurst, D.L., Appelo, C.A.J., 1999. User's Guide to PHREEQC (Version 2): A Computer Program for Speciation, Batch-Reaction, One-Dimensional Transport, and Inverse Geochemical Calculations. U.S. Geological Survey Water-Resources Investigations Report 99-4259, 310 p.

Pollard, W.H., 1983. A study of seasonal frost mounds, North Fork Pass, northern interior Yukon Territory. Unpublished PhD Thesis, University of Ottawa.

Pollard, W.H., 2005. Icing processes associated with High Arctic perennial springs, Axel Heiberg Island, Nunavut, Canada. Permafrost and Periglacial Processes 16, 51-68.

Sharp, M., Tison, J.L., Fierens, G., 1990. Geochemistry of subglacial calcites: implications for the hydrology of the basal water film. Arctic and Alpine Research 22, 141-152.

Socki, R.A., Romanek, C.S., Gibson Jr., E.K., Golden, D.C., 2001. Terrestrial aufeis formation as martian analog: Clues from laboratory-produced C-13 enriched cryogenic carbonate. In,

Lunar and Planetary Science XXXII abstract #2032. Lunar and Planetary Institute, Houston, TX.

Souchez, R.A., Lemmens, M., 1985. Subglacial carbonate deposition – an isotopic study of present-day case. Palaeogeography, Palaeoclimatology and Palaeoecology 51, 357-364.

Swett, K., 1974. Calcrete crusts in an arctic permafrost environment. American Journal of Sciences 274, 1059-1063.

St-Jean, G., 2003. Automated quantitative and isotopic (^{13}C) analysis of dissolved inorganic carbon and dissolved organic carbon in continuous flow using a total carbon organic carbon analyser. Rapid communications in mass spectrometry 17, 419-428.

Tolsikhin, N.I., Tolsikhin, O.N., 1976. Groundwater and surface water in the permafrost region. Canada Inland Waters Directorate, Water Resources Branch, Ottawa. Technical Bulletin No.97, 1-27.

Van Everdingen, R.O., 1974. Groundwater in permafrost regions of Canada. In: Permafrost Hydrology, Proceedings o f a Workshop Seminar, Canadian National Committee, International Hydrological Decade, Environment Canada, Ottawa.

Van Everndingen, R.O., 1988. Perennial discharge of subpermafrost groundwater in tow small drainage basins, Yukon, Canada. In: Proceedings, 5th International Conference on Permafrost, August 1988, Trondheim, Norway, p. 639–643.

Van Everdingen, R.O., Allen, H., 1983. Ground movements and dendrogeomorphology in a small icing area of the Alaska Highway, Yukon, Canada. In: Proceedings, 4th International Conference on Permafrost, July 1983, Fairbanks, USA, p. 1292–1297.

Zak, K., Urban, J., Cilek, V., Hercman, H., 2004. Cryogenic cave calcite from several Central European caves: age, carbon and oxygen isotopes and a genetic model. Chemical Geology 206, 119-136.

Zuddas, P., Mucci, A., 1994. Kinetics of calcite precipitation from seawater. I. A classical chemical kinetics description for strong electrolyte solutions. Geochemical Cosmochimica Acta 58, 4353-4362.

Manuscript 2

Origin, age and paleo-environmental significance of carbonate precipitates from a granitic environment, Akshayuk Pass, southern Baffin Island, Canada.

Lacelle, D., Lauriol, B. and Clark, I.D.

Canadian Journal of Earth Science (accepted)

Abstract

This study documents the discovery of calcite crusts on the upper surface of clasts within morainic complexes in Akshayuk Pass, southern Cumberland Peninsula (Baffin Island), a region underlain by granitic and gneissic rocks of the Precambrian Canadian Shield. Strontium isotope ratios ($^{87}Sr/^{86}Sr$) indicate that the major source of calcium is derived from the local dissolution of fracture-filling calcite and a minor source is derived from silicate weathering. The calcite crusts have $\delta^{13}C$ values between 1.6 and 12.0‰ and $\delta^{18}O$ values in the –13.0 and –7.9‰ range. These values are highly enriched over the predicted isotopic values based on the $\delta^{13}C_{DIC}$ and $\delta^{18}O$ of the local water and temperature at which calcite precipitation occurred. The isotopic enrichments are attributed to a combination of both equilibrium and kinetic evaporation and were verified experimentally. The series of evaporative experiments indicate that kinetic evaporation produces a far-from-equilibrium isotope effect on both the $\delta^{13}C$ and $\delta^{18}O$ composition of the precipitating calcite (^{13}CKIE $\varepsilon CaCO_3$-CO_2 between 20.2 and 40.5‰; ^{18}OKIE between 0.6 and 9.1‰). Based on these results, the formation of the calcite crusts is ascribed to the evaporation of stagnating ephemeral lakes and streams following the retreat of valley glaciers. Given the > 1500 m difference in heights between the highland and the valley, the katabatic winds originating from the Penny Ice Cap can act as a catalyst to increase the rate of evaporation. In addition, radiocarbon dating of ten of these crusts yielded Holocene ages (7640 cal BP to modern). These results suggest that the maximum expansion of Holocene valley glacier in Akshayuk Pass, previously thought to have occurred during the Little Ice Age, is probably much older.

1. Introduction

The presence of carbonate deposits, in the form of crusts and / or pendants, is common in polar regions. Carbonate crusts, or pendants, have been observed in permafrosted limestone environments on the underside of clasts within soil profiles (Washburn 1969; Swett 1974; Bunting and Christensen 1978; Forman and Miller 1984; Marlin et al. 1993; Courty et al. 1994), on the upper surface of clasts and bedrock (Ford et al. 1970; Hallet 1976; Hillaire-Marcel et al. 1979; Souchez and Lemmens 1985; Sharp et al. 1990; Fairchild et al. 1993) within fissures in bedrock outcrops (Clark et al. 2004) and in freezing caves (Lauriol et al. 1997). In this study, the presence of white calcite crusts found within morainic complexes in Akshayuk Pass, a glacial valley on southern Cumberland Peninsula (Baffin Island, Nunavut) is documented (Fig. 1). These calcite crusts are unlike most of the others reported in the literature as they are found in an area of granitic bedrock. Akshayuk Pass has a geology consisting primarily of granitic rocks of the Precambrian Canadian Shield, medium to coarse-grained gneiss and quartz monzonites (Dyke et al. 1982). Carbonate bedrock outcrops are absent from the area, however calcite is present as a fracture-filling mineral.

To our knowledge, the only other occurrence of carbonate precipitates in an area of crystalline bedrock in the Arctic is on glacially sculptured Precambrian granitic and gneissic bedrock in east-central Ellesmere Island, Nunavut (Blake 1999, 2005). Besides the geological setting, an additional unifying characteristic between the Akshayuk Pass and the Ellesmere Island calcite crusts is their stable isotope ratios of carbon ($^{13}C/^{12}C$) and oxygen ($^{18}O/^{16}O$), which are among the highest measured in carbonate precipitates in cold regions ($\delta^{13}C$ up to 12.0‰; $\delta^{18}O$ up to 7.9‰). Although the stable isotope ratios of carbon and oxygen are commonly used to determine the processes that initiated the precipitation of carbonates, the origin of the Ellesmere Island carbonate crusts remains unknown. Biotic, cryogenic and weathering mechanisms have all been advanced by Blake (2005) to explain their origin. However, an interesting aspect of the Ellesmere Island carbonate deposits is that they provided information regarding the timing of Neoglacial deglacation in the area. Radiocarbon ages obtained from the carbonate crusts led Blake (2005) to suggest that they provide minimum ages of the exposed ice-sculpted surface on which they occur. Recent work by Waragai (2005) on calcrete crusts precipitated on the surface of moraines of the Batura glacier, northern Pakistan, further illustrate the potential of using ^{14}C dating to obtain minimum ages of moraines or surfaces on which the

carbonate crusts precipitated. Given these recent advances, determining the origin and age of the Akshayuk Pass calcite crusts is important since the origin of such deposits are poorly understood, especially from a granitic landscape, and can provide reliable information regarding the glacial history of the region in which they occur.

The objectives of this study is to determine the origin and age of the calcite crusts discovered on the surface of moraines in Akshayuk Pass and to provide information regarding the Holocene glacial chronology of valley glaciers in this area. These objectives were reached by using a combination of microscopic (SEM), mineralogical (XRD and XRF) and isotopic ($\delta^{13}C$, $\delta^{18}O$, $^{87}Sr/^{86}Sr$, ^{14}C) methods. To verify the reliability of the radiocarbon ages of the calcite crusts, the geochemical composition and the stable isotope ratios of oxygen, hydrogen and carbon of the waters draining the study area were also analyzed to determine the mechanism (physico-chemical or biological) and to assess the isotopic condition (equilibrium or kinetic) under which the calcite crusts precipitated. In addition, to account for the highly enriched $^{13}C/^{12}C$ and $^{18}O/^{16}O$ values of the carbonate crusts, a series of laboratory experiments were performed to shed light on the probable enrichment mechanism.

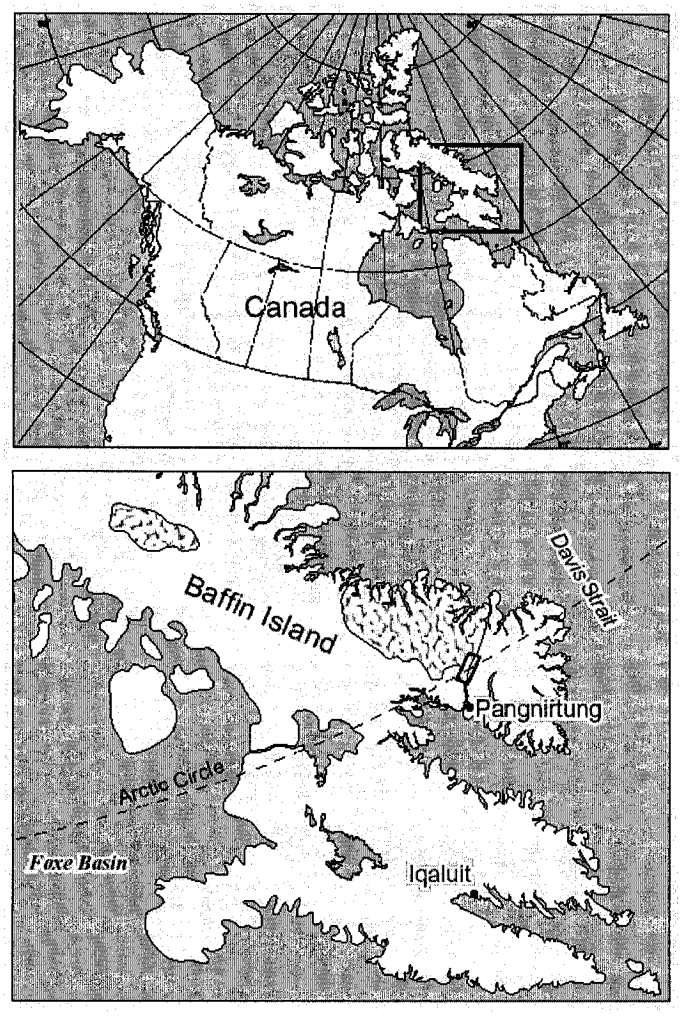

Figure 1: Map showing location of Akshayuk Pass, southern Baffin Island, NU.

2. Study area and glacial history

Akshayuk Pass (66°44'N; 65°00'W) is a 98 km long U-shaped glacial valley incised into the Penny highlands on southern Cumberland Peninsula (NU), and is occupied by the Weasel and Owl rivers (Fig. 2). Elevation in the Pass ranges from sea level at North Pang Fjord and South Pang Fjord to 500 m a.s.l. at Summit Lake. The climate in Akshayuk Pass is part of the polar maritime regime and is highly variable due to the presence of the Penny Ice Cap in the highlands. The climate recorded at the nearest meteorological station, the hamlet of Pangnirtung, reports a mean annual air temperature of –10.4 °C (January T °C: –28 °C; July T °C: 7 °C) and total annual precipitation amounts to nearly 400 mm (Environment Canada 2004). Vegetation in Akshayuk Pass ranges from very patchy and open on the slopes to lush tundra meadows near the flood plain. Arctic shrubs such as dwarf birch, willow, heather, and blueberry form a continuous carpet in sheltered valleys, while tussocks of grasses and sedges grow in less favourable areas.

The modern landscape of Akshayuk Pass is dominated by active alpine glaciation with numerous cirque glaciers and the 6000 km^2 Penny Ice Cap found at an elevation of > 1900 m a.s.l. Lichenometric studies (Davis 1985; Mercier 2004) indicate that the moraines presently visible beyond the terminus of modern glaciers in Akshayuk Pass have formed during the Little Ice Age, in phase with the Holocene thermal minimum on southern Cumberland Peninsula (Bradley 1990; Overpeck et al. 1997; Kerwin et al. 2004; Miller et al. 2005). For most of the alpine glaciers, ice-cored lateral moraines form a series of distinct parallel ridges and lichen density cover indicates that the outer ridges are considerably older than the inner ones (Davis 1985). This suggests that the Little Ice Age expansion could have been more restricted for some of the glaciers. In the foreland of the moraines, outwash streams, ephemeral lakes and streams as well as glacial and fluvio-glacial features, such as kettle lakes and kames, are observed.

The last major glaciation that took place on southern Cumberland Peninsula occurred during the Late Wisconsin and is referred to as the Foxe Glaciation. The ice filling Akshayuk Pass during the Foxe Glaciation probably came from an expansion of outlet glaciers from the Penny Ice Cap that merged with the expanding Laurentide Ice Sheet in the Foxe Basin and Cumberland Sound region. Cosmogenic exposure dating from the Duval moraines, a major moraine system located in the highland, suggests either a continuous ice cover from 24 000 to 9000 BP or multiple ice-cover events during the same period (Bierman et al. 1999; Davis et al. 1999). Large-scale retreat of the Penny Ice Cap and adjoining alpine glaciers began around 10 000 BP

(Marsella et al. 2002) as a result of the abrupt climatic amelioration causing rapid drawdown and calving in the fjords of Akshayuk Pass. According to Miller (1973), the recession of the ice cap from Akshayuk Pass was completed by 9000 BP.

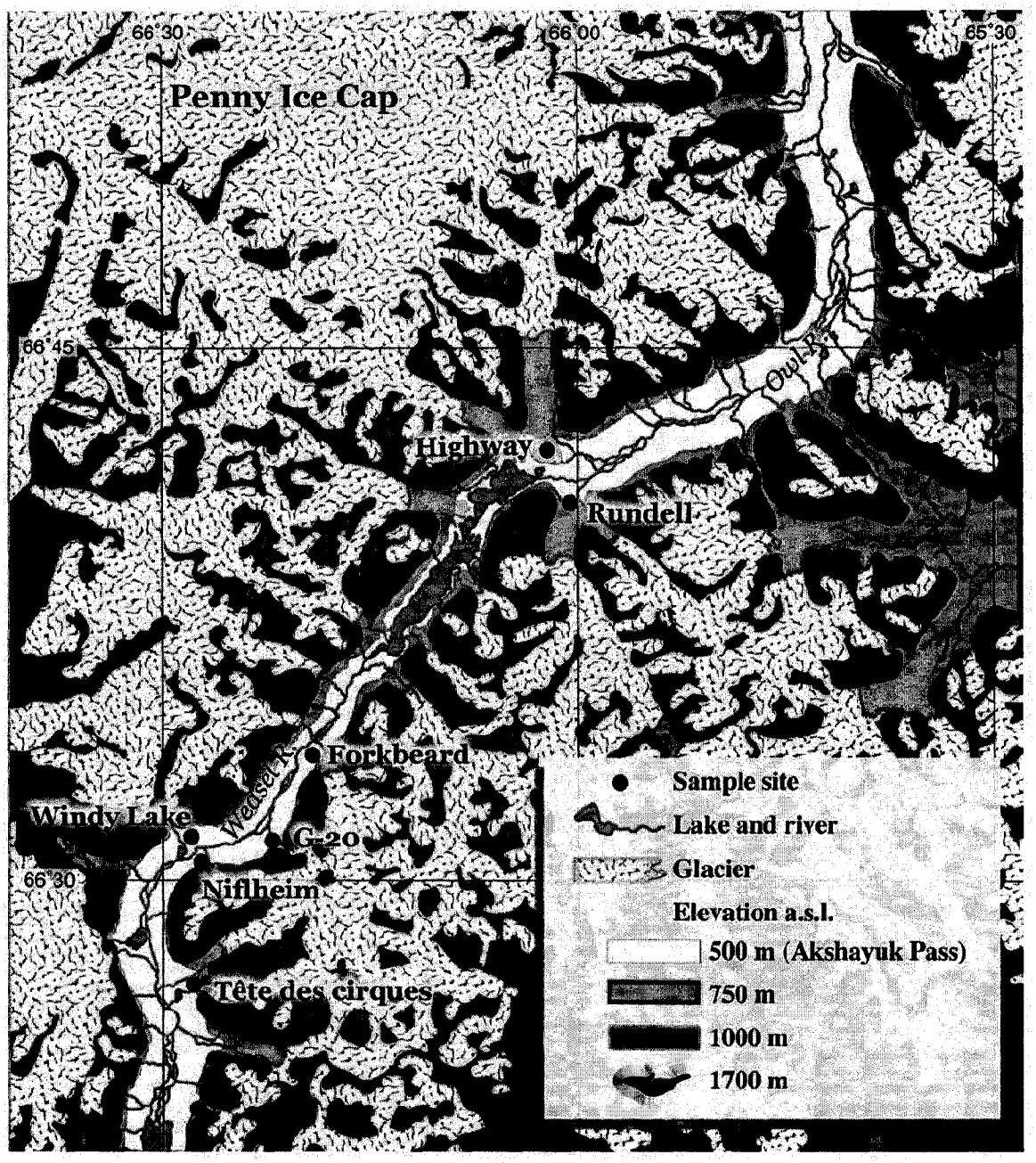

Figure 2: Location map of sites sampled in Akshayuk Pass, southern Baffin Island, NU.

3. Sampling and analytical methods

3.1 Carbonate precipitates

The carbonate crusts, which are up to 5 mm thick, were collected from the upper surface of clasts within the morainic complex of five alpine glaciers in Akshayuk Pass (Tête des Cirques, Windy Lake, G-20, Nifhleim and Forkbeard glaciers) using a chisel and a hammer (Fig. 2). Samples of fracture-filling calcite were collected near Rundell Glacier on an opportunity basis. The carbonate crusts are not restricted to the lee-side of the clasts (Fig. 3), as is often the case for subglacially precipitated calcite deposits (Hallet 1976; Souchez and Lemmens 1985; Sharp et al. 1990; Fairchild et al. 1993). Furthermore, none of the carbonate crusts in Akshayuk Pass is striated, suggesting that they have not been over-ridden by ice since depostion as they could not have resisted glacial abrasion (Watts 1981; Arocena and Hall 2003). The carbonate crusts in Akshayuk Pass are present not only on the surface of moraines; but on the surface of large boulders at the bottom of talus slopes, and on occasion, on the surface of clasts in abandoned stream channels (Fig. 3).

The mineral composition of the carbonate deposits was determined by powdering the samples, which were then mixed with acetone and spread over a glass slide and analyzed using a Phillips PW-1800 x-ray diffractometer with a step size of 0.02 and scanning speed of 0.4 seconds per step to record the XRD spectra. The chemical composition of the carbonate deposits was determined from X-ray fluorescence (XRF) measurements on powdered samples using a Phillips PW-2400 spectrometer.

The micro-morphologies of the carbonate deposits were examined under scanning electron microscope (SEM; JEOL 6400) equipped with an electron dispersion spectrometer (EDS) at Carleton University. The samples were mounted onto an aluminum stub using doubled-sided carbon tape and then sputter-coated with gold for 60 seconds prior to examination under SEM.

The $^{18}O/^{16}O$ and $^{13}C/^{12}C$ ratios of the carbonate deposits were determined on CO_2 gas produced by reacting the powdered calcite with 100% phosphoric acid (H_3PO_4) in glass septum vials for 24 hours at 25 °C. The evolved CO_2 gas was analyzed in continuous flow using a Gas Bench II interfaced with a Finnigan Mat Delta$^+$ XP isotope mass spectrometer at the G.G. Hatch Isotope Laboratory, University of Ottawa. Stable isotope data for C and O are expressed in δ-notation, where δ represents the parts per thousand difference of $^{13}C/^{12}C$ and $^{18}O/^{16}O$ in a sample

with respect to the Vienna Pee-Dee Belemnite standard (VPDB). Analytical reproducibility is ± 0.15‰ for both isotopes.

The strontium isotope ratio ($^{87}Sr/^{86}Sr$) of the carbonate deposits and local bedrock was measured to provide insights into the potential source of calcium (Ca) to the calcite crusts because the chemical properties of strontium are similar to calcium (i.e. radius, charge and electron configuration). Consequently, strontium can easily substitute for calcium in carbonate mineral during their formation and act as a proxy for the source of calcium. The $^{87}Sr/^{86}Sr$ ratios were determined by thermal ionization mass spectrometry (TIMS) at Carleton University. The samples, dissolved in 2.5N HCl, were pipetted into a 14-ml Bio-Rad borosilicate glass chromatography column containing 3.0 ml of Dowex AG50-X8 cation resin. The purified strontium was then loaded onto a single Ta filament with H_3PO_4 and was run at filament temperatures of 1480-1520°C on a Finnigan Mat Triton solid source mass spectrometer. Measured ratios were corrected for mass discrimination using exponential normalization to $^{86}Sr/^{88}Sr = 0.1194$. Results are expressed relative to a mean value of $^{87}Sr/^{86}Sr = 0.71025$ in NIST standard SRM-987. The analytical reproducibility is ± 0.0001.

Radiocarbon measurements of the carbonate crusts and fracture-filling calcite were made at IsoTrace (University of Toronto) by accelerator mass spectrometry (AMS) to determine the possible sources of carbon and the age of the calcite crusts. In all cases, the material used for dating originated from individual crusts. The ^{14}C activities are presented as pMC (percent Modern Carbon) and the radiocarbon ages are presented as calibrated ^{14}C yr BP (cal BP) using Libby's ^{14}C half-life (5568 years).

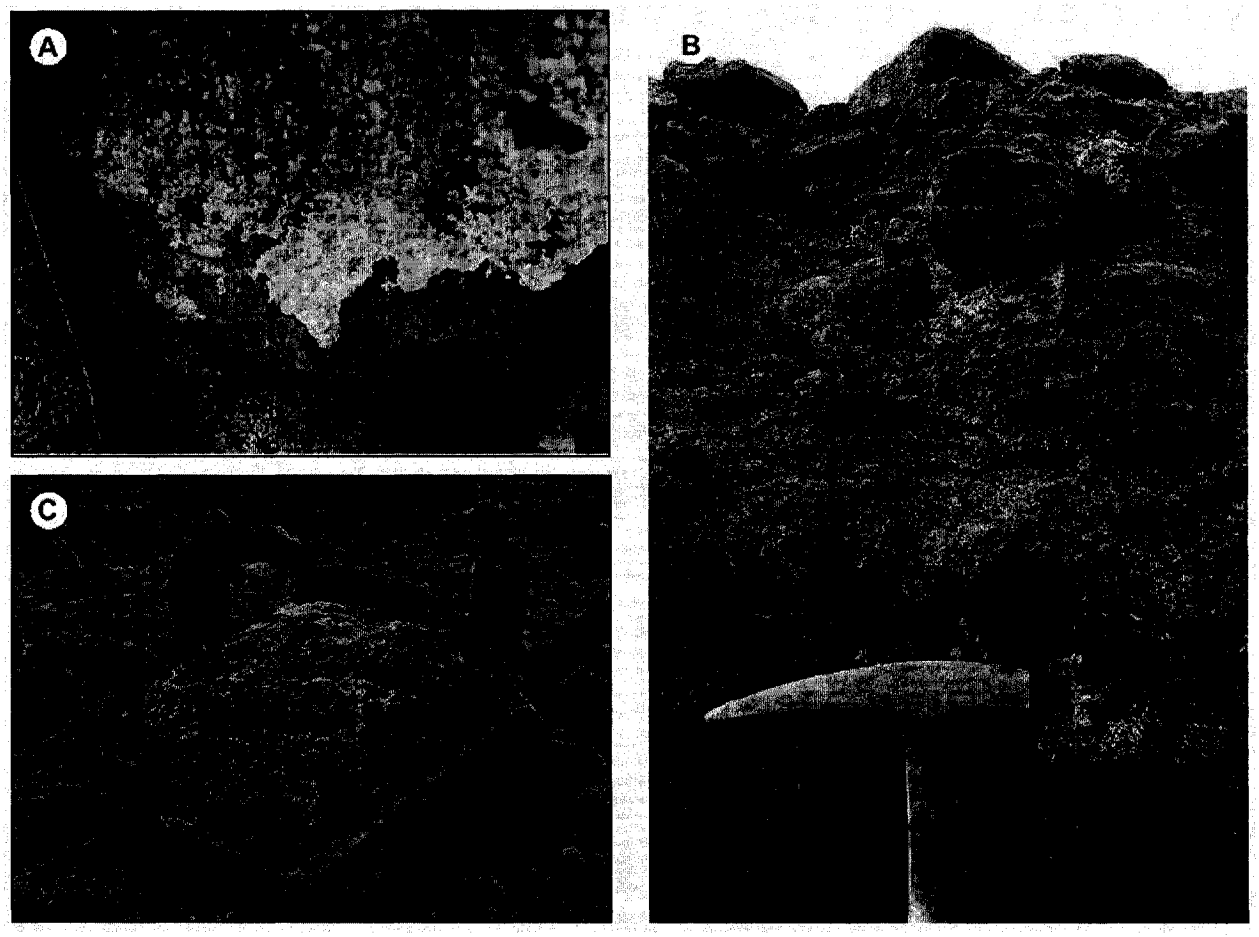

Figure 3: Photographs of calcite crusts sampled in Akshayuk Pass. A) Calcite crusts collected from the upper surface of a granitic clast. B) Calcite crusts on the surface of a large supra-glacial boulder at Rundell Glacier; C) Calcite crusts on the surface of clasts in an abandoned stream channel.

3.2 Surface waters

Glacial meltwater samples from Tête des Cirques, Windy Lake, G-20, Nifhleim, Forkbeard and Rundell glaciers outwash streams were collected daily during the month of July in 2003 and 2004. Single samples from non-glacial streams located near the hamlet of Pangnirtung and from non-glacial tributaries of the Owl River were also collected for comparison purposes.

In 2003, the pH was determined in the field using an Oakton pH meter 3^{+}. In 2004, pH measurements were made back in the laboratory using a Fisher Accumet 610A pH meter. Water samples for cations analysis were field filtered (0.45μm pore diameter) and collected in 20 ml pre-rinsed polyethylene bottles, with subsequent acidification using ultra-pure nitric acid. Filtered, unacidified samples were collected for anions analysis in 20 ml pre-rinsed polyethylene bottles. Major cations were analyzed by Inductively Coupled Plasma Atomic Emission Spectroscopy (ICP-AES). The anions were analyzed using a Dionex DX-100 ion chromatograph. The mean charge balance error for the glacial meltwaters and non-glacial streams was 21% and 14% respectively. These high charge balance errors are attributed to the low concentrations of solutes in the sampled waters (average TDS < 5 mg/L), which are close to the detection limits of the instruments, resulting in greater errors in the measurements.

Water samples for the measurement of the stable isotope ratios of oxygen and hydrogen were collected unfiltered in 20 ml polyethylene bottles. The $^{18}O/^{16}O$ ratio of water samples was measured on CO_2 equilibrated with the water at 25 °C (analytical reproducibility of ± 0.1‰). The D/H ratio was measured on H_2 equilibrated with the water at 25 °C using a Pt based catalyst (analytical reproducibility of ± 1.5‰). Both stable isotope measurements were made on the same sample using a Gas Bench II interfaced with a Finnigan Mat Delta XL mass spectrometer at the G.G. Hatch Laboratory. Results are presented using the δ-notation ($\delta^{18}O$ and δD), where δ represents the parts per thousand differences for $^{18}O/^{16}O$ or D/H in a sample with respect to Vienna Standard Mean Ocean Water (VSMOW).

Filtered water samples were collected unpreserved in 40 ml glass amber bottles for the determination of dissolved inorganic carbon (DIC) and its stable isotope ratio ($^{13}C/^{12}C_{DIC}$). The DIC concentrations and $^{13}C/^{12}C_{DIC}$ ratio in the water samples were determined on a TIC-TOC analyser model OI-1010 interfaced to a Finnigan Mat Delta^{+} isotope ratio mass spectrometer at the G.G. Hatch Laboratory following the wet oxidation technique described by St-Jean (2003). Phosphoric acid (5% H_3PO_4) was added to the water sample to convert the DIC to CO_2 gas. The

amount of CO_2 gas released was measured by a non-dispersive infrared detector calibrated to quantitatively measure DIC released through acidification of the water sample. The DIC concentration data was normalized using internal standards and the analytical precision is ± 0.002 ppm. The evolved CO_2 gas was then carried by a continuous He flow to the mass spectrometer for $^{13}C/^{12}C_{DIC}$ analysis. Stable isotope data for C is expressed in δ-notation, where δ represents the parts per thousand difference of $^{13}C/^{12}C$ in a sample with respect to the Vienna Pee-Dee Belemnite standard (VPDB). Analytical precision is ± 0.2‰.

4. Results

4.1 Mineralogy, micromorphology and isotopic composition of carbonate precipitates

The presence of calcite as the dominant mineral in the crusts collected from Tête des Cirques, Nifhleim, G-20, Windy Lake and Forkbeard glaciers and from the fracture-filling calcites was confirmed by X-ray diffraction analyses. The chemical composition of the calcite crusts, fracture-filling calcites and local bedrock are presented in Table 1. Normative analysis of metals as oxides in the calcite crusts shows them to be composed mostly of CaO (up to 61%), with trace amounts of MgO, Al_2O_3, Na_2O and Fe_2O_3 (< 1%). By comparison, the local bedrock is dominated by SiO_2 (64%), Al_2O_3 (15%) and Fe_2O_3 (6%), with minor amounts of K_2O, CaO and Na_2O (< 5%). The fracture-filling calcites are also composed mostly of SiO_2 (43%), followed by CaO (21%) and Al_2O_3 (14%). Assuming that the loss-on-ignition results represents CO_2, then the calcite crusts are composed of up to 43% of calcite, the remaining are impurities of silicate derived from the bedrock.

The calcite crusts and fracture-filling calcites have distinct micro-morphologies (Fig. 4). SEM images show that the calcite crusts are composed of microcrystalline calcite crystals (< 4μm). By contrast, the fracture-filling calcites tend to develop large (> 10μm) platelet calcite crystals, suggestive of calcite formed within the restricted width of a thin fracture. These crystal morphologies are highly suggestive of an inorganic origin for the formation of the calcite deposits.

The $\delta^{18}O$ and $\delta^{13}C$ composition of the calcite crusts and fracture-filling calcites are presented in Fig. 5 and a statistical summary is given in Table 2. The calcite crusts collected from Tête des Cirques, Nifhleim, G-20, Windy Lake and Forkbeard glaciers (n = 64) have $\delta^{18}O$ values ranging between –13.0 and –7.9‰ and $\delta^{13}C$ values in the 1.6 to 12.0‰ range, which are

among the highest $\delta^{13}C$ values measured in secondary carbonate deposits in the Canadian Arctic. By contrast, the fracture-filling calcites ($n = 3$) have much lower $\delta^{18}O$ and $\delta^{13}C$ values, averaging $-18.5 \pm 0.9‰$ and $-16.7 \pm 0.1‰$ respectively.

A further distinction between the calcite crusts and fracture filling calcites is observed in their radiocarbon measurements (Table 3). The calcite crusts provided ^{14}C ages in the 7640 ± 70 cal BP to modern range ($n = 10$), while the analysis of one sample of fracture-filling calcite yielded a ^{14}C activity of 4.4 pMC, indicating that the latter are much older, and likely of a hydrothermal origin within fractures in the crystalline bedrock. The minor radiocarbon activity in the fracture filling calcite could also be attributed to contamination during exposure in the surface environment of the moraine deposit.

Strontium isotope data of the calcite crusts, fracture-filling calcite and local bedrock are shown in Fig. 6 and summarized in Table 2. Both the fracture-filling calcites ($^{87}Sr/^{86}Sr$ between 0.7261 and 0.7409; $n = 2$) and the calcite crusts ($^{87}Sr/^{86}Sr$ between 0.7235 and 0.7544; $n = 5$) have much lower strontium isotope ratios than the local granitic bedrock ($^{87}Sr/^{86}Sr$ between 0.7804 and 0.7965; $n = 5$).

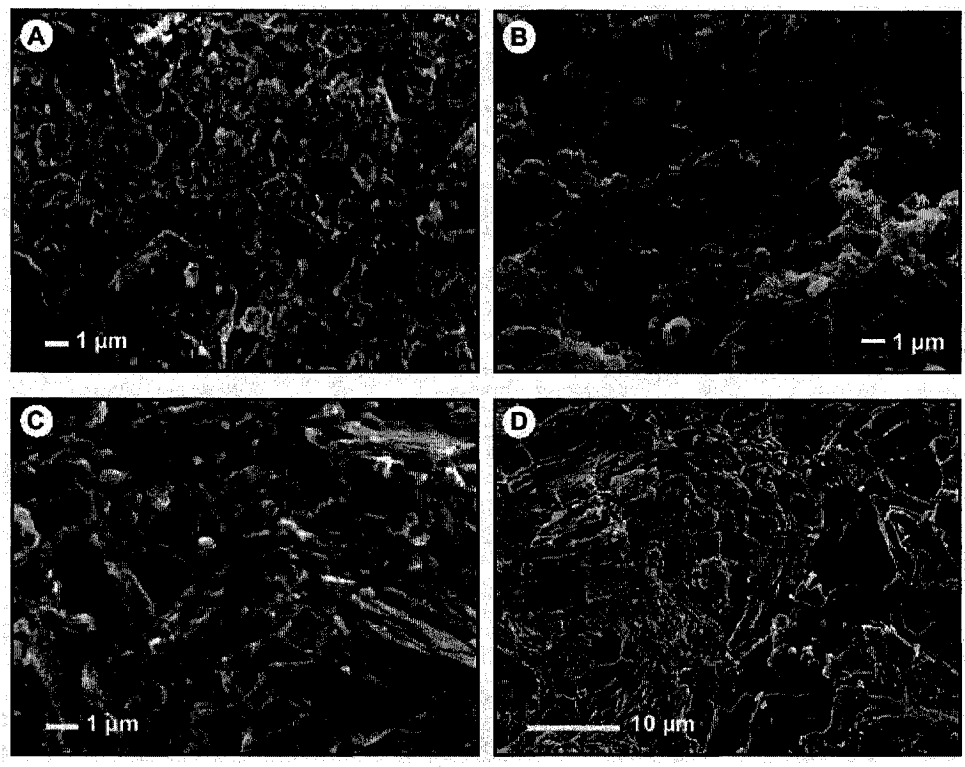

Fig. 4: Scanning electron images (SEM) of calcite crusts (a – b) and fracture-filling calcite (c – d) collected in Akshayuk Pass, southern Baffin Island, NU.

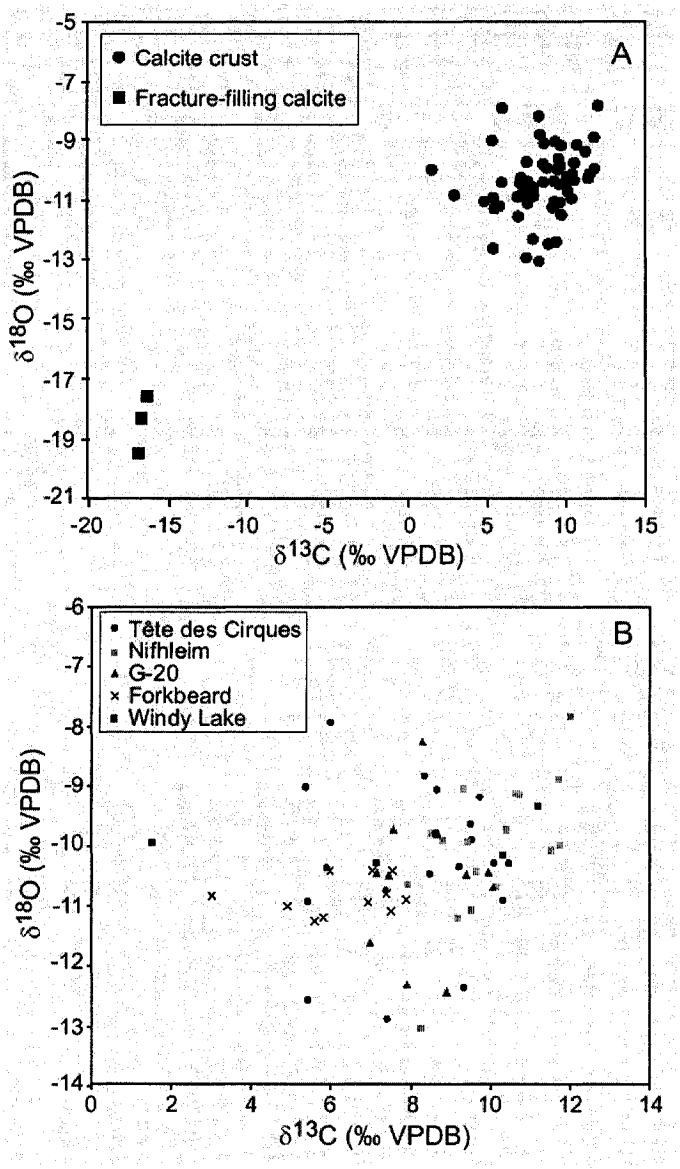

Figure 5: A) Stable isotope ratios of carbon and oxygen of calcite crusts and fracture-filling calcite collected in Akshayuk Pass. B) Close-up of the isotopic composition (^{13}C and ^{18}O) of calcite crusts collected from the various sites.

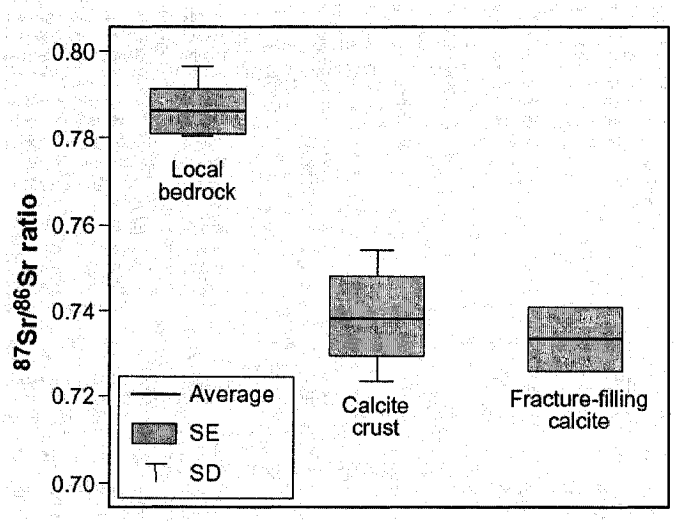

Figure 6: Strontium isotope ($^{87}Sr/^{86}Sr$) results of local bedrock, fracture-filling calcite and calcite crusts collected in Akshayuk Pass, southern Baffin Island, NU.

Table 1. Major (%) and trace elements (ppm) of the local bedrock, fracture-filling calcites and calcite crusts from Akshayuk Pass, Nunavut, Canada, as measured by X-ray fluorescence (XRF) on a Phillips PW-2400 spectrometer.

	Major elements (%)											Trace elements (ppm)										Ratio
Sample	SiO_2	Al_2O_3	CaO	K_2O	MgO	MnO	Na_2O	P_2O_5	Fe_2O_3	TiO_2	LOI	Ba	Ce	Co	Cr	Ga	La	Ni	Pb	Rb	Sr	Sr:Ca
Local bedrock																						
TCG-07-03	67.1	14.6	3.4	4.4	1.3	0.1	2.8	0.2	5.3	0.7	--	1087	81	14	26	19	27	<10	21	138	146	0.004345
TCG-10-03	65.4	13.6	3.2	4.4	1.6	0.1	2.7	0.2	6.2	1.0	--	1245	78	17	24	18	35	<10	20	153	135	0.004206
NG-44-03	64.2	16.8	3.7	5.5	1.1	0.1	3.1	0.2	4.5	0.6	--	1536	80	10	16	21	24	<10	26	177	169	0.004592
NG-46-03	64.7	15.2	3.4	5.1	1.5	0.1	3.0	0.2	5.2	0.8	--	1577	74	14	21	17	45	<10	23	157	154	0.004570
Fracture-filling calcite																						
RG-18-04	43.6	14.1	21.2	0.8	0.2	0.0	0.9	0.0	0.5	0.1	21.6	143	16	<10	32	<10	10	36	10	32	137	0.000646
Calcite crusts																						
RG-38-04	0.8	0.1	61.0	0.0	0.6	0.0	0.2	0.0	0.1	0.0	43.1	<10	34	<10	12	<10	<10	<10	<10	<10	135	0.000221
NG-46-03	8.5	3.4	51.6	0.9	0.4	0.0	0.7	0.0	0.5	0.1	36.8	279	38	<10	26	<10	30	<10	<10	30	772	0.001496

[1]Sample code: NG = Nifhleim glacier, RG = Rundell glacier, TCG = Tete des Cirques glacier

Table 2. Statistical summary of isotopic composition of calcite crusts, fracture-filling calcite and local bedrock from Akshayuk Pass, Nunavut, Canada.

	n	Minimum	Maximum	Average	SD
Calcite crusts					
$\delta^{13}C$ (‰ VPDB)	64	1.6	12.0	8.3	2.2
$\delta^{18}O$ (‰ VPDB)	64	–13.0	–7.9	–10.4	1.1
$\delta^{18}O$ (‰ VSMOW)	64	17.6	22.8	20.3	1.1
$^{87}Sr/^{86}Sr$	5	0.7235	0.7544	0.7387	0.012
Fracture-filling calcite					
$\delta^{13}C$ (‰ VPDB)	3	–16.8	–16.6	–16.7	0.1
$\delta^{18}O$ (‰ VPDB)	3	–19.5	–17.5	–18.5	0.9
$\delta^{18}O$ (‰ VSMOW)	3	10.9	13.0	11.9	0.9
$^{87}Sr/^{86}Sr$	2	0.7261	0.7409	0.7335	0.0105
Local bedrock					
$^{87}Sr/^{86}Sr$	5	0.7804	0.7965	0.7885	0.0068

Note: $\delta^{18}O_{VSMOW}$ values converted using the following equation, $\delta^{18}O_{VSMOW} = 1.02354\ \delta^{18}O_{VPDB} + 30.92$ (Coplen et al. 1983)

Table 3. Radiocarbon measurements for calcite crusts and fracture-filling calcite in Akshayuk Pass, Nunavut, Canada.

Location	Type	Latitude	Longitude	$\delta^{18}O$ (‰)	$\delta^{13}C$ (‰)	^{14}C activity (pMC)	Uncalibrated ^{14}C age BP	Calibrated age (cal BP, 1 σ)	Calibrated median age	Laboratory number
Tête des Cirques	crust	66°26.77'N	65°27.81'W	–9.6	9.5	113.6	Modern			TO-11965
Tête des Cirques	crust	66°26.77'N	65°27.92'W	–9.9	9.5	103.7	Modern			TO-11964
Tête des Cirques	crust	66°26.78'N	65°27.92'W	–8.8	8.4	76.7	2130 ± 50	2040-2155	2095	TO-11966
Windy Lake	crust	66°30.59'N	65°29.35'W	--	--	81.3	1660 ± 50	1120-1625	1375	TO-11973
Niflheim	crust	66°30.91'N	65°26.28'W	–10.0	11.7	53.6	5000 ± 370	5430-6190	5810	TO-11243
Niflheim	crust	66°30.77'N	65°26.30'W	–10.6	7.9	46.6	6130 ± 420	6555-7425	6990	TO-11244
G-20	crust	66°30.97'N	65°23.83'W	–12.4	8.9	93.9	500 ± 350	265-745	505	TO-11970
G-20	crust	66°30.87'N	65°23.59'W	–9.7	7.6	42.3	6910 ± 70	7475-7800	7640	TO-11969
Forkbeard	crust	66°33.74'N	65°19.15'W	–10.4	7.5	69.2	2920 ± 60	2970-3160	3065	TO-11972
Forkbeard	crust	66°33.79'N	65°19.24'W	–11.0	4.9	62.7	3750 ± 390	3620-4625	4125	TO-11971
Rundell	vein	66°40.34'N	65°01.12'W	–19.5	-16.8	4.4	25140 ± 290			TO-11933

Note: Calibrated ages were calculated using CALIB Radiocarbon Calibration Program version 5.0 (Stuiver et al. 2005; Stuiver and Reimer 1993).

4.2 Chemical and isotopic composition of surface waters

The geochemical composition of the glacial meltwaters and non-glacial streams are presented in Table 4. The glacial meltwaters have the highest concentrations of solutes (up to 390 μeq/L) and are characterized by a Ca-Mg-SO_4 facies and pH in the 5.4 to 6.6 range. The log pCO_2 of the glacial meltwaters average –4.4 ± 0.2, which, according to Ek (1964), are typical of subglacial meltwaters collected near the snout of a glacier. These low log pCO_2 values suggest that weathering occurred under closed-system water-saturated conditions and that the acidity available was totally consumed by weathering of the bedrock. The glacial meltwaters are also highly under-saturated with respect to calcite mineral (SIcal < –5). The non-glacial streams have a much lower dissolved solids concentration (up to 170 μeq/L) but display a similar geochemical facies as the glacial meltwaters. However, the non-glacial streams have log pCO_2 averaging –3.8 ± 0.1 (Table 4), indicating that it is freely exchanging CO_2 with the atmosphere as they are close to equilibrium with the partial pressure of the atmosphere (log pCO_2 = –3.5 atm). The non-glacial streams have a calcite saturation index that is also highly under-saturated (SIcal < –5), characteristic of surface waters draining non-carbonated bedrock.

The $\delta^{18}O$ and δD composition of glacial meltwater and non-glacial streams is shown in Fig. 7 and can be compared to those from the ice core record from the Penny Ice Cap (67°15N; 65°46'W; 1900 m a.s.l.). The 1965-1995 $\delta^{18}O$ values from the Penny Ice Cap range from –29.3‰ in winter to –20.3‰ in summer (average $\delta^{18}O$: –24.2 ± 1.5‰; Fisher et al. 1998), and, due to its proximity to the study area, reflect the isotopic composition of the local precipitation in the area. The glacial meltwaters show a strong attenuation of the seasonal isotopic variations observed in modern precipitation with $\delta^{18}O$ values averaging –22.2 ± 0.3‰ (n = 22), but is similar to the modern average $\delta^{18}O$ composition of Penny Ice Cap and therefore represents a mixture a snow-derived meltwater and rainfall during surface flow. The $\delta^{18}O$ composition of the non-glacial streams ranges from –22.7‰ to –19.9‰ (n = 16), reflecting mostly rainfall values.

The $\delta^{13}C_{DIC}$ for the glacial meltwaters and non-glacial streams are presented in Table 4. The streams have invariant $\delta^{13}C_{DIC}$ values (–12.2 to –10.3‰; n = 10) as a result of continuous oxidation of the local vegetation, while the $\delta^{13}C_{DIC}$ values of the glacial meltwaters range from –11.3‰ to –3.1‰ (n = 22), due to varying degree of exposure to atmospheric CO_2 during surface flow on the vegetation-free moraines.

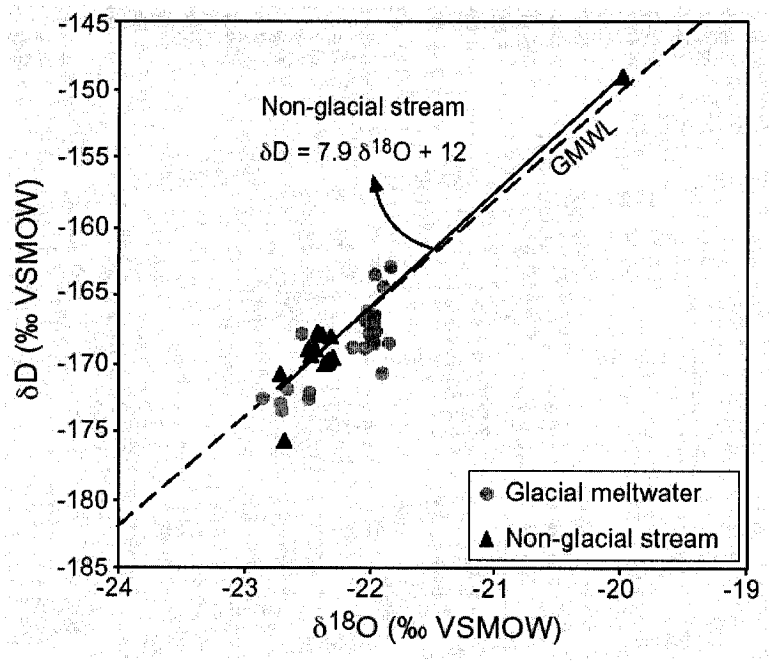

Figure 7: Stable isotope ratios of hydrogen and oxygen of glacial meltwaters and non-glacial streams. The non-glacial streams samples plot along a slope of 7.9 ($\delta D = 7.9\ \delta^{18}O + 7.9$). GMWL defines the Global Meteoric Water Line ($\delta D = 8\ \delta^{18}O + 10$; Craig1961).

Table 4. Geochemical (μeq/L) and isotopic (‰) data from surface waters in Akshayuk Pass.

Sample[1]	T°C	pH	Ca	Mg	Na	Cl	SO_4	HCO_3	SIcal	log pCO_2[2]	$\delta^{13}C_{DIC}$	$\delta^{18}O$	d[3]
Glacial meltwater													
FG-101-03	7.8	5.7	10.9	3.2	b.d	19.4	15.1	0.4	–7.3	–4.4	–9.6	–22.0	7.9
FG-110-03	9.2	5.7	12.1	3.1	b.d	12.1	19.6	0.4	–7.3	–4.4	–11.3	–22.0	7.1
G20-61-03	4.3	6.5	85.8	18.1	b.d	11.3	50.3	1.8	–5.7	–4.5	–4.1	–22.0	7.3
G20-71-03	4.3	6.5	73.9	15.6	b.d	23.0	47.0	1.9	–5.7	–4.5	–6.5	–21.9	6.3
G20-81-03	4.1	6.1	68.9	14.4	b.d	26.2	36.7	1.0	–6.3	–4.4	–6.6	–22.0	9.9
NG-41-03	5.6	5.9	85.3	32.3	41.0	48.7	74.0	0.7	–6.3	–4.3	–6.7	–22.0	7.5
NG-42-03	1.3	6.0	128.6	73.1	57.0	58.2	64.0	0.6	–6.2	–4.5	–5.3	–22.1	8.2
NG-51-03	5.5	6.4	67.9	25.2	28.4	6.0	45.7	1.6	–5.9	–4.5	–4.2	–21.9	4.4
NG-52-03	4.8	6.1	79.8	31.3	40.8	22.9	83.3	1.1	–6.2	–4.4	–5.9	–22.0	7.7
SG-82-03	3.6	6.5	105.2	15.5	19.8	8.6	43.3	1.7	–5.7	–4.6	–4.5	–21.8	11.7
SG-86-03	4.7	6.1	96.9	13.8	14.9	6.0	38.9	0.9	–6.1	–4.4	–4.5	–21.9	10.5
SG-90-03	4.1	6.5	100.3	11.7	13.4	29.1	52.9	1.6	–5.7	–4.6	–6.3	–22.0	12.3
SG-91-03	9.5	6.6	15.5	3.9	b.d	16.4	25.7	1.8	–6.3	–4.6	–9.9	–22.0	9.0
TCG-06-04	5.1	6.1	59.8	22.0	11.4	16.6	43.4	n.d.	n.d.	n.d.	n.d.	–22.7	8.2
TCG-07-04	4.5	6.1	52.7	20.0	10.7	17.1	39.9	n.d.	n.d.	n.d.	n.d.	–22.9	10.2
TCG-08-04	4.2	6.0	62.4	23.2	15.7	9.1	47.1	n.d.	n.d.	n.d.	n.d.	–22.7	8.8
TCG-09-04	5.0	5.6	63.3	23.4	17.6	23.6	b.d.	2.3	–6.4	–3.5	–9.9	–22.7	9.5
TCG-27-03	4.0	6.3	40.6	13.5	b.d	5.1	20.7	1.5	–6.3	–4.4	–10.8	–22.5	7.6
TCG-28-03	5.0	6.4	46.8	14.9	b.d	7.7	31.6	1.8	–6.0	–4.4	–9.2	–22.5	12.4
TCG-30-03	4.8	5.4	50.5	16.5	13.9	14.4	36.0	0.3	–6.7	–4.2	–8.6	–22.5	7.2
WLG-119-03	6.0	6.5	90.9	20.1	b.d	13.8	40.0	1.8	–5.7	–4.5	–3.7	–22.0	9.4
WLG-125-03	8.6	6.4	9.5	21.2	14.3	17.8	45.1	1.4	–5.8	–4.5	–3.1	–22.0	8.3
AVERAGE	*5.3*	*6.2*	*64.0*	*19.8*	*23.0*	*18.8*	*42.9*	*1.1*	*–6.2*	*–4.4*	*–6.9*	*–22.2*	*8.7*
SD	*1.9*	*0.3*	*32.6*	*14.2*	*14.5*	*13.2*	*16.7*	*0.7*	*0.5*	*0.2*	*2.6*	*0.3*	*1.9*
Non-glacial streams													
PG-01-04	7.2	6.0	13.5	b.d.	30.1	13.3	0.9	n.d.	n.d.	n.d.	n.d.	–20.0	10.7
OR-21-04	8.7	6.1	51.9	12.1	15.3	18.0	39.7	4.8	–6.0	–3.7	–11.8	–22.3	8.8
OR-22-04	9.2	6.3	49.2	12.1	15.6	45.3	39.0	6.3	–5.7	–3.8	–11.4	–22.3	10.4
OR-23-04	9.4	6.1	48.7	11.8	13.7	25.1	39.7	4.8	–6.0	–3.7	–11.2	–22.3	8.8
OR-24-04	9.1	6.0	48.2	11.7	12.6	13.9	35.0	4.6	–6.1	–3.7	–11.1	–22.4	11.3
OR-25-04	9.5	6.1	20.4	b.d.	6.9	10.3	39.4	5.4	–6.3	–3.7	–10.6	–22.4	11.1
OR-27-04	9.8	5.4	45.7	11.1	9.8	10.0	2.1	1.3	–7.3	–3.6	–12.2	–22.4	10.6
OR-28-04	10.1	6.1	25.9	b.d.	7.4	14.0	36.7	6.1	–6.1	–3.6	–10.3	–22.5	10.3
OR-30-04	9.5	6.0	55.5	12.9	13.8	16.5	39.7	6.0	–5.9	–3.5	–10.5	–22.4	8.9
OR-31-04	9.9	6.1	50.1	11.8	10.6	9.9	39.0	5.7	–5.9	–3.7	–10.4	–22.3	8.8
AVERAGE	*9.3*	*6.0*	*41.5*	*11.9*	*13.6*	*16.2*	*32.3*	*5.0*	*–6.1*	*–3.7*	*–11.1*	*–21.9*	*10.1*
SD	*0.8*	*0.2*	*14.4*	*0.5*	*6.2*	*10.3*	*14.5*	*1.4*	*0.5*	*0.1*	*0.6*	*1.1*	*1.1*

[1]Sample code: FG = Forkbeard glacier, G20 = G-20 glacier, NG = Nifhleim glacier, SG = Sivingavuk glacier, TCG = Tete des Cirques glacier, WLG = Windy Lake glacier, PG = Pangnirtung, OR = Owl river

[2]Partial pressure of CO_2 determined from pH and HCO_3^- measurements.

[3]d calculated as: d excess = $\delta D - 8 * \delta^{18}O$ (Dansgaard 1964).

n.d = no data; b.d. = below detection limit

5. Origin of calcite crusts

5.1 Sources of calcium

Since strontium can easily substitute for calcium during carbonate precipitation, the strontium isotope data provides insights into the potential calcium sources for the formation of the calcite crusts. In Akshayuk Pass, the amount of calcium contributed from the dissolution of the fracture-filling calcite versus calcium released by the weathering of the local bedrock can be estimated by the following mixing equation:

[1] $Ca^{2+}_{CaCO3}(\%) = ({}^{87}Sr/{}^{86}Sr_{CaCO3} - {}^{87}Sr/{}^{86}Sr_{LB}) \cdot Sr/Ca_{LB} / (({}^{87}Sr/{}^{86}Sr_{CaCO3} - {}^{87}Sr/{}^{86}Sr_{LB}) \cdot Sr/Ca_{LB} + ({}^{87}Sr/{}^{86}Sr_{FFC} - {}^{87}Sr/{}^{86}Sr_{CaCO3}) \cdot Sr/Ca_{FFC}) \cdot 100$ (Capo et al. 1998)

where LB = local bedrock and FFC = fracture-filling calcite

The Sr/Ca ratio from the fracture-filling calcites and bedrock, given in Table 1, controls the curvature of the mixing curve (Fig. 8). Based on the mixing curve, the weathering of the granitic bedrock is not an important source of Ca^{2+} ions for the precipitation of the calcite crusts. The mixing curve indicates that at least 85% of the Ca^{2+} in the calcite crusts originates from the dissolution of the fracture-filling calcites. These quantities were calculated assuming that the Sr/Ca ratio in the waters from which the calcite crusts precipitated had an identical Sr/Ca ratio to that of the fracture-filling calcite, which was not measured. However, the relative proportion of Ca^{2+} derived from the dissolution of the fracture-filling calcite is consistent with the geochemistry of the glacial meltwaters. Calcium ions dominate the ionic chemistry of the glacial meltwaters, while potassium (K^+), associated with the weathering of K-feldspars, and SiO_2 constitute minor species (< 0.5 ppm) (Table 4). These results suggest that calcite dissolution dominates silicate weathering, even in this granitic environment.

This is supported by experimental work done by White et al. (1999) who demonstrated that calcite dissolution dominates over silicate weathering, even when the bedrock comprises trace amounts (< 2%) of carbonate. In addition, Fairchild et al. (1999) demonstrated that finely abraded calcite particles in the subglacial environment have a higher chemical reactivity, rendering them more soluble then unabraded calcite. Therefore, the low permeability of the granitic bedrock, which may cause local increase in basal meltwater pressure, combined with the presence of soluble fracture-filling calcite, exerts a strong influence on the Ca^{2+} dominated chemistry of the glacial and subglacial meltwaters.

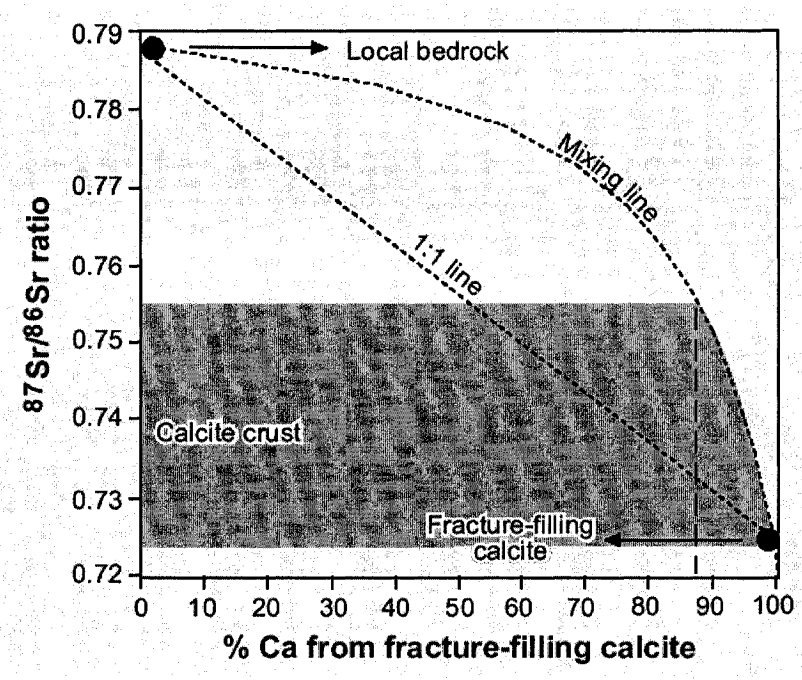

Figure 8: Model mixing curve showing the relative contribution of Ca released by the weathering of the fracture-filling calcite to the calcite crusts. The shaded areas represent the range of $^{87}Sr/^{86}Sr$ measured in the calcite crusts. The vertical dashed lines indicate the minimum Ca^{2+} contribution of fracture-filling calcite to the calcite crusts.

5.2 Origin of the ^{13}C and ^{18}O enrichments

The calcite crusts collected from the upper surface of clasts within morainic complexes in Akshayuk Pass have some of the highest $\delta^{13}C$ (1.6 to 12.0‰) and $\delta^{18}O$ (–13.0 to –7.9‰ VPDB or 17.6 to 22.8‰ VSMOW) values measured in carbonate deposits in cold regions. Under most circumstances, the $\delta^{13}C$ and $\delta^{18}O$ of calcite can be estimated from the $\delta^{13}C_{DIC}$ and $\delta^{18}O$ of the waters from which the calcite precipitated (Table 4) and temperature at which the precipitation occurred. Assuming that the calcite crusts precipitated in the temperature range observed in Akshayuk Pass (0 to 25 °C), then the $\delta^{13}C$ composition of the calcite crusts are enriched by up to 24‰ at 22 °C (21‰ at 0 °C) over the $\delta^{13}C_{DIC}$ composition of the local waters and the temperature at which calcite precipitated (Fig. 9). A similar enrichment is also found in the $\delta^{18}O$ composition of the calcite crusts (up to 15‰ at 22 °C) over the $\delta^{18}O$ values of the local water and temperature at which calcite precipitated (Fig. 9). Given the strong $\delta^{13}C$ values of the calcite crusts (up to 12‰), their precipitation from water previously in equilibrium with atmospheric CO_2 ($\delta^{13}C = -8‰$) can be ruled out since it would yield a maximum $\delta^{13}C$ value of 6.4‰ ($\varepsilon^{13}C$ $CaCO_3$-CO_2 = 14.4‰ at 0 °C; Bottinga 1968) during equilibrium freezing of bicarbonate-rich water, still well below the heaviest $\delta^{13}C$ values measured in the Akshayuk Pass calcite crusts (Fig. 9). Further, the freezing of water under equilibrium condition would tend to precipitate

calcite with a depleted $\delta^{18}O$ value with respect with the initial $\delta^{18}O$ composition of the parent water (Lacelle et al. 2006),which is not the case for the Akshayuk Pass calcite crusts.

There is only a few processes that are capable to generate calcite deposits with an enriched $\delta^{13}C$ and or $\delta^{18}O$ composition, *i*) non-equilibrium freezing conditions; *ii*) biogenic processes (i.e. methanogenesis / photosynthesis) or *iii*) evaporation of the parent water prior to the calcite crusts being precpitated. A close examination of the conditions that control these processes will help to determine which one is most possible to have caused precipitation of the calcite crusts in Akshayuk Pass.

Freezing under non-equilibrium conditions (i.e. within seconds) of Ca^{2+}- HCO_3^- waters produces calcite with enriched $\delta^{13}C$ and $\delta^{18}O$ relative to the initial isotopic composition of the parent water. The rapid rate of freezing causes a kinetic partitioning between CO_2 and calcite ($\varepsilon^{13}C$ $CaCO_3$-CO_2 = 31.2 ± 3.1‰ VPDB; Clark and Lauriol 1992) and between water and calcite ($\varepsilon^{18}O$ $CaCO_3$-H2O = 36.7 ± 1.3‰ VSMOW; Clark and Lauriol 1992), which are much greater than their respective equilibrium fractionation factors. However, kinetic ^{13}C and ^{18}O enrichment associated with the rapid freezing of bicarbonate-rich water is an unlikely mechanism to explain the origin of the calcite crusts in Akshayuk Pass since it requires the freezing of water within seconds. The calcite crusts are located on the surface of clasts, where thermal variations occur on the scale of hours rather than seconds.

Biogenic processes, such as methanogenesis and photosynthesis, are also able to generate ^{13}C enriched carbonates relative to the isotopic composition of the parent water. Both of these reactions prefer to metabolize the isotopically light organics (^{12}C), which generates a ^{13}C enrichment in the various phases involved (DIC and calcite). CO_2 reduction by methanogenic bacteria has proposed for the growth of endostromatolites within fissures in limestone bedrock outcrops (Lauriol and Clark 1999; Clark et al. 2004). These endostromatolites have $\delta^{13}C$ values in the –1.7 to 11.4‰ range (Clark et al. 2004), similar to the values measured in our calcite crusts. However, carbonate precipitation associated with CO_2 reduction during acetate-methanogenesis is an anaerobic process involving bacteria and can be ruled out given the aerobic setting of our calcite crusts (on the upper surface of clasts). Sharp et al. (1990) invoked that photosynthesis, through the removal of light CO_2 (^{12}C) from the water, played a role to explained the enriched $\delta^{13}C$ values (up to 8‰) of the "white calcite deposits" precipitated on the upper surface of clasts at Glacier de Tsanfleuron, Switzerland. However, evidence of biomineralization was not detected in the crystal morphologies of the Akshayuk Pass calcite

crust (Fig. 4). Further, biogenic processes, such as methanogenesis or photosynthesis, does not explain the $\delta^{18}O$ enrichment observed in the calcite crusts over the local waters since the kinetics of reaction of organics with O_2 are not quantitatively important and of little importance in geochemical evolution (Drever, 1997).

The only known mechanism capable to generate an enrichment in both $\delta^{18}O$ and $\delta^{13}C$ in carbonate deposits under open aerobic condition is evaporation. It is well known that evaporation imparts a progressive enrichment and increase in the $\delta^{18}O$ composition and solute concentration in the residual water due to a Rayleigh-type fractionation. The effect of evaporation on the SIcal and $\delta^{18}O$ composition of the water collected from Akshayuk Pass was modeled using the PHREECQ computer code (Fig. 10). During evaporation, the SIcal of the water progressively increases as the solutes are concentrated in the residual water. The $\delta^{18}O$ of water also progressively increases due to the preferential removal of the lighter ^{16}O in the vapor phase and extreme enrichments of up to 37‰ are found when the bulk of the water has evaporated. Given the low calcite saturation state of the glacial meltwaters in Akshayuk Pass (SIcal < -5; Table 4) and the fact that calcite does not precipitate until SIcal > 0, calcite precipitating from such waters would be enriched by several permil over the initial $\delta^{18}O$ composition of its parent water as calcite saturation would be exceeded to be reached only in the late stage of evaporation (Fig. 10). Regarding the effect of evaporation on the $\delta^{13}C$ composition of carbonates, Knauth et al. (2003) proposed that it could generate calcite with highly enriched $\delta^{13}C$ values. For example, caliche developed on the surface of basalt in the Arizona volcanic field had $\delta^{13}C$ values in the 4 to 12‰ range, which Knauth et al. (2003) attributed to the preferential degassing of light CO_2 and an unknown kinetic isotope effect during evaporation. Although the loss of ^{13}C-depleted carbon during degassing of CO_2 can produce $\delta^{13}C$ enriched calcite as observed occasionally in speleothems (Michaelis et al. 1985; Dulinski and Rozanski 1990; Mickler et al. 2004), it is difficult to image that such a process is responsible for the ^{13}C enrichment observed in the calcite crusts, since the waters collected in Akshayuk Pass have log pCO_2 values between –4.6 and –3.5 (Table 4), which are near the atmospheric partial pressure ($\log pCO_2 = -3.5$), limiting CO_2 degassing. However, given the low relative humidity and strong winds in Akshayuk Pass (Gilbert and Neuman 1988), strong (kinetic) evaporation of ephemeral streams and lakes stagnating inside the moraines in Akshayuk Pass is a possible mechanism for the formation of the calcite crusts on the surface clasts

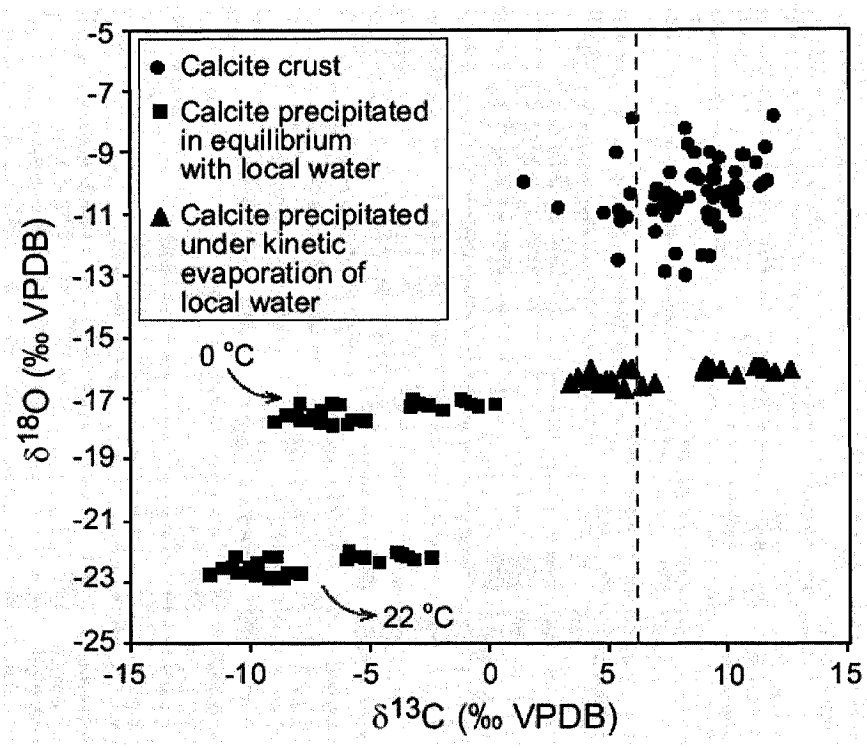

Figure 9 Stable isotope ratios of carbon and oxygen of calcite crusts collected in Akshayuk Pass. Also shown is the theoretical $\delta^{13}C$ and $\delta^{18}O$ composition of calcite crusts that precipitated under equilibrium and under non-equilibrium conditions with the $\delta^{13}C_{DIC}$ and $\delta^{18}O$ of local waters. The $\delta^{13}C$ equilibrium values were calculated using the fractionation factor between $CaCO_3$ and HCO_3^- (Mook et al. 1974). The $\delta^{18}O$ equilibrium values were calculated using the fractionation factor between $CaCO_3$ and H_2O (Kim and O'Neil et al. 1997) and then converted to the VPDB-scale using Coplen's equation ($\delta^{18}O$ VPDB = 0.97001 $\delta^{18}O$ VSMOW - 29.99‰; Coplen et al. 1983). The non-equilibrium $\delta^{13}C$ and $\delta^{18}O$ values were calculated using the average ε^{13}CKIE and ε^{18}OKIE obtained during the kinetic evaporation experiment (Table 6). The vertical dashed line represents the maximum $\delta^{13}C$ of calcite obtained by equilibration with atmospheric CO_2 ($\delta^{13}C = -8‰$):

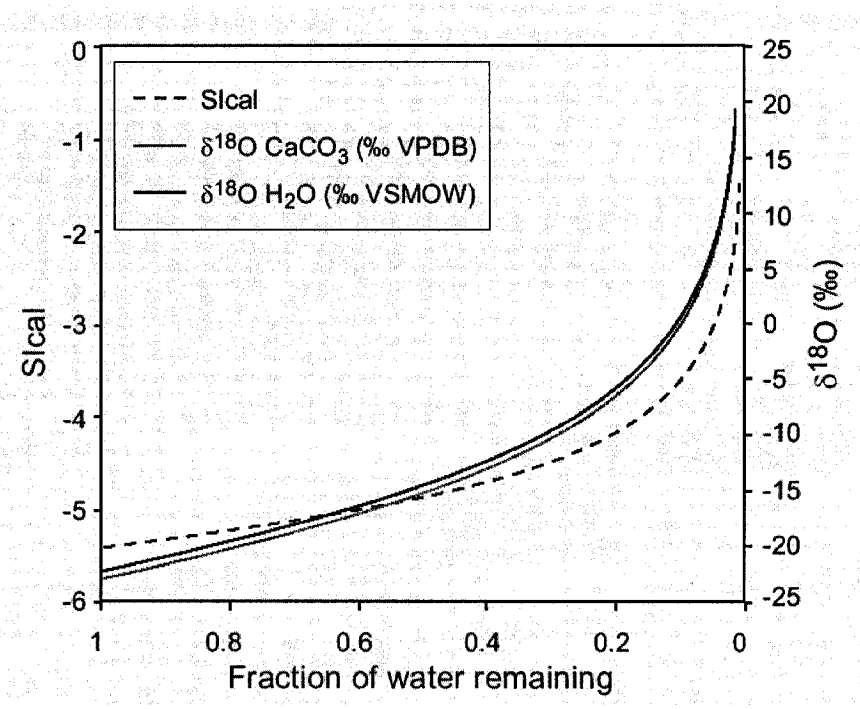

Figure 10: The evolution of the SIcal of water collected in Akshayuk Pass during evaporation as simulated by the PHREECQ hydrogeochemical software (Parkhurst and Appelo 1999). The solubility product of calcite used by PHREECQ at 22 °C is $10^{-8.45}$. Also modeled is the $\delta^{18}O$ composition of calcite precipitating in equilibrium with the $\delta^{18}O$ of the water using a Rayleigh-type fractionation during open system evaporation. In δ(‰) nomenclature, the Rayleigh equation is expressed as: $\delta = \delta_0 + \varepsilon \cdot \ln f$ where δ_0, δ are the initial and final $\delta^{18}O$ (‰) values respectively, $\varepsilon = (\alpha - 1) \cdot 1000$ *where* α is the fractionation factor, and *f* is the fraction of water remaining in solution. For the modeling, an initial $\delta^{18}O$ value of the water of –22.2‰ was used with an ε value of 9.6‰, which is the fractionation factor between water and vapour at 22 °C (Majoube 1971). The $\delta^{18}O$ values of the water where then corrected for the fractionation between water and calcite ($\varepsilon CaCO_3$-H_2O = 28.1‰ at 22 °C; Kim and O'Neil et al. 1997) and then converted to the VPDB-scale (Coplen et al. 1983) to obtain the $\delta^{18}O$ composition of calcite.

5.3. Laboratory investigation on ^{13}C enrichment during equilibrium and kinetic evaporation

The only known laboratory experiment to verify the effect of evaporation on the $\delta^{13}C$ of carbonate was done by Stiller et al. (1985) from evaporating brines of the Dead Sea. Therefore, the highly enriched $\delta^{13}C$ values of the Akshayuk Pass calcite crusts with respect to the $\delta^{13}C_{DIC}$ of the local water, which is attributed to an evaporative enrichment effect of low ionic strength waters, were investigated more closely by a series of laboratory experiments. Two experiments were undertaken at ambient laboratory air temperature (22 °C). The first experiment verified the ^{13}C partitioning between calcite and bicarbonate during evaporation of a synthetic calcium bicarbonate solution in continuous contact with atmospheric CO_2, which simulated evaporation under equilibrium conditions. The second experiment examined the ^{13}C composition of calcite during rapid (kinetic) evaporation of synthetic calcium bicarbonate solutions.

The synthetic calcium bicarbonate solutions were prepared by purging air with 2% CO_2 for 30 minutes in double distilled water to which powdered reagent-grade calcium carbonate was added. Table 5 summarizes the geochemical and isotopic composition of the solutions used in the experiments.

Table 5. Geochemical and isotopic composition of the solutions used in evaporative experiments.

Parameter	Solution UO-A	Solution UO-B
Water		
pH	6.2	6.3
log pCO_2	–3.5	–3.5
HCO_3^- mmol l^{-1}	0.007	0.006
DIC mmol l^{-1}	0.015	0.013
Ca^{2+} mmol l^{-1}	4.19	7.58
SIcal	0.2	0.4
$\delta^{13}C$ (‰ VPDB)	–33.2	–31.1
$\delta^{18}O$ (‰ VSMOW)	–13.3	–14.5
Calcite[1]		
$\delta^{13}C$ (‰ VPDB)	–32.5	–30.4
$\delta^{18}O$ (‰ VPDB)	–13.9	–15.1

[1]: Predicted $\delta^{13}C$ and $\delta^{18}O$ values of calcite precipitating in equilibrium with the $\delta^{13}C_{DIC}$ and $\delta^{18}O$ of the solutions at 22 °C.

5.3.1 Equilibrium evaporation

The equilibrium evaporation experiment consisted of six glass beakers, each containing 100 ml of a synthetic calcium bicarbonate solution (UO-1) that were left to evaporate at 22 °C in quiescent conditions for a total of 8 days. Samples were collected at regular intervals, which produced a static view of a Rayleigh distillation at successively decreasing residual water fractions. The remaining water fractions were analyzed for pH, DIC concentrations and $\delta^{13}C_{DIC}$. The DIC concentration was determined by reacting the solutions with 100% phosphoric acid under vacuum conditions, which converted the DIC to CO_2 gas. The concentration of CO_2 was measured at a pressure transducer calibrated to measure CO_2 yields and converted to μmoles of DIC. The CO_2 was then transferred into a glass septum vial for $^{13}C/^{12}C$ analysis on a Finnigan Mat Delta$^+$ XP isotope mass spectrometer following the techniques described earlier in the text.

Results of the equilibrium evaporation experiment are shown in Fig. 11. The progressive increase in $\delta^{13}C_{DIC}$ from –34.8 to 1‰ occurs concurrently with a decrease in acidity (pH increases from 6 to 8), alkalinity (DIC concentration drops from 207 to 16 μm) and partial pressure of CO_2 (from log pCO_2 –2.3 to log pCO_2 –3.4). The increase in $\delta^{13}C_{DIC}$ values cannot be solely attributed to a shift toward higher pH, since an increase in pH from 6 to 8 only causes a 4‰ increase in $\delta^{13}C_{DIC}$. Therefore, the progressive increase in $\delta^{13}C_{DIC}$ is more likely the result of an equilibration between the dissolved bicarbonate and gaseous CO_2 ($\varepsilon HCO_3^- - CO_2$ = 8.3‰ at 22 °C; Mook et al. 1974) during CO_2 degassing. However, in a graphic showing the normalized fraction of residual CO_2 against the $\delta^{13}C_{DIC}$ (Fig. 12), it is apparent that a Rayleigh-type enrichment on the $\delta^{13}C_{DIC}$ occurred during the evaporation of the calcium bicarbonate solution. During evaporation of a bicarbonate solution, gaseous CO_2 can leave the solution through the reaction:

[2] $Ca^{2+} + 2HCO_3^- \rightarrow CaCO_3 + H_2O + CO_2 \uparrow$

and since there is no significant change to the isotope composition of $\delta^{13}C_{DIC}$ during calcite precipitation (εHCO_3^- - $CaCO_3$ = 0.4‰ at 22 °C; Mook et al. 1974), it is the progressive degassing of light CO_2 (^{12}C) from the solution that would cause the observed $\delta^{13}C_{DIC}$ enrichment. During the experiment, calcite was formed at all stages (confirmed by XRD measurements).

Therefore, the $\delta^{13}C_{DIC}$ enrichment caused by the CO_2 degassing during calcite precipitation can be modeled according to a Rayleigh-type distillation using ½ (εCO_2-HCO_3^- + εHCO_3^--$CaCO_3$) as the fractionation factor since carbon is evenly divided between two phases (calcite and CO_2) (Fig. 12). A comparison of the data with the theoretical Rayleigh fractionation during calcite precipitation indicates that data deviates from the Rayleigh-type curve during evaporation, probably due to an isotopic exchange with atmospheric CO_2 or to a slightly larger fractionation factor than that of equilibrium between gaseous CO_2 and HCO_3^- at 22 °C (–8.3‰; Mook et al. 1974). A possible explanation for this increased fractionation factor is that evaporation proceeded under a two-stage process where equilibrium conditions are maintained between CO_2 and HCO_3^- during the initial part of evaporation, followed by non-equilibrium conditions between the escaping gaseous CO_2 and the precipitating calcite, which would increase the $\delta^{13}C_{DIC}$. A similar process was also observed in the evaporating brines (Stiller et al. 1985), indicating that a kinetic isotope effect on the $\delta^{13}C_{DIC}$ is observed during evaporation.

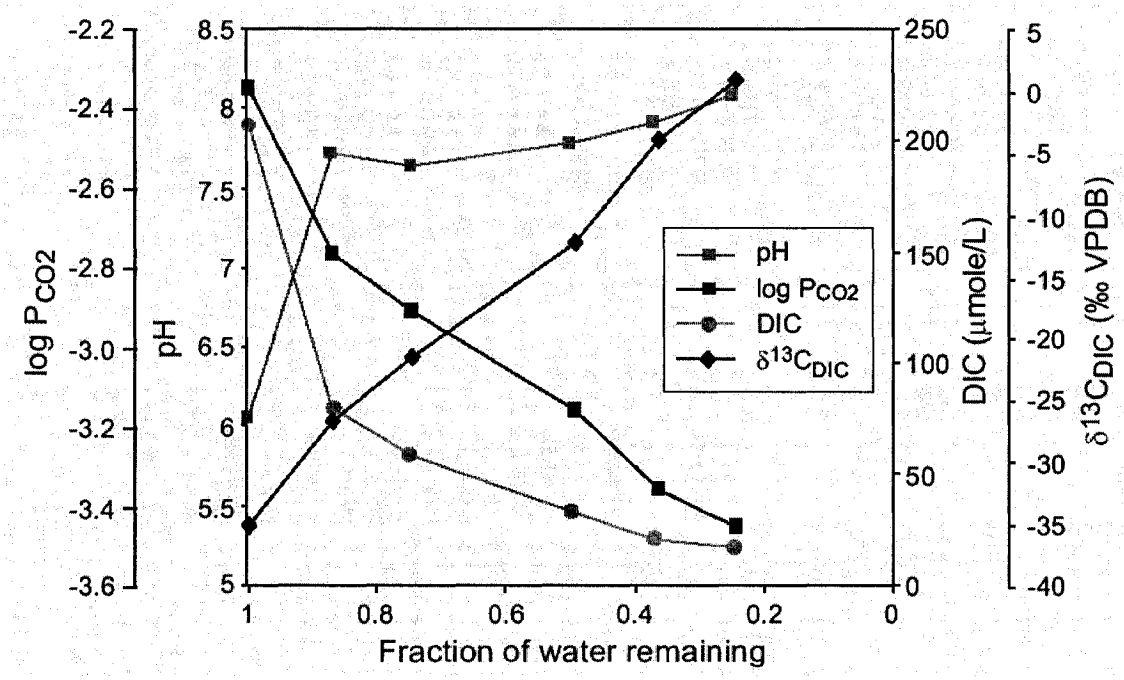

Figure 11: Evolution of pH, log P_{CO2}, DIC concentration and $\delta^{13}C_{DIC}$ during the equilibrium evaporation experiment.

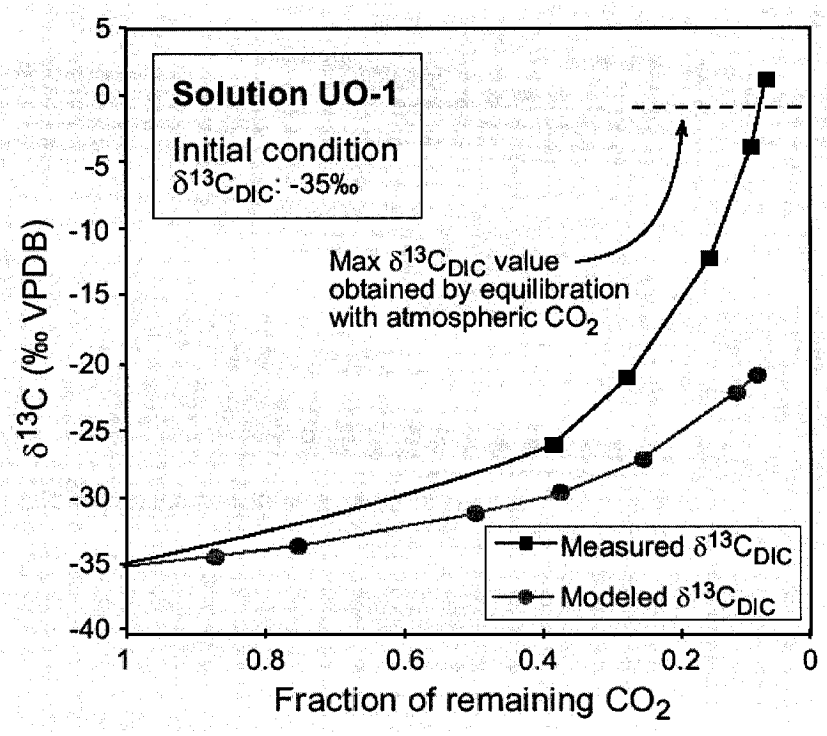

Figure 12: Evolution of $\delta^{13}C_{DIC}$ against the normalized fraction of residual CO_2. The modeled $\delta^{13}C_{DIC}$ line represents the enrichment caused by the CO_2 degassing during calcite precipitation and was modeled according to a Rayleigh-type distillation using ½ (εCO_2-HCO_3^- + εHCO_3^--$CaCO_3$) as the fractionation factor since carbon is evenly divided between two phases (calcite and CO_2). For the modeling an initial $\delta^{13}C_{DIC}$ value of -35‰ was used with an ε value of -5.6‰, which is ½ (εCO_2-HCO_3^- + εHCO_3^--$CaCO_3$) at 22°C.

5.3.2 Kinetic evaporation

The kinetic evaporation experiment consisted of purging compressed CO_2-free dry air (Praxair GP529318) through a 21G needle inside a glass septum vial which contained the synthetic bicarbonate solution (Fig. 13). A second needle allowed for excess air to evacuate. The fact that CO_2-free air was used in the experiments precluded any isotopic exchange (re-equilibrium) between CO_2 and the bicarbonate solution prior to calcite precipitating. The effect of the rate of reaction on the $\delta^{13}C$ of precipitating calcite was examined by changing the volume of solution used. The duration of the experiments ranged from 2 hours using volume of 0.1 ml to 5 hours using 0.2 ml. At the end of the experiments, the precipitated calcite was analyzed for its $\delta^{13}C$ and $\delta^{18}O$ composition following the techniques described earlier in the text.

Results of the kinetic evaporation experiments are shown in Table 6. The measured kinetic isotope effect ($\varepsilon^{13}C_{KIE}$) between CO_2 and $CaCO_3$ ranged between 20 and 40‰, which is much

greater than the equilibrium fractionation value of 10.8‰ ($\varepsilon^{13}C$ $CaCO_3$-CO_2; Bottinga 1968) at 22 °C, but within the same range as those obtained by Clark and Lauriol (1992) for cryogenically precipitated calcites (31.5‰). Given that the amount of fractionation during the precipitation of calcite between the dissolved bicarbonate (HCO_3^-) and calcite ($CaCO_3$) is relatively small (Mook et al. 1974; Turner 1982), the kinetic isotope enrichment must have occurred during the dehydration of bicarbonate ($HCO_3^- \rightarrow CO_2 + H^+$), where the weaker ^{12}C-O bonds of the bicarbonate are preferentially broken, producing a ^{13}C depleted CO_2 and reciprocal ^{13}C enrichment in calcite. Furthermore, the $\varepsilon^{13}C_{KIE}$ $CaCO_3$-HCO_3^- range (11.7 to 32.1‰) is within the observed enrichment of the calcite crusts over the $\delta^{13}C_{DIC}$ of local waters (15.2 ± 2.4‰; Fig . 9), suggesting that the ^{13}C enrichment observed in the Akshayuk Pass calcite crusts is probably due to the evaporation of bicarbonated water under non-equilibrium conditions.

The kinetic evaporation experiment also produced a kinetic isotope effect on ^{18}O (Table 6). Given that the calcite saturation state of synthetic solutions used in the experiment exceeded saturation with respect to calcite prior to being evaporated, then the difference in $\delta^{18}O$ between the $\delta^{18}O$ of the water and calcite represents ε^{18}OKIE. The ε^{18}OKIE during rapid evaporation ranges between 30.5 to 39.3‰, which is greater than the equilibrium fractionation factor at 22°C (28.1‰; Kim and O'Neil 1997), but similar to the average ε^{18}OKIE measured by Clark and Lauriol (1992) during rapid freezing of bicarbonated waters (ε^{18}OKIE = 36.7 ± 1.3‰). Figure 8 shows that, unlike the ε^{13}CKIE during kinetic evaporation, the ε^{18}OKIE does not re-produce the observed range in $\delta^{18}O$ values in the Akshayuk Pass calcite crusts. This was expected and is attributed to the lower calcite saturation state of local water from which the Akshayuk Pass calcite crusts precipitated (Fig. 10). Calcite precipitating from a solution that has a low initial calcite saturation state, such as those in Akshayuk Pass, will become enriched by several permil in ^{18}O over that of the initial $\delta^{18}O$ of the parent water as calcite precipitation does not occur until the solution reaches calcite saturation (Fig. 9).

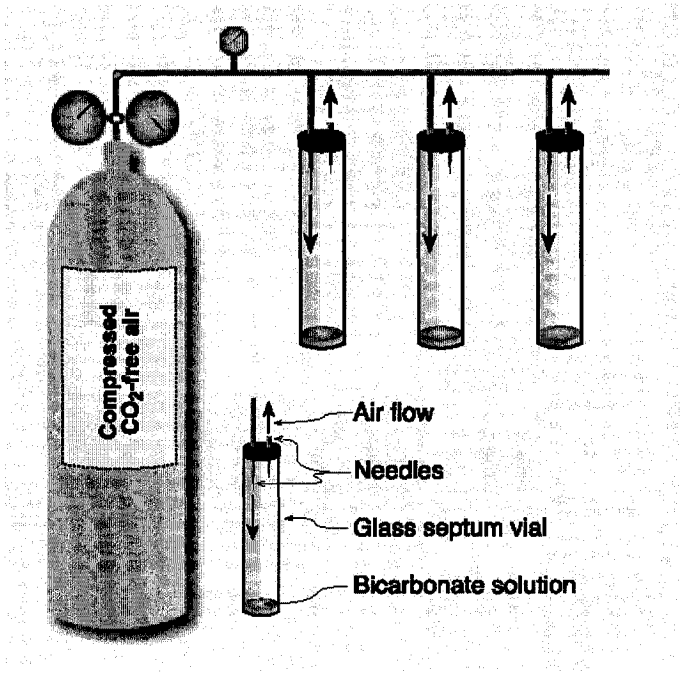

Figure 13: Configuration of the kinetic evaporation experiment.

Table 6. Results of kinetic evaporation experiments.

				^{13}C (‰ VPDB)			^{18}O (‰ VSMOW)		
Solution	Volume (ml)	Initial CO_2	Initial DIC	Fianl $CaCO_3$	εKIE $CaCO_3$-CO_2	εKIE $CaCO_3$-HCO_3	Initial. H_2O	Final $CaCO_3$	εKIE $CaCO_3$-H_2O
UO-A	0.1	–41.6	–33.2	–1.1	40.5	32.1	–13.3	17.2	30.5
UO-A	0.2	–41.6	–33.2	–20.3	21.3	12.9	–13.3	22.4	35.7
UO-A	0.2	–41.6	–33.2	–20.1	21.5	13.1	–13.3	18.3	31.6
UO-B	0.2	–39.6	–31.1	–19.4	20.2	11.7	–14.5	24.8	39.3
UO-B	0.2	–39.6	–31.1	–18.4	21.2	12.7	–14.5	22.8	37.3
Average					*19.9*	*16.5*			*34.9*
Stdev					*7.8*	*8.7*			*3.7*

Note: The final $\delta^{18}O$ $CaCO_3$ values were converted to the VSMOW-scale using using the following equation, $\delta^{18}O_{VSMOW} = 1.02354\ \delta^{18}O_{VPDB} + 30.92$ (Coplen et al. 1983)

5.4 Formation of calcite crusts

The calcite crusts discovered on the upper surface of clasts within morainic complexes in Akshayuk Pass must not be confused with the subglacially precipitated calcite in deglaciated regions (Ford et al. 1970; Hillaire-Marcel et al. 1979; Souchez and Lemmens 1985; Sharp et al. 1990; Fairchild et al. 1993). Subglacially precipitated calcite crusts are commonly found on the lee side of bedrock obstacles, are often striated and tend to be in isotopic equilibrium with the $\delta^{18}O$ and $\delta^{13}C_{DIC}$ of the basal meltwater from which they precipitated. In Akshayuk Pass, none of the calcite crusts observed was striated, suggesting that they did not originate beneath active ice, and their stable isotopic composition (C-O) is strongly enriched over the $\delta^{13}C$ and $\delta^{18}O$ values of calcite precipitating in equilibrium with the local waters (Fig. 9).

Given the geographical setting of the calcite crusts, three mechanisms of formation are plausible (Fig. 14). First, the calcite crusts observed in some abandoned stream channels could have originated from groundwater circulating through till and later drawn upwards by evaporation, causing the calcite to precipitate on the surface of the clasts. Secondly, the calcite crusts on the surface of clasts could have precipitated during the evaporation of ephemeral streams and lakes stagnating between the moraine and the glacier ice following the retreat of the valley glaciers. Given the > 1500 m difference in heights between the highlands and the valley where the crusts are situated, the strong katabatic winds originating from the Penny Ice Cap (Gilbert and Neuman 1988) could have acted as a catalyst to increase the rate of evaporation, creating far-from-equilibrium isotope effect, as they increase their hygrometric capacity. Thirdly, the calcite crusts found on the surface of large boulders at the bottom of talus slope did not form *in situ*, but given the same isotopic composition to those formed on clasts on the end-moraines, they can be attributed to a similar origin. Rockfalls are frequent in Akshayk Pass and therefore the calcite crusts could have formed on the exposed face/fissure of a cliff prior to falling (Fig. 3). Water circulating on the highlands can infiltrate through micro-fissures in the bedrock and acquired a $Ca\text{-}HCO_3$ load through the dissolution of the fracture-filling calcite. The groundwater eventually reaches the face of the cliff and dries, causing calcite precipitation. Weathering of the cliff caused the boulders to fall, either as supraglacial debris or at the bottom of slopes.

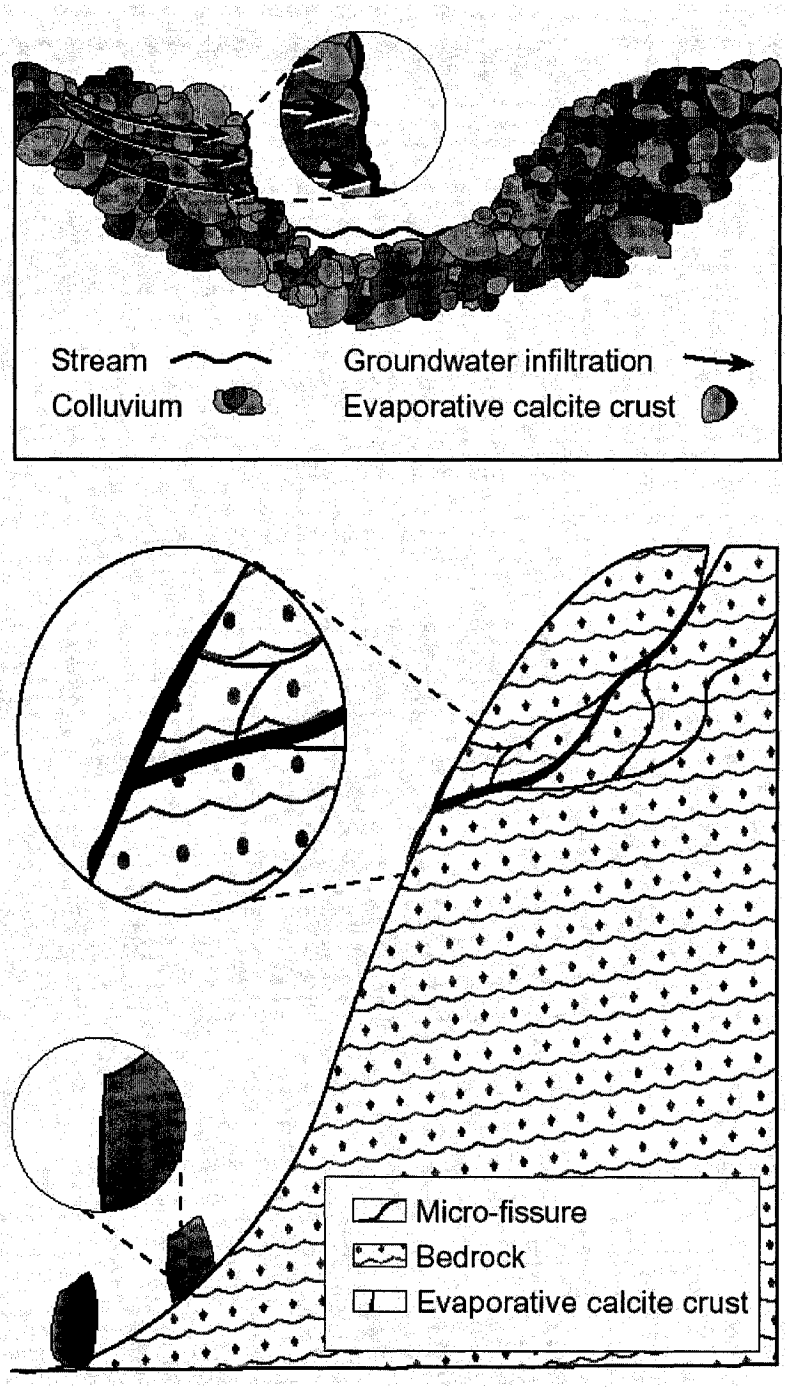

Figure 14: Schematic diagram showing the possible formation of calcite crusts in Akshayuk Pass, southern Baffin Island, NU.

6. Implications for Holocene glacial chronology

Currently, the Holocene glacial chronology in Akshayuk Pass is based entirely on ^{14}C lichenometric dates of the widespread *Rhizocarpon geographicum* colonizing the surface of the moraines. The ^{14}C lichenometric dates suggests that the moraines fronting the valley glaciers were deposited during the Little Ice Age (e.g. Davis 1985; Mercier 2004). However, little is known about the extent of previous Holocene alpine glaciations in Akshayuk Pass, except for the few lichenometric measurements from the outer ridges of some lateral moraines, which provided ^{14}C ages up to 5000 BP (Davis 1985). Recently, studies by Blake (2005) and Waragai (2005) have illustrated the potential of using ^{14}C dating of carbonate deposits to provide minimum ages of the moraine surface on which carbonate deposits precipitated. However, the ^{14}C ages of such deposits might be modified by ^{14}C dust supply and / or a hard water effect, thus yielding an older or younger age. However, both these effect can be neglected for the Akshayuk Pass calcite crusts given the compact structure and the absence of microscopic pores on the surface of the crusts and the formative process of the deposits, which allows for ^{14}C to re-equilibrate with atmospheric CO_2 prior to precipitating.

If we accept that the ^{14}C content of the calcite crusts collected from the upper surface of clasts within the morainic complexes in Akshayuk Pass was nearly 100% modern at the time of their formation then the ^{14}C ages obtained from calcite crusts provide minimum ^{14}C ages of ice retreat and moraine deposition of the Holocene valley glacier in Akshayuk Pass. The spatial variation of the ^{14}C ages derived from the calcite crusts are shown in Fig. 15. Three radiocarbon measurements obtained within a surface area of 5000 m^2 from Tête des Cirques Glacier yielded ^{14}C ages between 2095 ± 50 cal BP to modern. The oldest sample dated (7640 ± 70 cal BP) was from a single crust near the snout of G-20 Glacier. Two radiocarbon measurements from crusts collected at Nifhleim Glacier yielded ^{14}C ages of 6990 ± 420 cal BP and 5810 ± 370 cal BP. The youngest age was obtained the farthest away from the snout of the glacier, while the oldest ^{14}C age is from an outer ridge near the snout of the glacier, suggesting that the calcite crusts were precipitated following the retreat of the glacier.

Based on this new information, it appears that some of the moraines did not form during the Little Ice Age, but that their formation pre-dates the Neoglacial period (Fig 16). Two potential scenarios exist to explain a pre-Neoglacial formation of the moraines. First, it is possible that some moraines in Akshayuk Pass represent a standstill of the late Pleistocene – early Holocene deglaciation, as Akshayuk Pass was apparently only ice-free after 9000 BP (Miller 1973;

Marsella et al. 2002). However, the stable isotope ratio of oxygen of the ice-cored lateral moraines seems to reject this hypothesis. Ice exposed in the ice-cored moraines at Nifhleim Glacier has $\delta^{18}O$ values in the –24.3 to –21.6‰ range (n = 7), suggesting that the moraines are Holocene in age. Alternatively, the formation of the moraines could be associated with the 8200 cal BP cold event. This event, which was cold and wet (Barber et al. 1999), could have caused a re-advance of alpine glaciers in Akshayuk Pass from their receeding Late Pleistocene position. Miller et al. (2005) presented evidence from Donard Lake and Lake Jake, which are nearby sites on southern Cumberland Peninsula, that alpine glaciers responded positively to the 8200 cal BP cold event. The ^{14}C age distribution of the calcite crusts seems to support this hypothesis as none is greater than 7640 ± 70 cal BP. However, it would imply that the moraines in Akshayuk Pass preserved their core of ice since the early Holocene, which contradicts with Miller (1973), who suggested that early Holocene moraines on Cumberland Peninsula lost their ice cores during the middle Holocene warm interval. The latter is highly unlikely because it would require an unrealistically rapid dissipation of deep permafrost (e.g., Dyke 1993). In any case, according to the mode of formation of the evaporative calcite crusts and their ^{14}C age distribution, it is suggested that the moraines in Akshayuk Pass pre-date the Little Ice age. This is not to say that the Late Holocene cooling during the Little Ice Age did not result in an expansion of valley glaciers as evidenced by the ^{14}C lichenometric dates. In fact, the extension of glaciers during the Little Ice Age was probably of similar magnitude for most glaciers to their early Holocene position, but it did not override the moraines established earlier. It is suggested that the Little Ice Age expansion of alpine glaciers in Akshayuk Pass probably created a lichen-kill event, which is produced when lichens are covered for many years by > 30 cm of snow/ice. Such an event would explain the ^{14}C lichenometric age distribution, which are concentrated during the Little Ice Age period.

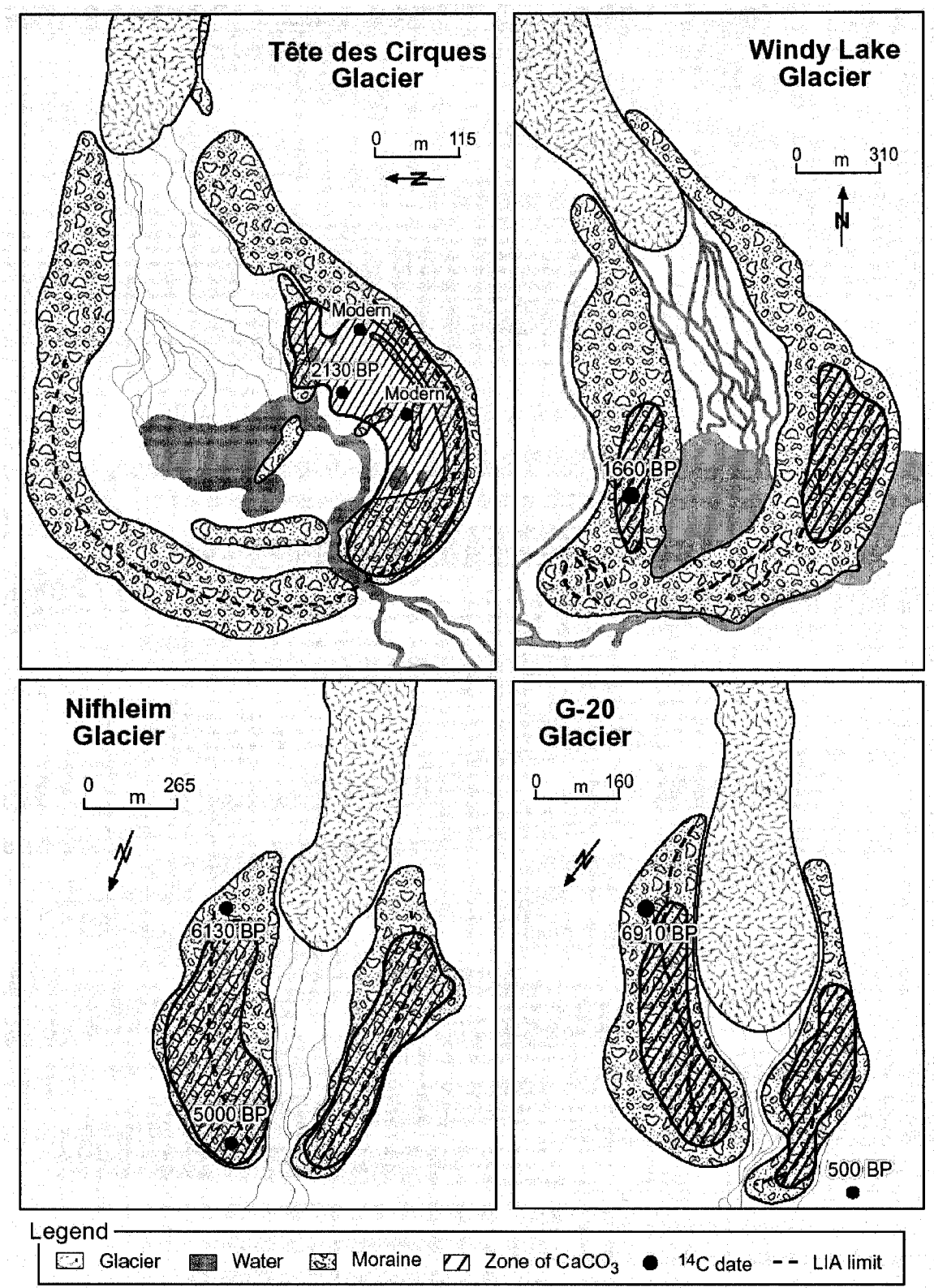

Figure 15: Detailed geomorphic maps of Tête des Cirques, Nifhleim, Windy Lake and G-20 glaciers showing areas where calcite crusts were discovered and locations of ^{14}C ages.

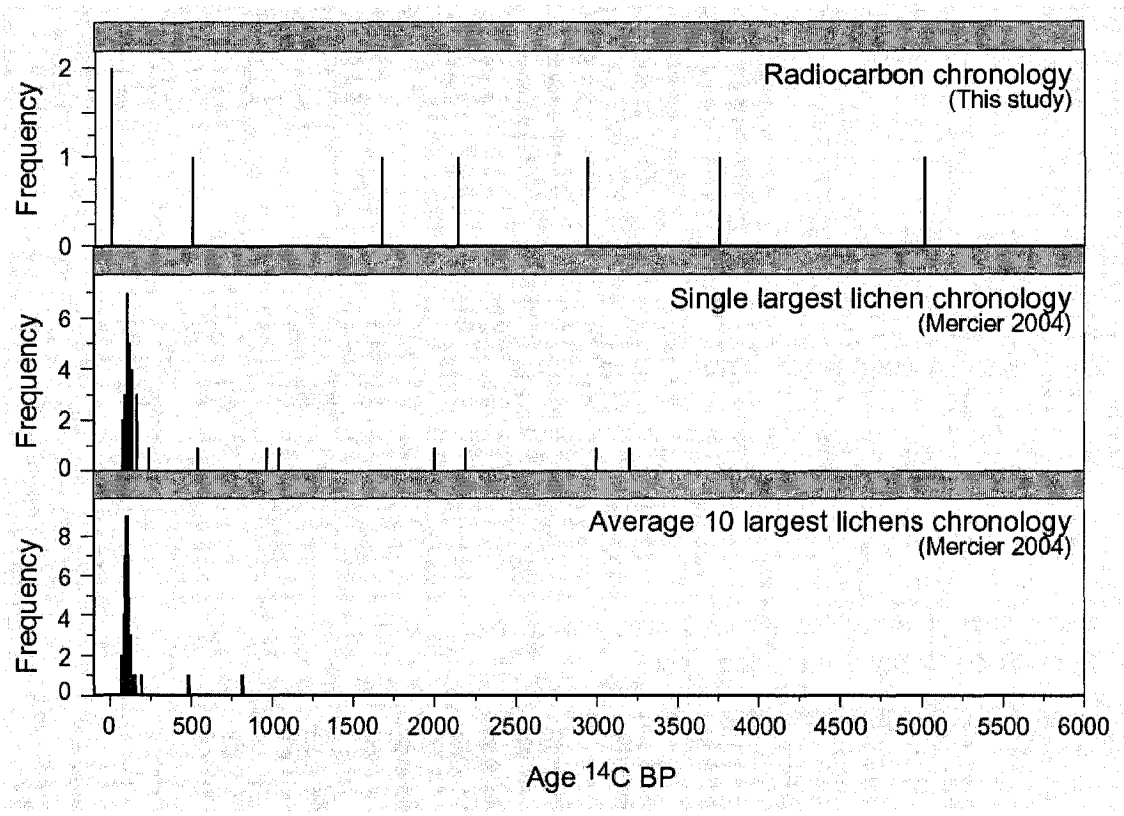

Figure 16: Comparison of radiocarbon age distribution obtained from evaporative calcite crusts that formed within the moraines and lichenometrically-derived ages of moraines in Akshayuk Pass.

7. Conclusions

Based on the results presented above, the following conclusions can be reached regarding the origin, age and paleo-environmental significance of the Akshayuk Pass calcite crusts:

1) The discovery of calcite crusts on the surface of clasts in a region underlain entirely by granitic and gneissic rocks of the Precambrian Canadian Shield indicates that carbonate deposits are not limited to limestone environments.
2) Strontium isotope ratio measurements indicate that the major source of calcium to the evaporative calcite crusts is the preferential dissolution of fracture-filling calcites and a minor source is derived from silicate weathering. This shows that carbonate weathering tends to dominate, even in regions where carbonates occur in trace amounts, and contributes to the chemistry of surface runoff.

3) The calcite crusts have a highly enriched $\delta^{13}C$ composition (1.6 to 12‰). The $\delta^{13}C$ values of the calcite crusts are enriched by up to 24‰ over that of the $^{13}C_{DIC}$ of the local waters and temperature at which calcite precipitation occurred. Such an enrichment was attributed to kinetic evaporation, where under controlled laboratory conditions, the rapid rate of reaction produced a $\varepsilon^{13}C_{KIE}$ $CaCO_3$-CO_2 (between 20 and 40‰) at 22 °C. This $\varepsilon^{13}C_{KIE}$ $CaCO_3$-CO_2 is much greater than the equilibrium fractionation factor of 10.8‰ at 22 °C (Bottinga 1968).
4) The highly enriched $\delta^{18}O$ composition of the calcite crusts (–13.0 to –7.9‰ VPDB) over that of the local waters (up to 15‰) supports that their formation is associated with evaporation. It is well known that evaporation imparts a progressive increase in ^{18}O and solute concentration on the residual water due to a Rayleigh-type fractionation. Given the initial condition of the water from which the calcite crusts precipitated (SIcal < –5) and that calcite precipitation does not occur until SIcal > 0, the $\delta^{18}O$ composition of the calcite crusts is expected to be enriched by several permil of that of the initial $\delta^{18}O$ of the parent water as calcite saturation will only be reached in the late stage of evaporation.
5) The formation of the calcite crusts collected in Akshayuk Pass is ascribed to the evaporation of stagnating ephemeral lakes and streams following the retreat of valley glaciers. The strong katabatic winds originating from the Penny Ice Cap can increase the rate of evaporation, creating far-from-equilibrium isotope effects as observed in the $\delta^{13}C$ and $\delta^{18}O$ composition of the calcite crusts.
6) The ^{14}C age distribution of the calcite crusts (7640 cal BP to modern) provides minimum ages for ice retreat and morainic deposition and indicates that the maximum glacier advance didn't occur during the Little Ice Age, as previously thought. Two potential scenarios exit to explain a pre-Neoglacial formation. First, it is possible that the moraines in Akshayuk Pass represent a standstill of the late Pleisotocene – early Holocene deglaciation, as Akshayuk Pass was apparently only ice-free after 9000 BP. Alternatively, the 8200 cal BP event, which was cold and wet, could have caused a readvance of valley glaciers in Akshayuk Pass from their receeding Late Pleistocene position as evidenced from elsewhere on southern Cumberland Peninsula.

Acknowledgements

This work was funded by Natural Science and Engineering Research Council of Canada (NSERC) discovery grants to B. Lauriol and I.D. Clark, by an Ontario Graduate Scholarship (OGS) and Northern Scientific Training Program (NSTP) grant to D. Lacelle. We would like to thank W. Abdi and P. Middlestead (G.G. Hatch Laboratory, University of Ottawa), L. Ling (SEM Laboratory, Carleton University), B. Cousens (strontium isotope analyses, Carleton University) and M. Alewany for their technical assistance. The radiocarbon measurements were made at IsoTrace (University of Toronto). J.F. Dion, J. Clark and G. Mercier provided valuable field assistance. Special thanks to B. Etooangat and P. Smiley (Parks Canada) for providing logistical support during our stay in Pangnirtung and Auyuittuq National Park (research permit number ANP 2004-001). We would like to thank the reviewers R. Léveillé, T. Waragai and G. Dix (associate editor) for their constructive reviews of the manuscript.

References

Arocena, J.M., and Hall, K. 2003. Calcium phosphate coatings on the Yalour Islands, Antarctica: formation and geomorphic implications. Arctic, Antarctic and Alpine Research, **35**: 233-241.

Barber, D.C., Dyke, A., Hillaire-Marcel, C., Jennings, A.E., Andrews, J.T., Kerwin, M.W., Bilodeau, G., McNeely, R., Southon, J., Morehead, M.D., and Gagnon, J.M. 1999. Forcing of the cold event of 8200 years ago by catastrophic drainage of Laurentide lakes. Nature, **400**: 344-348.

Bierman, P.R., Marsella, K.A., Patterson, C., Davis, P.T., and Caffee, M. 1999. Mid-Pleistocene cosmogenic minimum-age limits for pre-Wisconsinan glacial surfaces in southwestern Minnesota and southern Baffin Island : a multiple nuclide approach. Geomorphology, **27**: 25-39.

Blake, W Jr. 1999. Glaciated landscape along Smith Sound, Ellesmere Island, Canada and Greenland. Annals of Glaciology, **28**: 40-46.

Blake, W. Jr. 2005. Holocene carbonate precipitates on Precambrian bedrock in the High Arctic: age and potential for paleoclimatic information. Geografiska Annaler, **87A**: 175-192.

Bottinga, I. 1968. Calculation of fractionation factors for carbon and oxygen exchange in the system calcite-CO_2-water. Journal of Physical Chemistry, **72**: 800-808.

Bradley, R.S. 1990. Holocene paleoclimatology of the Queen Elizabeth Islands, Canadian High Arctic. Quaternary Science Reviews, **9**: 365-384.

Bunting, B.T., and Christensen L. 1978. Micromorphology of calcareous crusts from the Canadian High Arctic. Geologiska Foreningens Forhandlinger, **100**: 361-367.

Capo, R.C, Stewart, B.W., and Chadwick, O.A. 1998. Strontium isotopes as tracers of ecosystem processes: theory and methods. Geoderma **82**: 197-225.

Clark, I.D., and Lauriol, B. 1992. Kinetic enrichment of stable isotopes in cryogenic calcites. Chemical Geology, **102**: 217-228.

Clark, I.D., Lauriol, B., Marschner, M., Sabourin, N., Chauret, Y., and Desrochers, A. 2004. Endostromatolites from permafrost karst, Yukon Canada: paleoclimatic proxies for the Holocene thermal hypsithermal. Canadian Journal of Earth Sciences, **41**: 387-399.

Coplen, T.B., Kendall, C., and Hopple, J. 1983. Comparison of isotope reference samples. Nature, **302**: 236.

Courty, M.A., Marlin, C., Dever, L., Tremblay, P., and Vachier, P. 1994. The properties, genesis and environmental significance of calcitic pendants from the high Arctic (Spitsbergen). Geoderma, **61**: 71-102.

Craig, H. 1961. Isotopic variations in meteoric waters. Science, **133**: 1702-1703.

Dansgaard, W. 1964. Stable isotopes in precipitation. Tellus, **16**: 436-468.

Davis, P.T. 1985. Neoglacial moraines on Baffin Island. *In* Quaternary environments, eastern Canadian Arctic, Baffin Island and western Greenland. *Edited by* J.T. Andrews, Boston: Allen and Unwin.

Davis, P.T, Bierman, P.R., Marsella, K.A.,Caffee, M.W., and Southon, J.R. 1999. Cosmogenic analysis of glacial terrains in the eastern Canadian Arctic: A test for inherited nuclides and effectiveness of glacial erosion. Annals of Glaciology, **28**: 181-188.

Drever, J.I. 1997. The geochemistry of natural waters: surface and groundwater environments. 3rd edition. Prentice Hall, Upper Saddle River, New Jersey. 436p.

Dulinski, M., and Rozanski, K. 1990. Formation of $^{13}C/^{12}C$ isotope ratios in speleothems; a semi-dynamic model. Radiocarbon, **32**: 7-16.

Dyke, A.S. 1993. Landscapes of cold-centred Late Wisconsinan ice caps, Arctic Canada. Progress in Physical Geography, **17**: 223-247.

Dyke, A.S., Andrews, J.T., and Miller, G.H. 1982. Quaternary geology of Cumberland Peninsula, Baffin Island, District of Franklin. Geological Survey of Canada, Memoir 403, 32p.

Ek, C. 1964. Note sur les eaux de fonte des glaciers de la Haute Maurienne. Leur actions sur les carbonates. Revue belge de Géographie, **1-2**: 127-156.

Environment Canada. 2004. Canadian Climate Normals 1971–2001. Canada Atmospheric Environment Service, Minister of Supply and Services Canada, Ottawa, Ontario, Canada.

Fairchild, I., Bradly, L. and Spiro, B. 1993. Carbonate diagenesis in ice. Geology, **21**: 901-904.

Fairchild, I., Killawee, J.A., Hubbard, B., and Dreybrodt, W. 1999. Interactions of calcareous suspended sediment with glacial meltwater: a field test of dissolution behaviour. Chemical Geology, **155**: 243-263.

Fisher, D.A., Koerner, R.M., Bourgeois, J.C., Zielinski, G., Wake,C., Hammer, C.U., Clausen, H.B., Gundestrup, N., Johnsen, S., Goto-Azuma, K., Hondoh, T., Blake, E., and Gerasimoff, M. 1998. Penny Ice Cap cores, Baffin Island, Canada, and the Wisconsinan Foxe dome connection: Two states of Hudson Bay ice cover. Science, **279**: 692-695.

Ford, D.C., Fuller, P.G., and Drake, J.J. 1970. Calcite precipitates at the sole of temperate glaciers. Nature, **226**: 441-442

Forman, S.L., and Miller, G. 1984. Time-dependent soil morphologies and pedogenic processes on raised beaches. Broggerhalwoya, Spitsbergen, Svalbard archipelago. Arctic and Alpine Research, **16**: 381-393.

Gilbert, R., and Neuman, C.M. 1988. Occurrence and potential significance of warm weather during winter in the eastern Canadian Arctic. Arctic and Alpine Research, **20**: 395-403.

Hallet, B. 1976. Deposits formed by subglacial precipitation of $CaCO_3$. Geological Society of America Bulletin, **87**: 1003-1015.

Hillaire-Marcel, C., Soucy, J.M., and Cailleux, A. 1979. Analyse isotopique de concrétions sous-glaciaire de l'inlandsis laurentidiens et teneur en oxygène 18 de la glace. Canadian Journal of Earth Sciences, **16**: 1494-1498.

Kerwin, M.W., Overpeck, J., Webb, R., and Anderson, K.H. 2004. Pollen-based summer temperature reconstructions for the eastern Canadian Boreal Forest, Sub-Arctic and Arctic. Quaternary Science Reviews, **23**: 1901-1924.

Kim, S.T., O'Neil, J.R. 1997. Equilibrium and nonequilibrium oxygen isotope effects in synthetic carbonates. Geochimica et Cosmochimica Acta **61**: 3461-3475.

Knauth, P.L., Brilli, M., and Klonowski, S. 2003. Isotope geochemistry of caliche developed on basalt. Geochimica et Cosmochimica Acta, **67**: 185-195.

Lacelle, D., Lauriol, B., and Clark, I.D. 2006. Effect of chemical composition of water on the oxygen-18 and carbon-13 signature preserved in cryogenic carbonates, Arctic Canada: implications in paleoclimatic studies. Chemical Geology **234**: 1-16.

Lauriol, B., Ford, D.C., Cinq-Mars, J., and Morris, W.A., 1997. The chronology of speleothem deposition in northern Yukon and its relationships to permafrost. Canadian Journal of Earth Sciences, **34**: 902-911.

Lauriol, B., and Clark, I.D. 1999. Fissure calcretes in the arctic: a paleohydrologic indicator. Applied Geochemistry, **14**: 775-785.

Majoube, M. 1971. Fractionnement en oxygene-18 et en deuterium entre l'eau et sa vapeur. Journal of Chemical Physics, **197**: 1423-1436.

Marlin, C., Dever, L., Vachier, P., and Courty, M-A., 1993. Variations chimiques et isotopiques de l'eau du sol lors de la reprise en gel d'une chouche active sur pergélisol continu (Presqu'ile de Brogger, Svalbard). Canadian Journal of Earth Sciences, **30**: 806-813.

Marsella, K.A., Bierman, P.R., Davis, P.T., and Caffee, M.W. 2002. Cosmogenic 10Be and 26Al ages for the Last Glacial Maximum, eastern Baffin Island, Arctic Canada. Geological Society of America Bulletin, **112**: 1296-1312.

Mercier G. 2004. Fluctuations des fronts glaciaires dans le sud de la Passe d'Akshayuk, Parc National d'Auyuittuq, Nunavut. Unpublished MSc. Thesis, University of Ottawa.

Michaelis, J., Usdowski, E., and Menschel, G. 1985. Partitioning of ^{13}C and ^{12}C on the degassing of CO_2 and the precipitation of calcite-Rayleigh type fractionation and a kinetic model. American Journal of Science, **285**: 318-327.

Mickler, P.J., Banner, J.L., Stern, L., Asmerom, Y., Edwards, R.L., and Ito, E. 2004. Stable isotope variations in modern tropical speleothems: evaluating equilibrium vs. kinetic isotope effects. Geochimica et Cosmochimica Acta, **68**: 4381-4393.

Miller, G.H. 1973. Late Quaternary glacial and climatic history of northern Cumberland Peninsula, Baffin Island, N.W.T., Canada. Quaternary Research, **3**: 561-583.

Miller, G.H., Wolfe, A.P., Briner, J.P., Sauer, P.E., and Nesje, A. 2005. Holocene glaciation and climate evolution of Baffin Island, Arctic Canada. Quaternary Science Reviews, **24**: 1703-1721.

Mook, W.G., Bommerson, J.C., and Staverman, W.H. 1974. Carbon isotope fractionation between dissolved bicarbonate and gaseous carbon dioxide. Earth and Planetary Science Letters, **22**: 169-176.

Overpeck, J, Hughen, K., Hardy, D., Bradley, R., Case, R., Douglas, M., Finney, B., Gajewski, K., Jacoby, G., Jennings, A., Lamoureux, S., Lasca, A., MacDonald, G., Moore, J., Retelle, M., Smith, S., Wolfe, A., and Zielinski, G. 1997. Arctic environmental change of the last four centuries. Science, **278**: 1251-1256.

Parkhurst, D.L., and Appelo, C.A.J. 1999. User's Guide to PHREEQC (Version 2): A Computer Program for Speciation, Batch-Reaction, One-Dimensional Transport, and Inverse Geochemical Calculations. U.S. Geological Survey Water-Resources Investigations Report 99-4259, 310 p.

Sharp, M., Tison, J.L., and Fierens, G. 1990. Geochemistry of subglacial calcites: implications for the hydrology of the basal water film. Arctic and Alpine Research, **22**: 141-152.

Souchez, R.A., and Lemmens, M. 1985. Subglacial carbonate deposition – an isotopic study of present-day case. Palaeogeography, Palaeoclimatology and Palaeoecology, **51**: 357-364.

St-Jean, G. 2003. Automated quantitative and isotopic (^{13}C) analysis of dissolved inorganic carbon and dissolved organic carbon in continuous flow using a total carbon organic carbon analyser. Rapid communications in mass spectrometry, **17**: 419-428.

Stiller, M., Rounick, J.S., and Shasha, S. 1985. Extreme carbon-isotope enrichments in evaporating brines. Nature, **316**: 434-435.

Stuiver, M., and Reimer, P.J. 1993. Extended ^{14}C database and revised CALIB 3.0 ^{14}C age radiocarbon calibration program. Radiocarbon, **35**: 215-230.

Stuiver, M., Reimer, P.J., and Reimer, R.W. 2005. CALIB 5.0 (computer program and documentation). Available from: http://radiocarbon.pa.qub.ac.uk/calib/

Swett, K. 1974. Calcrete crusts in an arctic permafrost environment. American Journal of Science, **274**: 1059-1063.

Turner, J.V. 1982. Kinetic fractionation of carbon-13 during calcium carbonate precipitation. Geochimica Cosmochica Acta, **46**: 1183-1191.

Waragai, T. 2005. Holocene calcrete crust deposits on the moraine of Batura Glacier, northern Pakistan. The Island Arc **14**: 368-377.

Washburn, A.L. 1969. Weathering, frost action, and patterned ground in the Mesters Vig district, Northeast Greenland. Medelelser om Gronland 176, 303p.

Watts, S.H. 1981. Near-coastal and incipient weathering features in the Cape Hershel – Alexandra Fjord area, Ellesmere Island, District of Franklin. *In* Current Research, Geological Survey of Canada Paper 81-1A, 389-394.

White, A.F., Bullen, T.D., Vivit, D.V, Schulz, M.S., and Clow, D.W. 1999. The role of disseminated calcite in the chemical weathering of granitoid rocks. Geochimica et Cosmochima Acta, **63**: 1939-1953.

Manuscript 3

Cold-climate carbonate precipitates - a review of their stable C-O isotope composition and evaluation of their potential as paleoclimatic proxies

Lacelle, D., Lauriol, B. and Clark, I.D.

Manuscript submitted to Quaternary Science Reviews

Abstract

Given the growing interest in carbonate deposits from polar regions as both paleoclimatic proxies and analogues to Mars, this study presents a review of the various types of cold-climate carbonate precipitates. This review paper first provides a morphologically classification of the carbonate deposits to facilitate inter-studies comparison followed by a summary of the stable isotope (C-O) of the carbonate deposits and that of the parent water (C and O) from which the carbonates precipitated. The cold-climate carbonate precipitates were classified into three categories: *powders, crusts* and *speleothems*. The carbonate powders include those that precipitated in relation to aufeis aggradation (cryogenic aufeis calcite) and in relation to the growth of various annual and perennial ice formations in caves (cryogenic cave calcite). The carbonate crusts can be further subdivided based on their lithic environment; those that precipitated on the upper surface of bedrock/clasts (i.e. subglacially precipitated calcite and evaporative calcite crusts); those that are located on the underside of clasts (i.e. active layer carbonates); and those that precipitated in rock outcrop fissures (i.e. endostromatolites). The cold-climate carbonate precipitates have a highly variable isotopic composition with $\delta^{18}O$ values ranging between –6.5 and 36‰ and $\delta^{13}C$ values in the –5 to 17‰ range. However each type of carbonate precipitates has a specific $\delta^{13}C$ and $\delta^{18}O$ range, suggesting that their environmental setting and the mechanism by which they formed controls their ^{13}C and ^{18}O signature. The measurement of the difference (Δ) in stable isotope composition of the carbonate deposits and of the parent water from which they precipitated provided valuable insights into the formative mechanism that led to their precipitation. It was found that carbonate deposits that precipitated under equilibrium physico-chemical conditions had a $\delta^{13}C$ value that is in equilibrium with that of the parent water, while its $\delta^{18}O$ composition was more variable, as it is in part controlled by the temperature of reaction and by the $\delta^{18}O$ and calcite saturation state of the parent water. By contrast, the $\delta^{18}O$ composition of biologically precipitated carbonate deposits (endostromatolites) reflected that of the parent water, while its $\delta^{13}C$ composition was enriched over that of the parent water because bacteria prefer to metabolize the light C (^{12}C) in the DIC pool. In the case of kinetically precipitated carbonate deposits, the $\delta^{18}O$ and $\delta^{13}C$ values are far-from-equilibrium relative to that of the parent water due to the faster rate of reactions which precludes isotopic equilibrium to be reached. Overall, this study has implications for regarding the use of cold-

climate carbonate precipitates as paleoclimatic proxies and in the interpretation of the stable isotope variations in carbonate in the Martian meteorites (i.e. ALH84001).

1. Introduction

In cold climatic regions, carbonate precipitates are widely developed features at the rock, sediment or ice surface, wherever there is or was flowing or standing water. For instance, carbonate precipitates have been observed on the surface of aufeis along riverbeds (Hall, 1980; Pollard, 1983; Lauriol et al., 1991; Clark and Lauriol, 1997; Omelon et al., 2001; Lacelle et al., 2006), in dry lakebeds (Nakai et al., 1975), on the upper surface of clasts and bedrock (Ford et al., 1970; Hallet, 1976; Hanshaw and Hallet, 1978; Hillaire-Marcel et al., 1979; Souchez and Lemmen, 1985; Sharp et al., 1990; Fairchild et al., 1993; Blake, 2005; Waragai, 2005; Lacelle et al., 2007), in fissures in bedrock outcrops (Lauriol and Clark, 1999; Clark et al., 2004), on the underside of clasts in soil profiles (Washburn, 1969; Swett, 1974; Vogt, 1977; Bunting and Christensen, 1978; Forman and Miller, 1984; Vogt, 1989; Courty et al., 1994; Vogt and Corte, 1996; Parnell et al., 2006), in sand dunes (Dijkmanns et al., 1986), in freezing caves, either as cryogenic calcite (Clark and Lauriol, 1992; Zak et al., 2004) or speleothems (Ford, 1976; Brook and Ford, 1980; Lauriol et al., 1997), and in shock-impacted rocks (Martinez et al., 1994; Osinski and Spray, 2001).

Cailleux (1964), in his studies of authigenic mineralization in seasonally frozen soils, first suggested that the formation of calcium carbonate precipitates in cold climatic regions was related to cryogenic process (i.e. freezing). Experimental work later done by Adolphe (1972), Hallet (1976) and Killawee et al. (1998) have shown that the formation of calcite minerals related to freezing involved a series of chemical processes and unique kinetics of dissolution leading to the precipitation of carbonates. During initial freezing of a calcium bicarbonate solution, the Ca^{2+} and HCO_3^- solutes increases to a point where eventually their ion activity product might reach and exceed the calcite saturation point, causing calcite to precipitate. However, other physico-chemical processes, such as cryo-dessication (Marlin et al., 1993) and intense evaporation (Bunting and Christensen, 1978; Lacelle et al., 2007) of calcium bicarbonate solutions have also been suggested as possible formative processes of calcite in cold climate environments. Besides those abiotic processes, calcite precipitates that carry a biological signature suggest that some might have a biotic origin (Swett, 1974; Clark et al., 2004; Parnell et al., 2006).

The stable isotope ratios of C and O are useful in helping to understand the conditions under which the carbonate deposits have formed. The various physical and biological processes that

operate in cold-climate regions (i.e. freezing, evaporation, photosynthesis and methanogenesis) can modify the stable C-O isotope composition of the solution from which the carbonate precipitated and, accordingly, such effect should be imprinted in the stable C-O isotope composition of the carbonate. However, many studies suggested that a kinetic isotope effect, which has the potential of creating large isotopic disequilibrium when the rate of reaction is increased, occurs during the precipitation of cold-climate carbonates (Clark and Lauriol, 1992; Socki et al., 2001; Zak et al., 2004). If this is the case, cold-climate carbonate precipitates would have a far-from-equilibrium C-O isotopic composition with respect to the initial C-O isotopic composition of the water from which the carbonates precipitated and, accordingly, the isotopic composition of the carbonates would potentially not be very useful in determining the principal formative mechanism.

In this study, we first describe the environmental setting, morphology and micro-morphologies of various cold-climate carbonate precipitates and then review the stable isotope ratios of C and O records of 29 published cold-climate carbonate precipitates (Fig. 1) to: *i*) evaluate if the principle formative mechanism by which the carbonate precipitated can be determined from their isotopic record; and *ii*) to assess the degree of isotopic disequilibrium, if any, during the precipitation of the carbonates. These objectives were reached by calculating the difference (Δ) in the stable C-O isotope composition of the carbonate and water from which the carbonate precipitated which will then be compared to the theoretical C-O equilibrium isotope fractionation. This study will further expand our knowledge on carbonate precipitated in cold environments and facilitate paleoclimatic, paleoenvironmental and paleohydrological interpretations derived from these deposits. In addition, this study also has implications regarding the formation of the carbonate in the Martian meteorite ALH84001, for which many hypotheses have been advanced to explain their origin (Mittlefehldt, 1994; Romanek et al., 1994; Anders, 1996; Mackay et al., 1996; Niles et al., 2005), since cold-climate carbonates are highly regarded as analogues.

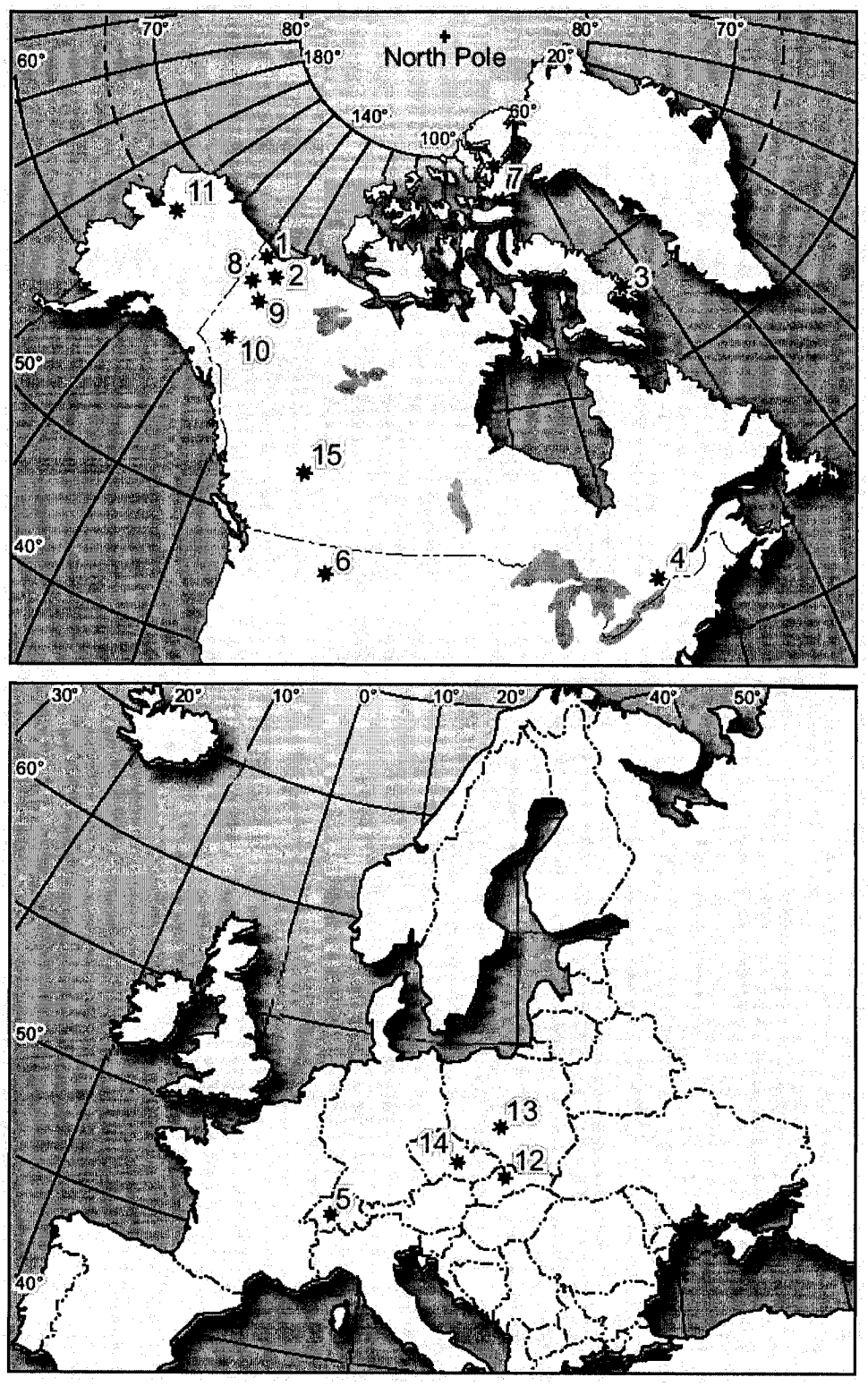

Figure 1. Map showing location of cold-climate carbonate precipitates discussed in the text. See Table 1 for description of location and type of carbonate.

2. Environmental setting and morphological description of cold-climate carbonates

Despite all the various mineralogical, geochemical, petrographical and stable isotopic techniques used so far to characterize carbonate precipitates in cold climate environments, there is still no clear classification of the carbonate deposits to facilitate inter-studies comparison and relatively few studies discussed the process that led to their precipitation. Based on their morphological appearance, cold-climate carbonate precipitates can be classified into three broad categories: *powders, crusts* and *speleothems* (Fig. 2). The carbonate powders include the cryogenic aufeis calcite and cryptocrystalline cave calcite. The carbonate crusts can be further subdivided based on their lithic environment; those that precipitated on the upper surface of bedrock/clasts (i.e. subglacially precipitated calcite and evaporative calcite crusts); those that are located on the underside of clasts (i.e. active layer carbonates); and those that precipitated within fissures in rock outcrops (i.e. endostromatolites). The speleothems (i.e. stalagmites, stalactites and flowstones) consist of a group on their own, because they are not restricted to cold climate regions, and, with the exception of caves located in areas of sporadic to discontinuous permafrost (Ford, 1976; Brook and Ford, 1980), speleothems growth is currently inactive due to the presence of permafrost, which impedes groundwater circulation (Lauriol et al., 1997). For these reasons, speleothems will not be discussed further in this study.

A summary of the site characteristics of each type of carbonate precipitates discussed in this study is presented in Table 1. An interesting aspect that emerged from this compilation is that cold-climate carbonate deposits are not limited to limestone terrains, as many were found in areas of granitic bedrock, where generally, the surface and ground waters are far from equilibrium with respect to calcite mineral.

2.1 Carbonate powders

2.1.1 Cryogenic aufeis calcite

Aufeis are sheet-like masses of horizontally layered ice that accumulate on river channels by successive overflow of perennial groundwater-fed springs upon exposure to cold air (Fig. 3). Cryogenic aufeis calcite powders are associated with the process of aufeis aggradation, which occurs under closed-system conditions (Clark and Lauriol, 1997; Heldmann et al., 2005). The most common mineral precipitated during aufeis growth are calcite ($CaCO_3$), gypsum ($CaSO_4 \cdot 2H_2O$), halite (NaCl) and ikaite ($CaCO_3 \cdot 6H_2O$) (Hall, 1980; Clark and Lauriol, 1997; Pollard,

2005). Micro-morphologically, the cryogenic aufeis calcite powders consist of randomly arranged smooth acicular crystals that are up to 10 μm wide and 150 μm long (Fig. 3). The minerals precipitate within the ice and are released from the aufeis during the thaw season. Residual accumulations of calcite powders of up to 18,000 m^3 were reported by Hall (1980) on the surface of aufeis along the north slopes of Alaska.

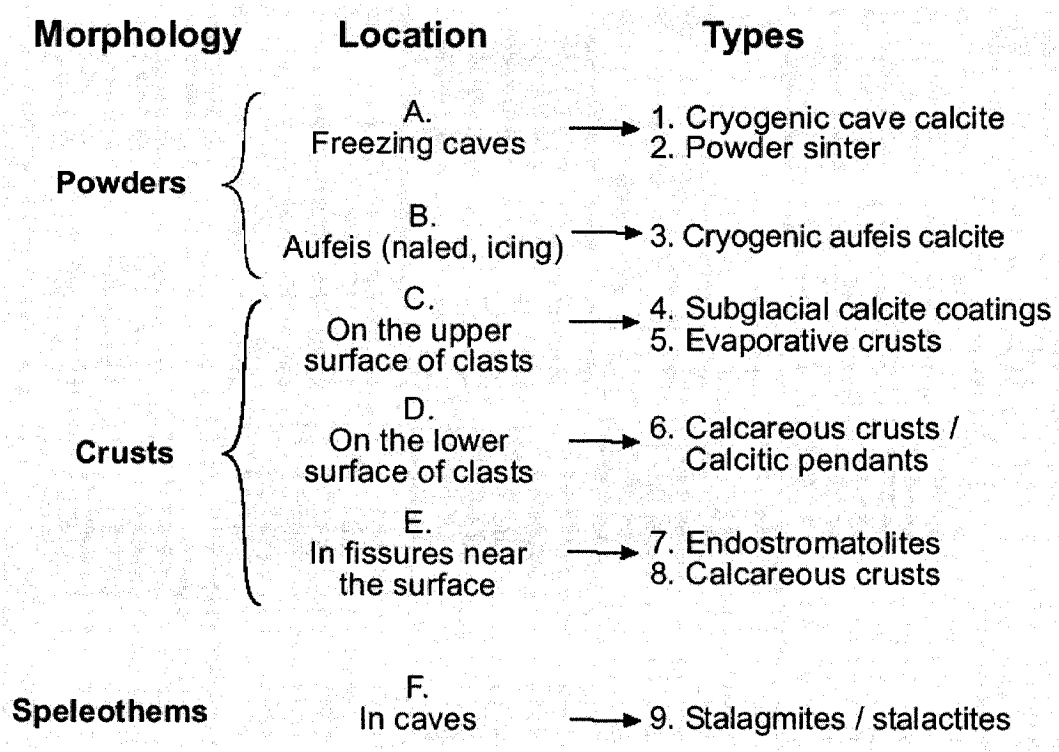

Figure 2. Morphological classification of cold-climate carbonate precipitates.

Table 1: Site characteristics of cold-climate carbonate precipitates discussed in this study.

Type of carbonate	Latitude	Longitude	Geology[a]	Code[b]
Powders				
Cryogenic aufeis calcite				
Timber Creek, YT				1
Fish Hole, YT	68°48'N	138°47'W	L-D	1
Babbage River, YT	68°48'N	138°47'W	L-D	1
Little Fish Creek, NWT	67°45'N	136°19'W	L-D	2
Highway Glacier, Baffin Island, NU	66°44'N	65°00'W	Q-Gn	3
Cryptocrystalline cave calcite				
Bear Cave, YT	66°42'N	139°18'W	L	8
Grande Caverne Glacé, YT	66°42'N	139°18'W	L	8
Caverne-85, YT	66°46'N	139°17'W	L	8
Lusk Cave, QC	45°39'N	75°38'W	L	4
Caverne de l'Ours, QC	45°40'N	75°39'W	L	4
Cave calcite pearls				
Stratenska Cave, Slovakia	49°15'N	21°5'E	L	12
Jaworznicka / Chelosiowa Jame caves,	50°40'N	18°30'E	L	13
Bulm Cave, Czech Republic	49°10'N	16°20'E	L	14
Crusts				
Subglacially precipitated carbonate				
Cantley, QC	45°35'N	75°47'W	L-G	4
Glacier de Tsanfleuron, Switzerland	46°5'N	16°20'E	L	5
Blackfoot glacier, Montana, USA	48°35'N	113°40'W	D	6
Evaporative calcite crusts				
Akshayuk Pass, Baffin Island, NU	66°44'N	65°00'W	Q-Gn	3
Cape Hershel, Ellesmere Island, NU	78°00'N	78°45'W	Gr-Gn	7
Lake Vanda, Antarctica	77°32'S	161°30'E	L	--
Active layer carbonate				
Kluane Lake, YT	61°05'N	138°22'W	L	10
Nye Alesund, Svalbard	79°N	12°E	L-D-Q	--
Calcretes				
Great Kobuk sand dunes, AK	67°00'N	159°00'W	L	11
Endostromatolites				
Bear Cave, YT	66°42'N	139°18'W	L	8
Caverne Helicoidale, YT	66°42'N	139°18'W	L	8
Ogilvie Mountains, YT	66°40'N	139°19'W	L	9
Speleothems				
Bear Cave, YT	66°42'N	139°18'W	L	8
Tsi-it-toh-Choh, YT	66°41'N	139°18'W	L	8
Castleguard, AB	51°10'N	115°33'W	L	15

a: L - Limestone; D - Dolomite; Q - Quartz; Gr - Granite; Gn - Gneiss
b: Location of site shown in Fig. 1.

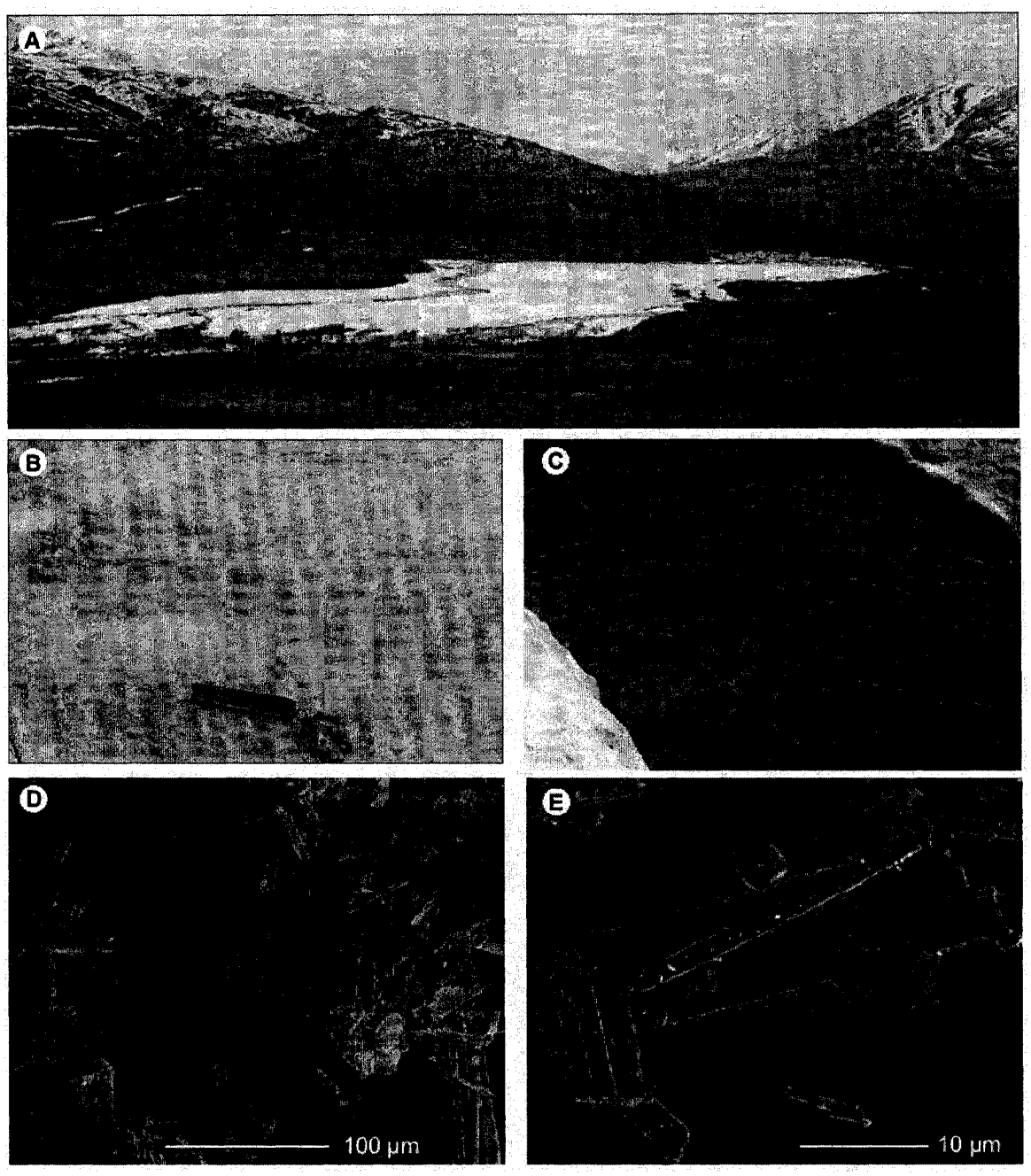

Figure 3. A) Tombstone range aufeis, central Yukon Territory. B-C) Residual accumulation of cryogenic aufeis calcite powders on the surface of the aufeis. D-E) Micro-morphology (SEM images) of cryogenic aufeis calcite.

2.1.2 Cryogenic cave calcite

Cryogenic cave calcite occurs naturally in caves where bicarbonate-rich water discharges into sub-freezing openings (Fig. 4). These deposits have been observed on the surface of ice formations (i.e. ice stalagmites, ice plugs) and on the floor of freezing caves in the northern Yukon Territory (Clark and Lauriol, 1992), in central Europe (Zak et al., 2004) and in caves where temperatures fall below the freezing point for at least a few months. The cryogenic cave calcite tend to precipitate either as cryptocrystalline powders (a few μm in diameter) or as loose calcite pearls (< 1 mm to > 1 cm). The cryptocrystalline powders are composed of 3-8 μm euhedral and rhombohedral calcite crystals (Fig. 4) that are formed during non-equilibrium (kinetic) freezing of a calcium bicarbonate solution and are released on the floor of caves or surface of ice formations (e.g ice plugs, ice stalagmites, ice stalactites) through sublimation or melting of the ice (Clark and Lauriol, 1992). By contrast, the calcite pearls have highly variable morphologies including simple platy, pin-shaped and fan-shaped grains, to more complex aggregates of hemispheroidal and botryoidal shaped with smoothed surfaces as well as tubular, skeletal radiating and comb-shaped forms with sharp edges that range in size from less than 1 mm to more than 1 cm (Fig. 4). Zak et al. (2004) suggested that the calcite pearls tend to be formed during the slow freezing of water under equilibrium conditions.

2.2 Carbonate crusts

2.2.1 Subglacially precipitated carbonate

Thin calcite coatings are frequently observed on the lee side of clasts and on the surface of bedrock exposed by receding glaciers (Fig. 5). These calcite crusts, which are up to a few centimeters thick, have been reported near modern glaciers in the French Alps (Hallet, 1976; Souchez and Lemmens, 1985; Sharp et al., 1990; Fairchild et al., 1993; Hubbard and Hubbard, 1998), in the Rockies (Ford et al., 1970; Hanshaw and Hallet, 1978) and on bedrock in the Ottawa-Valley region which was glaciated by the Laurentide Ice Sheet during the late Pleistocene (Hillaire-Marcel et al., 1979). Micro-morphologically, these deposits are commonly laminated and are composed of micritic calcite crystals (Fig. 5). According to Hallet (1976), Hanshaw and Hallet (1978) and Souchez and Lemmens (1985), the calcite coatings precipitated subglacially as a result of pressure-melting on the stoss side of a bedrock protuberance, which

dissolved carbonate, followed by refreezing of the subglacial calcium bicarbonate meltwater on the lee side.

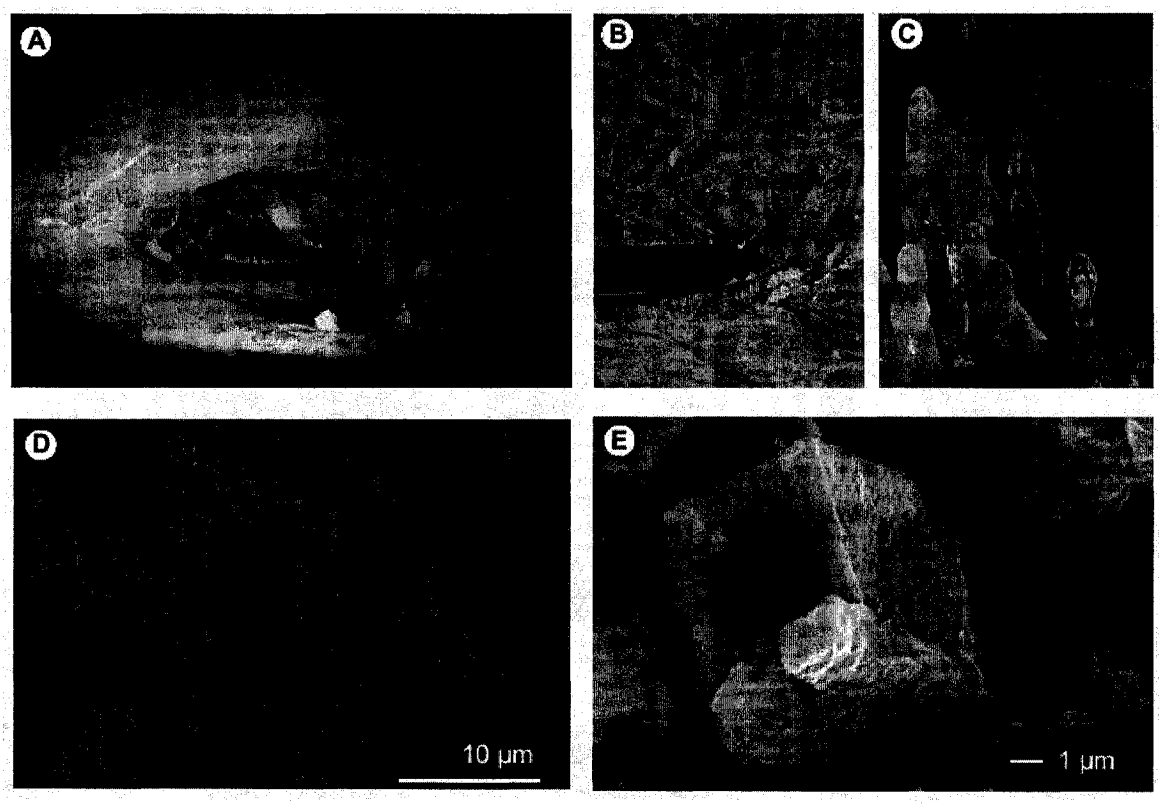

Figure 4. A) Grande Caverne Glacée, northern Yukon Territory; B-C) Various ice formations inside the cave on which cryptocrystalline cave calcite powders can be found. D-E) Micro-morphology (SEM images) of cryptocrystalline cave calcite powders.

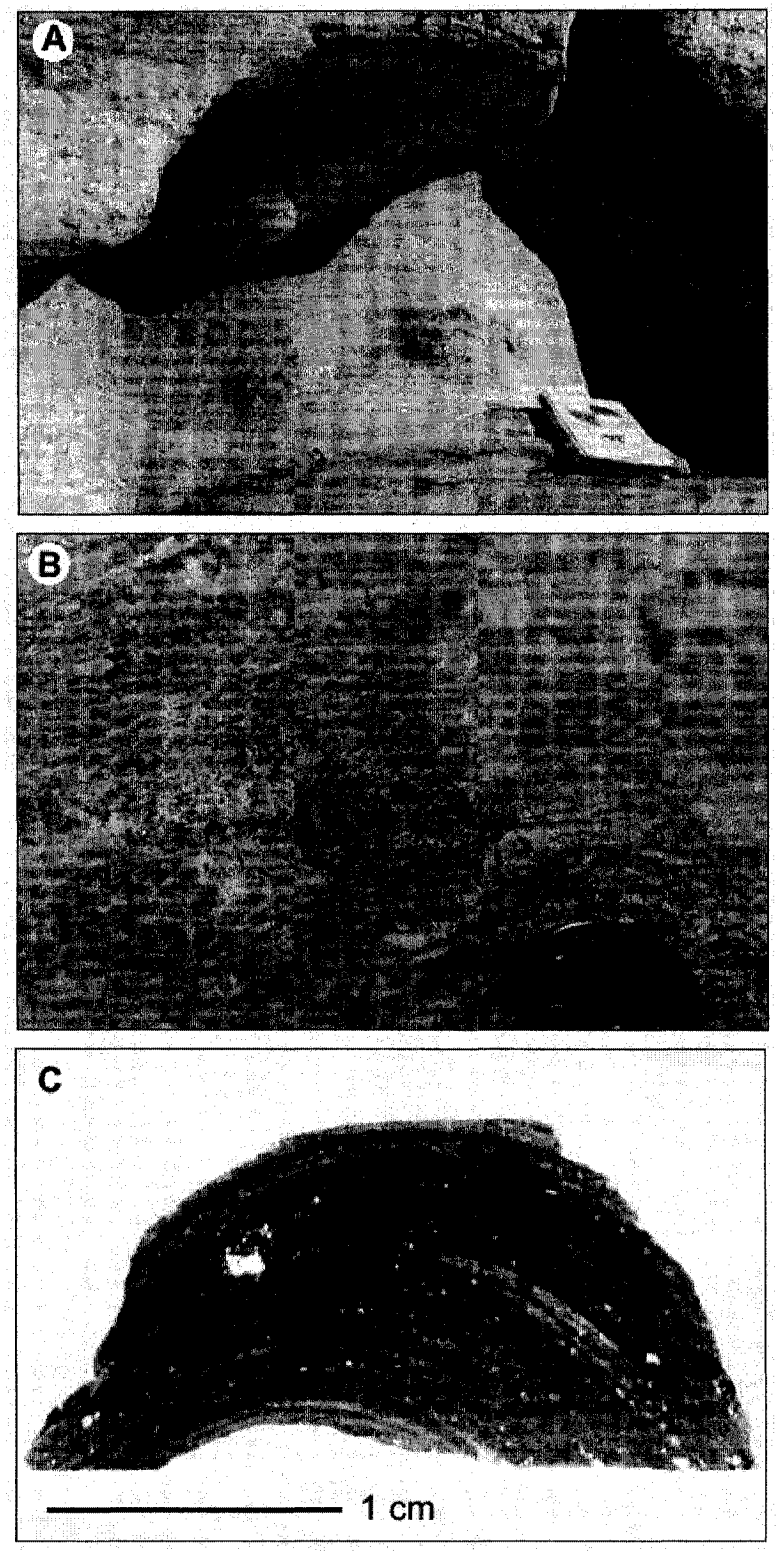

Figure 5. A-B) Pleistocene-age subglacially precipitated calcite on Grenvillian gneiss near Cantley, Québec. C) Thin-section of subglacially precipitated calcite showing laminations defined by dark and light colored bands.

2.2.2 Evaporative calcite crusts

Thin white calcite crusts that are located on the upper surface of clasts and bedrock in formerly glaciated regions, but which are not restricted to the lee-side of clasts, have been observed in southern Baffin Island (Lacelle et al., 2007), east-central Ellesmere Island (Blake, 2005) and northern Pakistan (Waragai, 2005 (Fig. 6). Micro-morphologically, these deposits appear unlaminated and are composed of micritic calcite crystals (Fig. 6). Although Blake (2005) didn't determine the exact nature of the east-central Ellesmere Island calcite crusts, Waragai (2005) and Lacelle et al. (2007) suggested that these deposits formed during the evaporation of proglacial streams or stagnating lakes following the retreat of glaciers. The similar morphology, micro-morphology and stable isotope composition of the east-central Ellesmere Island crusts with the southern Baffin Island calcite crusts suggest that it too might have a similar origin.

2.2.3 Active layer carbonates

Calcareous crusts developed on the lower surface of clasts within the active layer (surface layer of soil subjected to annual freezing and thawing) are the most common type of carbonate deposits reported in cold climate environments (Fig. 7). These deposits appear as thin (mm) to thick (cm) laminated crusts or pendants defined by alternating dark and light bands (Swett, 1974; Bunting and Christensen, 1978; Forman and Miller, 1984; Marlin et al., 1993; Courty et al., 1994; Vogt and Corte, 1996). The carbonates display a wide range of micro-morphologies consisting mostly of sparite and micrite crystals, suggestive of an inorganic precipitation, but fibrous piles of calcite platelets and acicular calcite crystals have also been observed (Vogt, 1977; 1989; Vogt and Corte, 1996). The precipitation of the calcareous deposits is thought to be induced by calcite supersaturation of a calcium bicarbonate solution during the freeze-back of the active layer, where the greater thermal conductivity of the gravels compared to the adjacent fine soil matrix allows for the freezing front to penetrate more rapidly to the underside of the clasts (Marlin et al., 1993; Courty et al., 1994; Vogt and Corte, 1996). However, intense evaporation (Bunting and Christensen, 1978) and biological (Swett, 1974; Parnell et al., 2006) processes have also been invoked to explain the formation of these deposits.

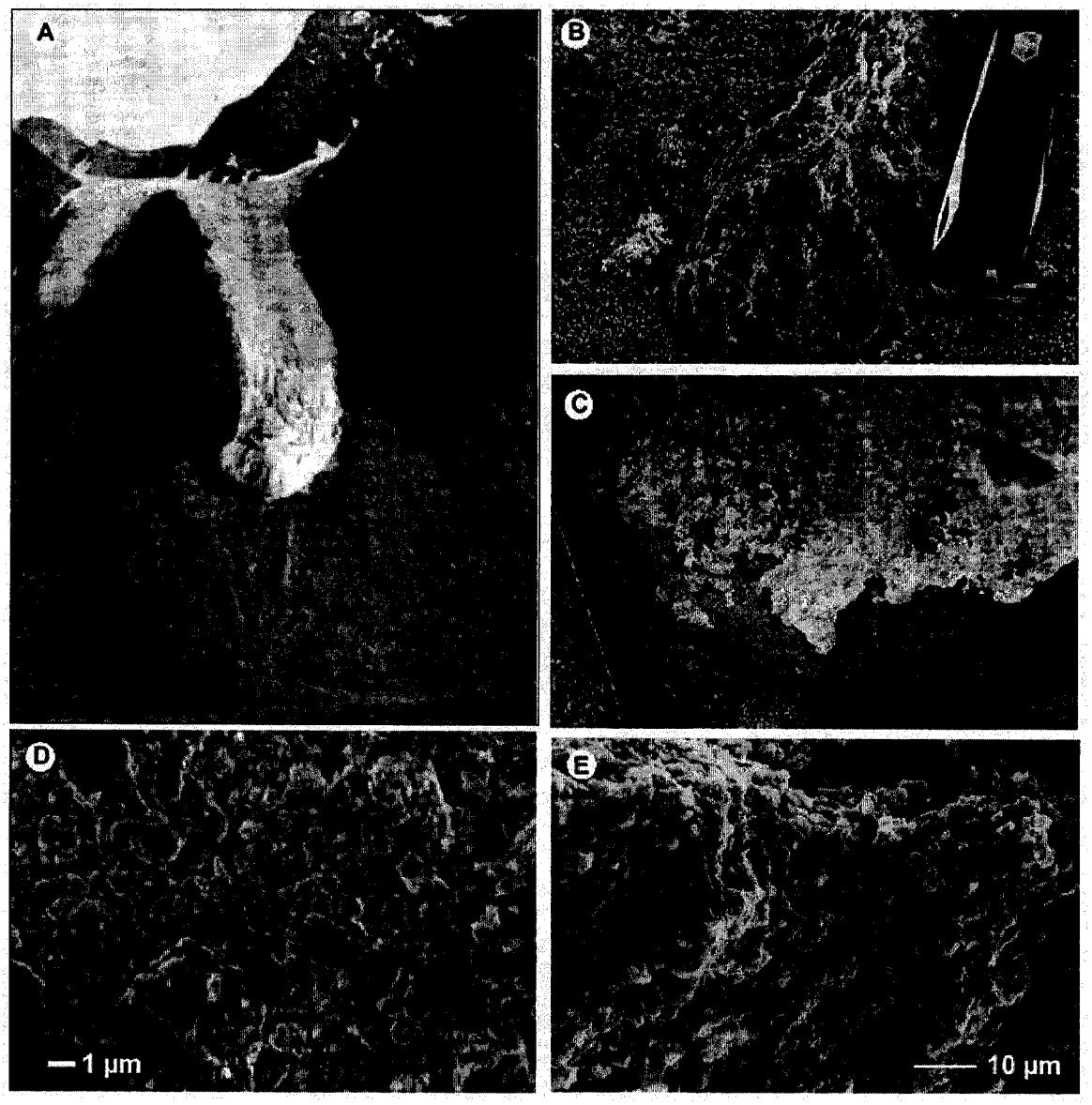

Figure 6 A) Nifhleim Glacier, Akshayuk Pass, southern Baffin Island, Nunavut. Evaporative calcite crusts are located on the upper surface of clasts within the moraine. B-C) Close-up of evaporative calcite crusts. D-E) Micro-morphology (SEM images) of evaporative calcite crusts.

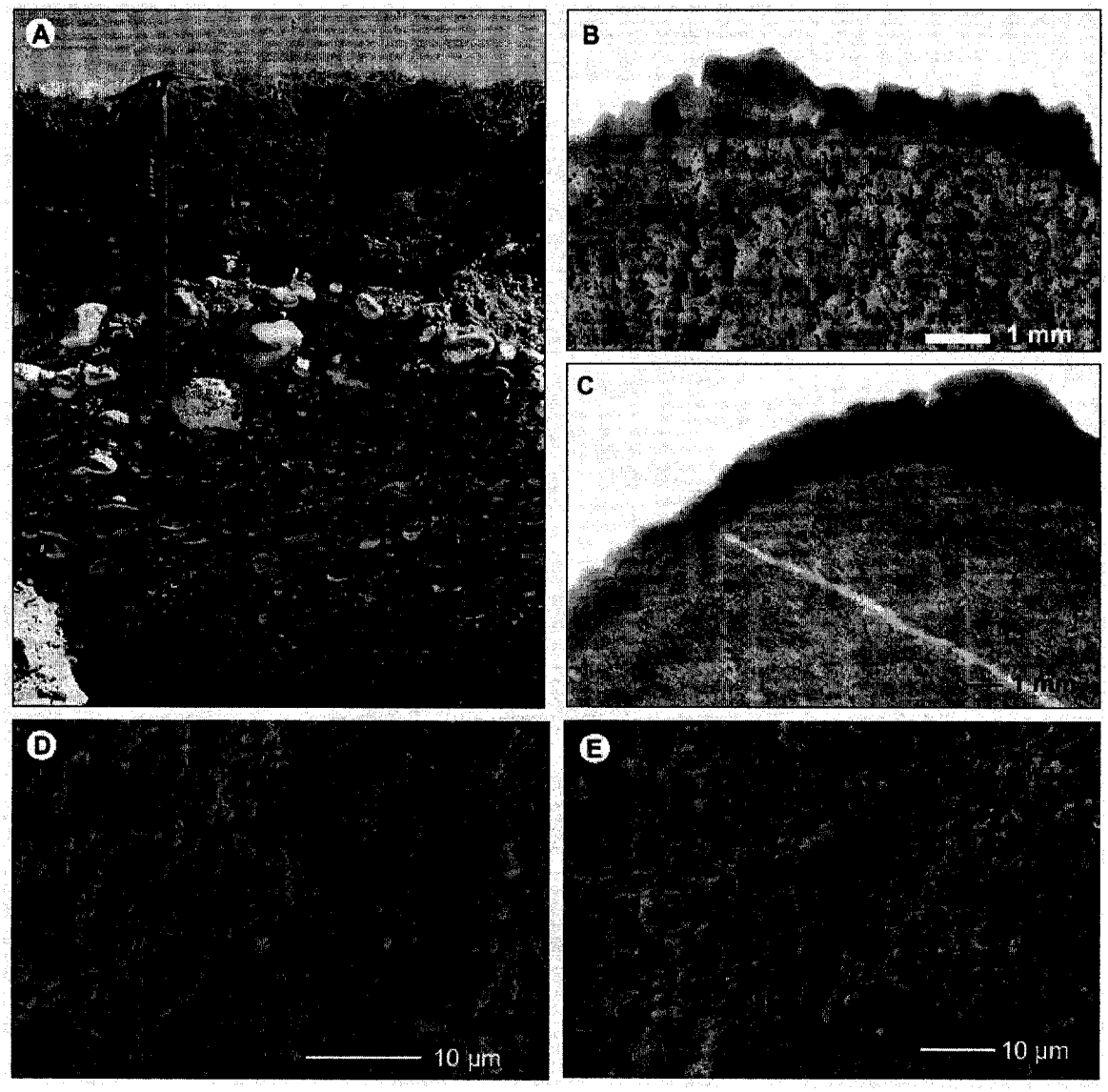

Figure 7. a) Pedogenic calcite crusts on the lower surface of clasts, Kluane Lake region, southern Yukon Territory. B-C) Thin sections of calcite crusts showing internal laminations. D-E) Micro-morphologies (SEM images) of calcite crusts.

2.2.4 Carbonate cemented crusts

Very little information is available about the origin of carbonate-cemented crusts in periglacial environments compared to the extensive literature of calcretes in (sub)tropical regions. Calcretes have been discovered in the Great Kobuk Sand Dunes (Alaska; Dijkmans et al., 1986) and at or near the soil surface in Patagonia (Argentina; Vogt and Del Valle, 1994). Morphologically, the carbonate-cemented crusts varied in width from a few mm to several decimeters and up to 5 cm thick. Two main processes have been advanced to explain their formation: 1) evaporation of the calcium bicarbonate solution which would eventually lead to calcite supersaturation of the solution and 2) degassing of CO_2 when the groundwater approaches the surface.

2.2.5 Endostromatolites

Endostromatolites have been observed within fissures on south facing limestone bedrock outcrops in the northern Yukon Territory and in / around the Haughton Impact Structure, Devon Island, Nunavut (Fig. 8). Endostromatolites consist of evenly-spaced laminated calcite columns that vary from less than 1 mm to 2-3 cm in height (Lauriol and Clark, 1999). Thin-sectioned endostromatolites reveal a 1 mm thick basal calcite layer that evolved into a 1-4 mm thick laminated calcite, which in turns developed into evenly spaced solitary or cauliflower texture columns of laminated calcite (Fig. 8). Laminations within the columns are defined by light and dark bands oriented across the individual columns, reminiscent of the internal structure of stromatolites. Viewed under SEM, the basal calcite layer is composed of sparite crystals, while the calcite columns and nodules are composed of micrite, micro-spartite and sparite crystals. The SEM images also allow to detect the presence of calcified microbiological structures that probably assisted in the precipitation of calcite during biomineralization (Fig. 8). The calcified micro-organisms consist of colonies of staphylocos, coccis parasites, non-organized bacilles, bacille parasites on unicellular organisms, streptobacillis and intertwined meshes of calcite needle fibers. Given the presence of calcified microbiological structures and a ^{13}C-NMR spectrum suggestive of a biogenic origin, Clark et al. (2004) ascribed the formation of endostromatolites to biomineralization in a methanogenic environment during anaerobic degradation of soil-derived organic carbon during periods of deepening of the active layer during the early Holocene warm interval and also probably around 80 ka BP (Ghaleb et al., 1997).

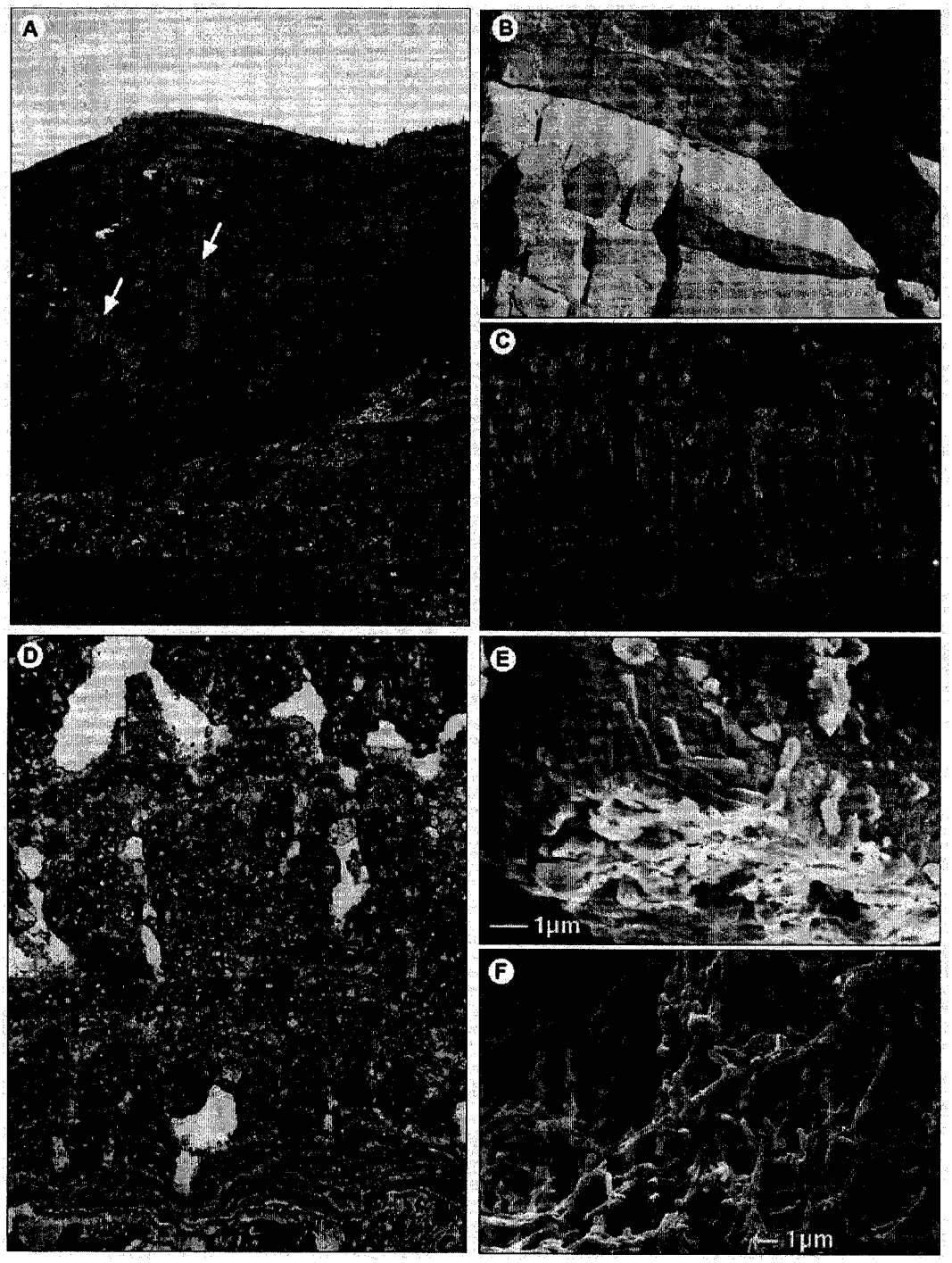

Figure 8. A) Landscape of the Ogilvie Mountains, central Yukon Territory. Endostromatolites are located in the bedrock outcrops indicated by arrows. B-C) Close-up of endostromatolites in fissures in limestone bedrock outcrops showing growth imprint on the inner face. D) Thin section of endostromatolites showing internal laminations and stromatolitic structures. E-F) Micro-morphology (SEM images) of endostromatolites.

3. Carbon and oxygen isotopic composition of cold-climate carbonates

3.1 Determining C-O equilibrium isotope exchange conditions

Carbonate isotope-exchange reactions involve the redistribution of heavy (^{13}C and ^{18}O) and light (^{12}C and ^{16}O) C-O isotopes among the various phases of carbonates, where the more condensed phase tends to be enriched in the heavier isotope (i.e. the $\delta^{13}C$ values of $CaCO_3$ > HCO_3^- > CO_2). There are two main phenomena that control isotope fractionation: equilibrium isotope exchange and kinetic processes, which depends primarily on the rate of reactions.

During equilibrium precipitation of calcite, the $\delta^{18}O$ of calcite is controlled by the $\delta^{18}O$ composition of the parent water and the temperature at which calcite precipitation occurred. At low temperature (i.e. freezing of calcium bicarbonate water), the $\delta^{18}O$ of calcite becomes enriched by 33.6‰ over the $\delta^{18}O$ of the parent water ($\varepsilon CaCO_3$-H_2O = 33.6‰ VSMOW at 0°C; Table 2), but the enrichment decreases to 28.1‰ at 25°C ($\varepsilon CaCO_3$-H_2O = 28.1‰ VSMOW at 25°C; Table 2). Likewise, the $\delta^{13}C$ of calcite represent a C isotope exchange reaction between dissolved bicarbonate (HCO_3^-) and calcite ($CaCO_3$), where the calcite is enriched by 3.6‰ at 0°C and by 2.4‰ at 25°C (Table 2). However, the $\delta^{13}C_{DIC}$ is set by the relative concentration of the DIC species ($CO_{2(g)}$ / HCO_3^- / CO_3^{2-}), which is controlled by the pH of the solution. As the solution evolves to higher pH through weathering processes, the $\delta^{13}C_{DIC}$ becomes progressively heavier (Fig. 9). The most enriched $\delta^{13}C_{DIC}$ occur at mid pH (6 – 8), where bicarbonate is the major component of DIC. Accordingly, the $\delta^{13}C$ of calcite is then mostly controlled by the initial pH and $\delta^{13}C_{DIC}$ of the solution and to a lesser extent temperature at which calcite precipitation occurred.

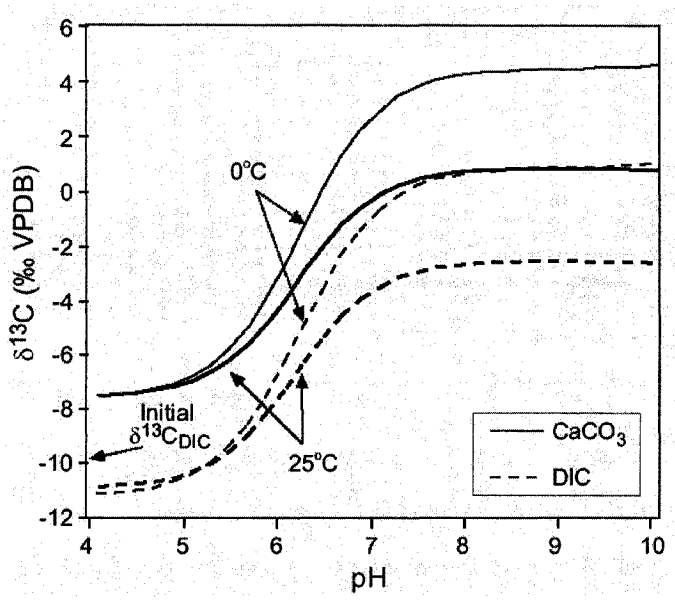

Figure 9. The $\delta^{13}C$ composition of DIC in equilibrium with a CO_2 of –10‰ at 0 and 25°C. Values are calculated using the relative contribution of the DIC species to weight their respective enrichment factor (Table 2). Also shown is the $\delta^{13}C$ of calcite precipitating in isotopic equilibrium with the solution.

Table 2: Equilibrium oxygen and carbon fractionation factors (1000 ln α) at 0 and 25°C.

Species pair	Enrichment factor (0°C)	Enrichment factor (25°C)	Reference
^{18}O $CaCO_3$-H_2O	33.6	28.1	Kim and O'Neil et al. (1997)
^{18}O CO_2-H_2O	45.6	40.1	Bottinga (1968)
^{13}C $CO_{2(g)}$-$CO_{2(aq)}$	−1.2	−1.1	Vogel et al. (1970)
^{13}C HCO_3-$CO_{2(g)}$	10.9	7.9	Mook et al. (1974)
^{13}C HCO_3-$CaCO_3$	3.6	2.4	Deines et al. (1974)
^{13}C CO_2-$CaCO_3$	14.4	10.4	Bottinga (1968)

3.2 Stable C-O isotope composition of cold-climate carbonates

A summary of the stable C-O isotope composition of cold-climate carbonate precipitates is presented in Fig. 10 and the complete compilation of the isotopic composition is given in Table 3. The cold-climate carbonate precipitates have a highly variable isotopic composition with $\delta^{18}O$ values ranging between –6.5 and 36‰ and $\delta^{13}C$ values in the –5 to 17‰ range. However each type of carbonate precipitates has a specific $\delta^{13}C$ and $\delta^{18}O$ range, suggesting that their environmental setting and the mechanism by which they formed controls their ^{13}C and ^{18}O signature. The most ^{18}O and ^{13}C enriched carbonates are the cryogenic cave calcite powders, followed by the evaporative calcite crusts and the endostromatolites. The most ^{18}O and ^{13}C depleted carbonates are the cryogenic aufeis calcite collected from an area of granitic bedrock, followed by Pleistocene-age subglacial calcite crusts.

Insights into the mechanistic controls on the $\delta^{18}O$ and $\delta^{13}C$ composition of calcite minerals are provided when the isotopic composition of the cold-climate carbonates (Table 3) is presented as a deviation (Δ) from the $\delta^{18}O$ and $\delta^{13}C_{DIC}$ of the water (Table 4) from which they precipitated (Fig. 11). Based on these values, cold-climate carbonates have $\Delta^{18}O_{CaCO3\text{-}H2O}$ and $\Delta^{13}C_{CaCO3\text{-}HCO3}$ that are consistent with precipitation under equilibrium to non-equilibrium conditions and can be divided into four groups: 1) Those that have $\Delta^{18}O$ and $\Delta^{13}C$ that are near equilibrium values (i.e. subglacially precipitated calcite; speleothems); 2) Those that have both $\Delta^{18}O$ and $\Delta^{13}C$ that are higher than the equilibrium values (i.e. cryptocrystalline cave calcite; evaporative calcite crusts); 3) Those that have $\Delta^{18}O$ lower than the equilibrium values but have $\Delta^{13}C$ near equilibrium values (i.e. cryogenic aufeis calcite; cave calcite pearls); 4) Those that have $\Delta^{13}C$ higher than the equilibrium values but have $\Delta^{18}O$ near equilibrium values (i.e. endostromatolites). In the following text, the potential mechanistic controls that can produce such groupings are discussed.

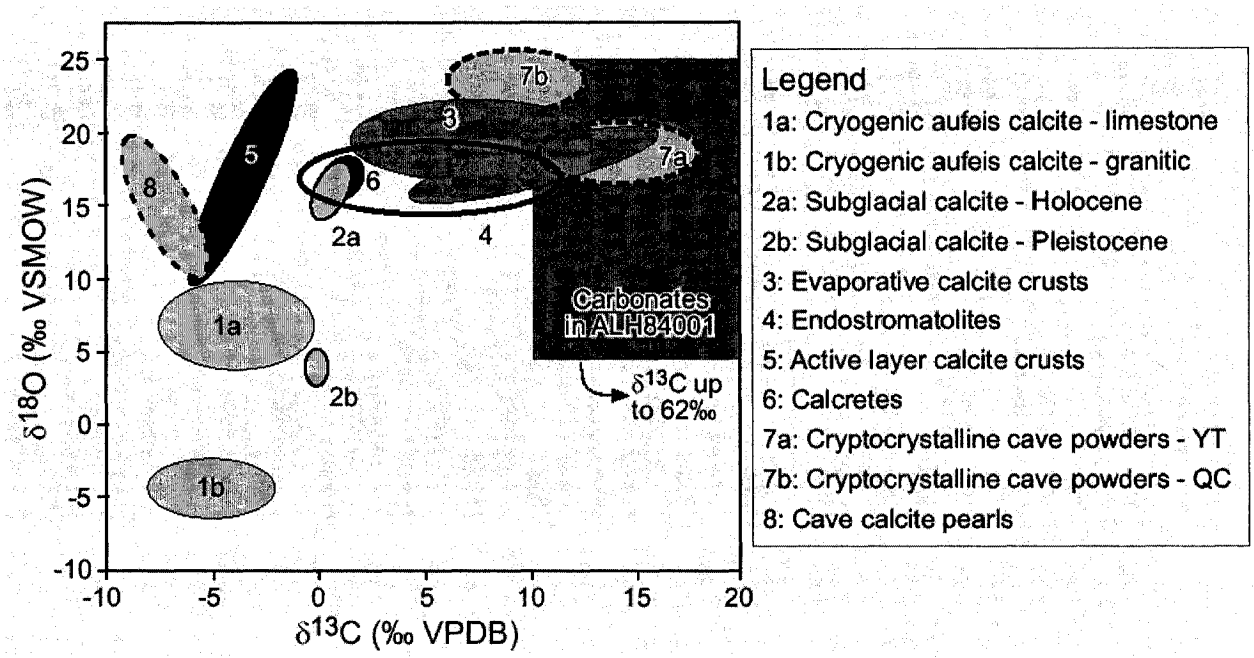

Figure 10. Summary of stable isotope composition of carbonate precipitates discussed in this study. The C-O range of the carbonate grains in ALH84001 is derived from Niles et al. (2005) and Leshin et al. (1998).

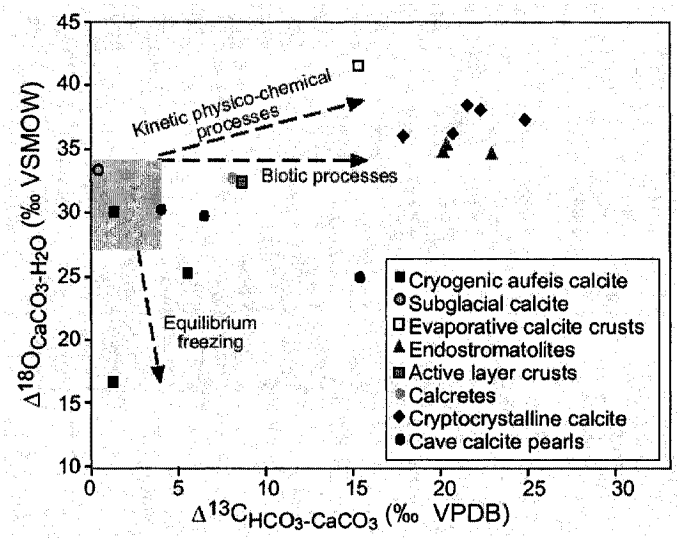

Figure 11. Deviation (Δ) of the C-O stable isotope composition of carbonate precipitates from that of the parent water. The average C-O stable isotope composition of the carbonates (Table 3) and waters (Table 4) was used in the calculation. The shaded box represents the range of equilibrium fractionation factors (0 to 25°C) between $CaCO_3$ -H_2O and $CaCO_3$ - HCO_3.

Table 3: Stable isotope ratios of oxygen and carbon of cold-climate carbonate precipitates discussed in this study.

Type of carbonate[a]	Oxygen-18 (‰ VSMOW)			Carbon-13 (‰VPDB)			Reference
	min	max	ave	min	max	ave	
Powders							
Cryogenic aufeis calcite							
Timber Creek, YT	8.3	8.7	8.5	–1.1	–0.9	–1.0	Lauriol et al. (1991)
Fish Hole, YT	4.7	8.8	6.7	–2.8	–2.3	–2.5	Lacelle et al. (2006)
Babbage River, YT	6.4	11.1	8.0	–7.2	–4.7	–5.8	Lacelle et al. (2006)
Little Fish Creek, NWT	3.5	3.8	3.6	–4.5	–4.4	–4.5	Lacelle et al. (2006)
Highway Glacier, Baffin Island,	–6.5	–2.7	–4.4	–7.6	–2.8	–5.6	Lacelle et al. (2006)
Cryptocrystalline cave calcite							
Bear Cave, YT	13.8	20.3	17.7	15.3	20.1	17.3	Clark and Lauriol (1992)
Grande Caverne Glacé, YT	14.0	21.7	18.9	9.7	17.0	14	Clark and Lauriol (1992)
Caverne-85, YT	10.8	19.3	15.5	6.8	13.2	9.9	Clark and Lauriol (1992)
Lusk Cave, QC	23.7	27.5	26.1	5.8	11.9	9.1	Clark and Lauriol (1992)
Caverne de l'Ours, QC	--	--	27.1	--	--	10.7	This study
Cave calcite pearls							
Stratenska Cave, Slovakia	6.2	13.4	*9.8*	3.0	6.0	*4.5*	Zak et al. (2004)
Jaworznicka Cave, Poland	10.3	19.6	*14.9*	–10.0	–4.0	*–7.0*	Zak et al. (2004)
Bulm Cave, Czech Republic	10.3	18.5	*14.4*	–6.0	–3.0	*–4.5*	Zak et al. (2004)
Crusts							
Subglacially precipitated							
Cantley, QC	3.1	4.6	4.0	–0.4	0.0	–0.1	Hillaire-Marcel et al. (1979)
Glacier de Tsanfleuron, Switzerland	22.9	25.2	23.9			–1.9	Souchez and Lemmens (1985) ; Sharp et al. (1990)
Blackfoot glacier, Montana, USA	14.5	17.6	15.7	–0.2	1.2	0.5	Hanshaw and Hallet (1978)
Evaporative calcite crusts							
Akshayuk Pass, Baffin Island,	16.7	22.0	19.4	1.6	12.0	8.4	Lacelle et al. (2007)
Cape Hershel, Ellesmere Island,	15.2	20.5	18.1	4.5	15.2	10.9	Blake (2005)
Lake Vanda, Antarctica	–0.4	22.3	*11.0*	–14.4	17.6	*1.6*	Nakai et al. (1975)
Active layer carbonate							
Kluane Lake, YT	9.8	16.2	12.8	–5.9	–4.3	–5.2	This study
Nye Alesund, Svalbard	23.3	25.2	*24.3*	–3	1.1	*–1.1*	Courty et al. (1994)
Calcretes							
Great Kobuk sand dunes, AK	16.1	17	16.5	0.05	1.8	1.1	Dijkmans et al. (1986)
Endostromatolites							
Bear Cave, YT	15.7	17.3	16.3	1.1	6.4	2.7	Lauriol and Clark (1999)
Caverne Helicoidale, YT	14.6	17.1	16.2	2.7	7.5	5.5	Lauriol and Clark (1999)
Ogilvie Mountains, YT	14.2	24.4	17	–0.1	11.4	2.9	Clark et al. (2004)
Speleothems							
Bear Cave, YT	–18.0	–15.0	*–17.5*	–8.0	–5.0	*–6.5*	Lauriol et al. (1997)
Tsi-it-toh-Choh, YT (ancient)	–20.0	–16.0	*–18.0*	–6.0	–5.0	*–5.5*	Lauriol et al. (1997)
Tsi-it-toh-Choh, YT	–20.0	–16.0	*–18.0*	–1.0	5.0	*2.0*	Lauriol et al. (1997)
Castleguard, AB	–19.0	–16.0	*–17.0*	–2.0	1.0	*–0.5*	Harmon et al. (1983)

Note: The stable isotope of oxygen ($\delta^{18}O$) and carbon ($\delta^{13}C$) is presented in the δ-notation, which is the normalized difference between the sample and a standard, i.e. $\delta^{18}O = [(^{18}O/^{16}O)spl / (^{18}O/^{16}O)std] - 1 \cdot 1000‰$.
a: See Fig. 1 and Table 1 for sample location and site description respectively.
Italic isotopic data represent estimated values.

Table 4: Stable isotope ratios of oxygen and dissolved inorganic carbon of water from which the carbonates discussed in this study precipitated from.

Type of carbonate[a]	Oxygen-18 (‰ VSMOW)			Carbon-13 (‰VPDB)			Reference
	min	max	ave	min	max	ave	
Powders							
Cryogenic aufeis calcite							
Timber Creek, YT	–23.9	–22.7	–23.3	--	--	--	Lauriol et al. (1991)
Fish Hole, YT	–22.6	–21.1	–21.9	--	--	--	Lacelle et al. (2006)
Babbage River, YT	–23.8	–20.7	–21.9	–9.0	–4.9	–7.2	Lacelle et al. (2006)
Little Fish Creek, NWT	–22.0	–20.8	–21.4	–10.6	–0.1	–10.0	Lacelle et al. (2006)
Highway Glacier, Baffin Island,	–22.4	–20.4	–21.1	–11.3	–3.1	–6.9	Lacelle et al. (2006)
Cryptocrystalline cave calcite							
Bear Cave, YT	--	--	–19.5	--	--	–7.6	Clark and Lauriol (1992)
Grande Caverne Glacé, YT	--	--	–19.5	--	--	–7.6	Clark and Lauriol (1992)
Caverne-85, YT	--	--	–20.5	–8.5	–7.6	–8.0	Clark and Lauriol (1992)
Lusk Cave, QC	--	--	–11.0	–13.4	–6.3	–10.6	Clark and Lauriol (1992)
Caverne de l'Ours, QC	–14.2	–9.0	–11.0	--	--	–11.5	This study
Cave calcite pearls							
Stratenska Cave, Slovakia	–17.0	–14.0	–15.0	--	--	–11.0	Zak et al. (2004)
Jaworznicka Cave, Poland	–17.0	–14.0	–15.0	--	--	–11.0	Zak et al. (2004)
Bulm Cave, Czech Republic	–17.0	–14.0	–15.0	--	--	–11.0	Zak et al. (2004)
Crusts							
Subglacially precipitated							
Cantley, QC	–31.8	–27.5	--	--	--	--	Hillaire-Marcel et al. (1979)
Glacier de Tsanfleuron, Switzerland	–15.8	–9.3	–12.1	--	--	–2.4	Souchez and Lemmens (1985) ; Sharp et al. (1990)
Blackfoot glacier, Montana, USA	--	--	–14.8	–0.1	1.6	0.9	Hanshaw and Hallet (1978)
Evaporative calcite crusts							
Akshayuk Pass, Baffin Island,	–22.5	–21.8	–22.2	–11.3	–3.1	–6.9	Lacelle et al. (2007)
Cape Hershel, Ellesmere Island,							Blake (2005)
Lake Vanda, Antarctica	–31.9	–29.9	--	--	--	--	Nakai et al. (1975)
Active layer carbonate							
Kluane Lake, YT	--	--	--	--	--	--	This study
Nye Alesund, Svalbard	--	--	–8.2	–10	–9	*–9.5*	Marlin et al. (1993)
Calcretes							
Great Kobuk sand dunes, AK	--	--	–16.0	–11.5	–3.0	*–7.0*	Dijkmans et al. (1986)
Endostromatolites							
Bear Cave, YT	--	--	–18.5	–20.0	–15.0	–17.5	Lauriol and Clark (1999)
Caverne Helicoidale, YT	--	--	–18.5	–20.0	–15.0	–17.5	Lauriol and Clark (1999)
Ogilvie Mountains, YT	--	--	–18.5	–20.0	–15.0	–17.5	Clark et al. (2004)

Note: The stable isotope of oxygen ($\delta^{18}O$) and dissolved inorganic carbon ($\delta^{13}C_{DIC}$) is presented in the δ-notation, which is the normalized difference between the sample and a standard, i.e. $\delta\,^{18}O = [(^{18}O/^{16}O)spl / (^{18}O/^{16}O)std] - 1 \cdot 1000‰$. Italic isotope data represent estimated values.

a: See Fig. 1 and Table 1 for sample location and site description respectively.

3.2.1 Group 1: $\Delta^{18}O$ and $\Delta^{13}C$ near equilibrium values

The subglacially precipitated calcite are the only cold-climate carbonate precipitates that have $\Delta^{18}O_{CaCO3\text{-}H2O}$ and $\Delta^{13}C_{CaCO3\text{-}HCO3}$ values that are near equilibrium ($\Delta^{18}O$ and $\Delta^{13}C$ of 33.3‰ and 0.5‰ respectively). Given that these deposits have only been discovered in areas of limestone bedrock, it is assumed that the subglacial meltwater from which they precipitated was at or near saturation with respect to calcite mineral and that the subglacial calcite crusts precipitated during the initial stage of freezing. At Glacier de Tsanfleuron, Fairchild et al. (1994) provided geochemical evidence that the subglacial meltwater is near calcite saturation. Therefore during the refreezing of the calcite saturated subglacial meltwater on the lee-side of bedrock obstacle, the ^{18}O and ^{13}C of the calcite crusts will tend to reflect that of the subglacial meltwater as the isotopic fractionation associated with freezing will be very limited.

3.2.2 Group 2: $\Delta^{18}O$ and $\Delta^{13}C$ higher than equilibrium values

Cold-climate carbonate precipitates that exhibit both $\Delta^{18}O_{CaCO3\text{-}H2O}$ and $\Delta^{13}C_{CaCO3\text{-}HCO3}$ higher than the equilibrium values (in the 15.3 to 24.9‰ range $\Delta^{13}C_{CaCO3\text{-}HCO3}$ and between 36.1 and 41.6‰ for $\Delta^{18}O_{CaCO3\text{-}H2O}$) include the cryptocrystalline cave calcite powders and evaporative calcite crusts (Fig. 11), for which the formation was ascribed to non-equilibrium freezing and evaporation respectively. Kinetic isotope exchange reactions occur when the rate of reaction is increased, which can be produced by a sudden change in temperature or relative humidity. The degree of isotopic disequilibrium is dependent on the ratios of the masses of the isotopes, their vibrational, translational and rotational energies (Urey, 1947). Although not systematic, kinetic fractionation generally leads to an enrichment of the heavy isotope in the more condensed phase (i.e calcite) (Kim and O'Neil, 1997).

Clark and Lauriol (1992) and Lacelle et al. (2007) produced a series of laboratory experiments to verify the degree of isotopic disequilibrium during freezing and evaporation (respectively) of low ionic strength water and synthetic calcium-bicarbonate solutions. It was found that the rapid freezing of a bicarbonate-rich solution produced a $\varepsilon^{18}O_{KIE}$ $CaCO_3$-H_2O = 36.7 ± 1.3‰ (Table 5), which is a few permil greater than the equilibrium fractionation value of 33.6‰ at 0°C. The kinetic evaporation experiment produced a lesser $\varepsilon^{18}O_{KIE}$ (34.9 ± 3.7‰; Table 5) relative to the non-equilibrium freezing experiment. This slight decrease in $\varepsilon^{18}O_{KIE}$ is not surprising considering that isotope fractionation is a thermodynamic reaction that is reduced

to unity at high temperature, even during kinetic reactions. The effect of non-equilibrium freezing of the bicarbonate-rich water is more drastic, as it produced a carbon isotope partitioning between $CaCO_3$ and HCO_3 of 16.7 ± 2.0‰ (Table 5), which is considerably greater than the isotopic fractionation under equilibrium conditions (10.3‰ at 0°C; Mook et al., 1974). The kinetic evaporation of the bicarbonate-rich water experiments produced a carbon isotope partitioning between $CaCO_3$ and HCO_3 of 16.5 ± 8.7‰ (Table 5). Therefore, the rapid rate of precipitation, whether it was induced by sudden changes in temperature or relative humidity, effectively precluded isotopic equilibrium to be reached and produced a strong isotopic disequilibrium between $CaCO_3$ and the escaping CO_2 through this reaction:

$$Ca^{2+} + 2HCO_3^- \rightarrow CaCO_3 + H_2O + CO_2 \uparrow \qquad [1]$$

The kinetic isotope enrichment most probably occurs during the dehydration of bicarbonate ($HCO_3^- \rightarrow CO_2 + H^+$), given that the amount of fractionation during the precipitation of bicarbonate as calcite is relatively small (Mook et al., 1974; Turner, 1982). The fact that the ^{13}C enrichment is much greater than the ^{18}O one is due to the fact that only one C atom participate in the reaction.

Table 5: Experimentally determined kinetic oxygen and carbon fractionation factors (1000 ln α) of low ionic strength water.

		^{13}C (‰ VPDB)					^{18}O (‰ VSMOW)			
Solution	Volume (ml)	CO_2	DIC	$CaCO_3$	$\Delta CaCO_3$-CO_2	$\Delta CaCO_3$-HCO_3	H_2O	$CaCO_3$	$\Delta CaCO_3$-H_2O	Reference
Freezing (-40°C)										
UO-3	5.0	–49.0	–33.1	–13.5	35.5	19.6	–10.5	25.0	35.6	Clark and Lauriol (1992)
UO-3	5.0	–49.0	–33.1	–17.7	31.3	15.4	–10.5	28.0	38.5	Clark and Lauriol (1992)
UO-3	5.0	–46.8	–33.1	–17.1	29.7	16.0	–10.5	25.7	36.2	Clark and Lauriol (1992)
UO-3	5.0	–45.7	–33.1	–17.5	28.2	15.6	–10.5	26.0	36.5	Clark and Lauriol (1992)
Average					*31.2*	*16.7*			*36.7*	
Stdev					*3.1*	*2.0*			*1.3*	
Evaporation (22°C)										
UO-A	0.1	–41.6	–33.2	–1.1	40.5	32.1	–13.3	17.2	30.5	Lacelle et al. (2007)
UO-A	0.2	–41.6	–33.2	–20.3	21.3	12.9	–13.3	22.4	35.7	Lacelle et al. (2007)
UO-A	0.2	–41.6	–33.2	–20.1	21.5	13.1	–13.3	18.3	31.6	Lacelle et al. (2007)
UO-B	0.2	–39.6	–31.1	–19.4	20.2	11.7	–14.5	24.8	39.3	Lacelle et al. (2007)
UO-B	0.2	–39.6	–31.1	–18.4	21.2	12.7	–14.5	22.8	37.3	Lacelle et al. (2007)
Average					*19.9*	*16.5*			*34.9*	
Stdev					*7.8*	*8.7*			*3.7*	

3.2.3 Group 3: $\Delta^{18}O$ lower than equilibrium values and $\Delta^{13}C$ near equilibrium values

Cold-climate carbonate precipitates that show $\Delta^{18}O_{CaCO3\text{-}H2O}$ that lower than equilibrium and $\Delta^{13}C_{CaCO3\text{-}HCO3}$ that is near equilibrium values include the cryogenic aufeis calcite and cave calcite pearls (Fig. 11). In fact, for these deposits, the $\Delta^{18}O$ (between 16.7 and 31.8‰) indicates that the carbonate precipitated from a water that had a very low $\delta^{18}O$ value.

There is only one mechanism that can produce such an isotopic effect, equilibrium freezing under closed-system. For the cryogenic aufeis calcite, this process is supported by field observations (Heldmann et al., 2005) and the $\delta^{18}O$ stratigraphy of aufeis ice (Clark and Lauriol, 1997). During the freezing of a solution, the $\delta^{18}O$ composition of the remaining solution is controlled by a Rayleigh-type fractionation, which is an exponential equilibrium function that describes the progressive partitioning of O isotope as the reservoir diminishes in size. In δ (‰) nomenclature, the Rayleigh fractionation can be expressed as:

$$\delta = \delta_0 + \varepsilon \ln f \qquad [2]$$

where δ and δ_0 are the final and initial $\delta^{18}O$ (‰) values respectively, $\varepsilon = (\alpha - 1)\ 1000$, where α is the ^{18}O fractionation factor between water and ice, and f is the fraction of water remaining in solution.

For example, as freezing of a solution proceeds the remaining water becomes progressively depleted in ^{18}O with respect to the initial $\delta^{18}O$ of the solution and extreme depletion of up to 12‰ are measured when the solution has completely frozen. The extent of ^{18}O depletion is in part controlled by the initial calcite saturation state of the solution, where those that are undersaturated with respect to calcite, such as the cryogenic aufeis calcite located in areas of granitic bedrock (Fig. 10), will tend to have highly depleted $\delta^{18}O$ values since the calcite saturation state is expected to be reached in the late stage of freezing (Lacelle et al., 2006).

The effect of freezing on the $\delta^{13}C_{DIC}$ is still not well understood, but some studies suggested that the $\delta^{13}C_{DIC}$ would progressively increase (Socki et al., 2001; Zak et al., 2004). During freezing of a calcium bicarbonate solution and prior to reaching calcite supersaturation, the pH of the residual water remains invariant (< 0.1 pH unit change; modeled using PHREEQC; Parkhurst and Appelo, 1999). However, once calcite supersaturation is reached, CO_2 solubility is

decreased due to the removal of water and gaseous CO_2 from the solution through reaction [1]. Since there is little carbon isotope fractionation between the $\delta^{13}C_{DIC}$ and $\delta^{13}C$ of calcite during calcite precipitation ($\varepsilon CaCO_3$-HCO_3 = 3.6‰; Table 2), the progressive removal of light CO_2 from the system can cause an enrichment in $\delta^{13}C_{DIC}$, and consequently on the ^{13}C of calcite. Therefore, the enrichment caused by the degassing of light CO_2 during calcite precipitation under closed-system freezing can be modeled according to a Rayleigh-type distillation [eq. 2] and using ½ (εCO_2-HCO_3^- + εHCO_3^--$CaCO_3$) as the fractionation factor since carbon is evenly divided between two phases (calcite and CO_2) (carbon all converted to CO_2 and calcite). The modeling shows a progressive, but slight increase (up to 4‰) relative to the initial $\delta^{13}C_{DIC}$ in the residual solution and calcite during closed-system freezing, but also an increase in the partial pressure of CO_2 gas. If this process is to operate during the precipitation of cryogenic aufeis calcite, the CO_2 gas must be able to escape from the system, either as occluded air bubbles in the ice or through the micro-fractures along the candle ice that form the aufeis to allow calcite to precipitate. Killawee et al. (1998) have experimentally demonstrated that the precipitation of calcite during closed-system freezing of a calcium bicarbonate solution produced CO_2 rich gas inclusions (ppm to 65% CO_2) within the ice, which allowed for calcite to precipitate. Such a process might also operate during the precipitation of cryogenic aufeis calcite, however, no field measurements exist to verify this hypothesis.

3.2.4 Group 4: $\Delta^{18}O$ near equilibrium values and $\Delta^{13}C$ higher than equilibrium values

Endostromatolites are the only cold-climate carbonate precipitates that have $\Delta^{18}O_{CaCO3\text{-}H2O}$ near equilibrium values and $\Delta^{13}C_{CaCO3\text{-}HCO3}$ higher than equilibrium values (Fig. 11). Endostromatolites are biogenically precipitated calcite by methanogenic bacteria (Lauriol and Clark, 1999; Clark et al., 2004). Biogenic processes, such as methanogenesis or photosynthesis, have little effect on the $\delta^{18}O$ composition of the water, since the kinetics of reaction of organics with O_2 are not quantitatively important and of little importance in geochemical evolution (Drever, 1997), which is why the $\delta^{18}O$ of calcite is in near equilibrium with the $\delta^{18}O$ of the parent water and the temperature at which the precipitation occurred.

By contrast, biologically mediated reactions (methanogenesis and photosynthesis) prefer to metabolize the isotopically light organics, which affects the C composition in the various phases

involved. Arctic environments are prone to methane (CH_4) production since the presence of permafrost restricts groundwater circulation and helps to maintain near-surface saturated soil conditions, a criteria necessary for the development of methanogenesis. There are two principal biologically mediated reactions associated with methanogenesis:

acetate fermentation,

$$CH_3COO^- + H_2O \rightarrow HCO_3^- + CH_4 \quad [3]$$

and CO_2 reduction,

$$CO_2 + 4H^+ \rightarrow CH_4 + 2H_2O \quad [4]$$

In both reactions, methanogenic bacteria preferentially metabolize ^{12}C, which generates strong thermo-dynamic fractionation between CO_2 and CH_4 (i.e. approximately 70‰ at 25°C; Whiticar et al. 1986). During acetate fermentation, the DIC concentration increases and the $\delta^{13}C_{DIC}$ values approaches the values near those of the organic matter in the aquifer. By contrast, the consumption of CO_2 imparts a Rayleigh distillation of ^{13}C enrichment on the residual $\delta^{13}C_{DIC}$ (e.g. Clark et al., 2004). The consumption of CO_2 also drives calcite supersaturation in the solution and consequently the precipitating calcite will be enriched in ^{13}C relative to equilibrium $\delta^{13}C$values.

Photosynthesis is another biologically mediated process that can progressively increase the $\delta^{13}C_{DIC}$ and calcite supersaturation in a solution during,

the consumption of CO_2,

$$CO_2 + H_2O \rightarrow CH_2O + O_2 \quad [5]$$

or by increasing alkalinity through the removal of HCO_3^- during the production of hydroxide,

$$HCO_3^- + H_2O \rightarrow CH_2O + O_2 + OH^- \quad [6]$$

The former process has been advanced by Sharp et al. (1990) to explain the enriched $\delta^{13}C$ composition (up to 8‰) of a few subglacially precipitated calcite at Glacier de Tsanfleuron. In a recent study, Léveillé et al. (2006) presented a summary of carbon isotope evolution during microbial photosynthesis based on the simultaneous measurements of ^{13}C of calcite and of the organic matter contained in the calcite. It was found that the microbial photosynthesis is accompanied by a $\Delta^{13}CCaCO_3$-OM of ~ 31‰. A similar value was measured in the biogenically-precipitated endostromatolites in the northern Yukon Territory ($\Delta^{13}CCaCO_3$-OM ~30‰). The similar spread between $\delta^{13}C_{org}$ and $\delta^{13}C$ of calcite is due to the fact that microbial photosynthesis (or methanogenesis) preferentially utilized the light C isotope (^{12}C) in the DIC carbon pool as their carbon source, leading to a congruent increase in $\delta^{13}C_{org}$ and $\delta^{13}C_{DIC}$ (Meyers and Lallier-Vergès, 1999). Therefore, the simultaneous measurement of ^{13}C in calcite and of the organic matter contained in the calcite deposit could be an efficient way of determining if biologically meditated reactions occurred prior / during the precipitation of carbonates in areas where the water cannot be sampled.

4. Implications

4.1 Paleoclimatic proxies

As our climate is warming, a better understanding of past climatic and environmental conditions is becoming necessary. Quantitative reconstructions of paleotemperatures generally rely on the $\delta^{18}O$ composition of glacier ice, such as the Greenland ice cores (GRIP; GISP2), Canadian Arctic ice cores (Fisher et al., 1998; Zdanowick et al., 2002) and Antarctic ice cores (Epica Community Members, 2004). In regions where glacier ice is not available, paleotemperature information are being retrieved from speleothems since it provides a record of the $\delta^{18}O$ of the water (e.g. McDermott 2004; Fairchild et al. 2006 and reference therein). The use of speleothems as paleoclimatic proxies relies on the $\delta^{18}O$ record preserved in the carbonate and the global $\delta^{18}O$-T°C relation ($\delta^{18}O = 0.69\ T°C - 13.6$) developed by Dansgaard (1964), providing that the water from which the carbonate formed reflects the local mean annual air temperature.

To date, few studies have explored the potential of carbonate deposits in polar regions as paleoclimatic proxies. Based on this review of the stable C-O isotope composition of cold-

climate carbonate precipitates and assessment of isotopic disequilibrium during their precipitation, it was found that the $\delta^{18}O$ composition of most cold-climate carbonate precipitate rarely reflect that of the parent water since the latter is being modified by equilibrium physico-chemical processes, such as freezing and evaporation, prior to the calcite being precipitated. Even in limestone environment, where the solution is near equilibrium with respect to calcite mineral, the $\delta^{18}O$ signature of calcite rarely reflect that of the $\delta^{18}O$ of water (Fig. 11). Consequently the $\delta^{18}O$ values of the carbonate deposits cannot be used in conjunction with Dansgaard's global $\delta^{18}O$-T°C relation to retrieve paleotemperature informations. There is however two exceptions, the subglacially precipitated calcite and the endostromatolites, and potentially other types of biogenic carbonate precipitates. Ford et al. (1970) and Hallet et al. (1978) suggested that subglacially-precipitated carbonate deposits may be used as paleoclimatic proxies because they thought the it recorded information about the $\delta^{18}O$ composition of the glacier ice meltwater at the time of precipitation. However, Souchez and Lemmens (1985) and Sharp et al. (1990) questioned the use of subglacially-precipitated carbonate as effective climatic proxies because they discovered that glacier ice is not necessarily at the origin of the meltwater that gives rise to the subglacially-precipitated carbonate deposits, but rather the melting of basal ice layers, which is usually slightly enriched over glacier ice. In comparison with most carbonate deposits, the $\delta^{18}O$ signal of endostromatolites is not modified by secondary physico-chemical processes, since the water-saturated conditions during the growth of the endostromatolites allowed for the $\delta^{18}O$ values of the groundwaters from which the calcite precipitated to be well-preserved. As a result, Clark et al. (2004) extracted a valuable $\delta^{18}O$ summer air temperatures record during the early Holocene period from the endostromatolites formed in fissures in bedrock outcrops in the northern Yukon Territory. Overall, these observations indicate that a complete understanding of the growth process of the carbonate deposits is necessary before any paleoclimatic and paleoenvironmental information can be retrieved.

4.2 Analogues to Martian meteorite ALH84001

Direct evidence of past water on Mars has been provided by the recent images of Mars Global Surveyor in the form of carved canyon, debris flows, polygonal ground and other geomorphological features (Kuzmin, 2005) and by the discovery of carbonate minerals in the

Martian meteorite ALH84001. The 3.9 Ga years old carbonate minerals in the meteorite consist of small (< 50 μm in diameter) ellipsoidal and disc-shaped grains that exhibit a strong chemical (Harvey and McSween, 1996) and isotopic zoning (Valley et al., 1997; Leshin et al., 1998), with maximum $\delta^{13}C$ values of 62‰ (10 – 62‰ VPDB) and $\delta^{18}O$ values of 25‰ (5 – 25‰ VSMOW) measured at the rim (Niles et al., 2005). Since its finding, many studies discussed the possible origins and environments by which these carbonates might have formed on Mars. So far, it was suggested that the carbonates grains in ALH84001 precipitated: *i*) from low-temperatures groundwater (0 to 80°C; Romanek et al., 1994); *ii*) from high pH groundwater discharging to the Martian surface (Anders, 1996); *iii*) from the mixing of chemically and isotopically distinct fluids (Niles et al., 2005); *iv*) from high-temperature shock-impact metamorphism (> 200°C; Mittlefehldt, 1994); and *v*) as a direct result of microbial action (Mackay et al., 1996).

Cold-climate carbonate precipitates are being regarded as potential analogues to the carbonate in ALH84001 (Omelon et al., 2001; Socki et al., 2001; Socki et al., 2003; Socki et al., 2004; Niles et al., 2004; Parnell et al., 2006). While key distinctions exist between Arctic regions and Mars, such as temperature minimums (–140 vs. –50°C) and atmospheric pressure (6 mbar vs. 1 bar), several features encountered in Arctic regions (i.e. continuous permafrost, polar deserts, glacial landscapes, perennial springs, meteorite impact craters and unique biological habitats) approximate those that may exist or have existed on Mars. In this study, the stable C-O isotope composition and formative mechanisms of various types of cold-climate carbonate precipitates have been examined. Of the list of 29 cold-climate carbonate precipitates compiled in this study, only the cryogenic cave calcite powders and evaporative calcite crusts have enriched ^{13}C and ^{18}O composition (Fig. 11). Although the maximum and range of $\delta^{13}C$ values obtained in these terrestrial carbonate precipitates is much lower and restricted than those of the carbonate grains in ALH84001 (Fig. 10), the larger spread in ^{13}C in the ALH84001 carbonate grains might be irrelevant since the ultimate control on the $\delta^{13}C$ composition of carbonate is the $\delta^{13}C$ of the carbon reservoir from which it is drawn. Right now, the overall composition of the Martian carbon pool is unknown and there is no reason to assume that it is similar to that of earth. Mars had presumably no large organic carbon reservoirs to interact with the inorganic carbon pools, as evidenced by the estimate of the $\delta^{13}C$ composition of the modern Martian atmosphere of 36‰ (Carr et al., 1985), which might be one of the reasons for much higher $\delta^{13}C$ values in the carbonate grains in ALH84001.

Freezing (Socki et al., 2001; Socki et al., 2003; Niles et al., 2004) and evaporative processes (Warren, 1998; McSween and Harvey, 1998) have already been suggested as plausible mechanism for the carbonate grains in ALH84001, but the latter was strongly criticized since it failed to appropriately explain the observed isotopic systematic in the carbonates in ALH84001. The problem with the evaporative models lied in the opposite effect of the ionic strength (degree of salinities) of the water on the isotopic composition of the residual water during evaporation. During evaporation of freshwater, enrichments > 20‰ in $\delta^{18}O$ can be measured in the residual water through equilibrium Rayleigh fractionation, but enrichments in $\delta^{13}C$ remained limited by the exchange with atmospheric CO_2. Conversely, during the evaporation of high ionic strength water, the $\delta^{18}O$ of the water is progressively decreased towards lower values due to the salinity effect (Sofer and Gat, 1975), while the $\delta^{13}C$ of the water can become highly enriched, as observed in evaporating brines (Stiller et al., 1985). However, the measurement of enriched $\delta^{13}C$ values in the evaporative calcite crusts by Lacelle et al. (2007), which was also reproduced in the laboratory from evaporating low ionic strength water (Table 5), could now make the evaporative setting more compelling and consistent with the isotopic composition of the carbonate grains in ALH84001, but the reaction would have had to happen under non-equilibrium condition.

5. Conclusion and pointers for future research

This review of the stable C-O isotope composition of cold-climate carbonate precipitates evaluated the formative mechanisms and degree of isotopic disequilibrium associated with their precipitation. Figure 12 presents a summary of the mechanisms discussed in the text to account for the ^{18}O and ^{13}C enrichments and depletions relative to the predicted equilibrium values. It was found that the cold-climate carbonate precipitates have a highly variable isotopic composition with $\delta^{18}O$ values ranging between –6.5 and 36‰ and $\delta^{13}C$ values in the –5 to 17‰ range. However each type of carbonate precipitates has a specific $\delta^{18}O$ and $\delta^{13}C$ range, suggesting that their environmental setting and the mechanism by which they formed controls their ^{18}O and ^{13}C signature. Although many studies suggested that such deposits precipitated under kinetic conditions with enriched C-O composition, it was found that only 2 of the 29 carbonates compiled in this study showed such an effect (cryogenic cave calcite powders and evaporative calcite crusts). Although most precipitated under equilibrium conditions, the $\delta^{18}O$ composition of these cold-climate carbonate precipitates can difficultly be used to derive paleo-

climatic information as the $\delta^{18}O$ of the water from which they precipitated was modified by equilibrium physico-chemical conditions (i.e. freezing or evaporation) resulting in a calcite that has a ^{18}O depleted or enriched relative to that of the water. Only the biologically precipitated carbonate deposits will tend to have a $\delta^{18}O$ composition that reflects that of the parent water.

Although expensive and time consuming, future studies of cold-climate carbonate precipitates should include the sampling of precipitation and local water to provide mechanistic constraint on the C-O isotopic composition of the carbonates. Future research also needs to investigate the evolution of pH and the partial pressure of CO_2 and their effect on the $\delta^{13}C_{DIC}$ of the solution and the $\delta^{13}C$ of the calcite precipitating from that solution under variable freezing and evaporation rates.

Acknowledgements

This work was funded by Natural Science and Engineering Research Council of Canada (NSERC) discovery grants to B. Lauriol and I.D. Clark, by an Ontario Graduate Scholarship (OGS) and Northern Scientific Training Program (NSTP) grant to D. Lacelle. We would like to thank W. Abdi, P. Middlestead (G.G. Hatch Laboratory, University of Ottawa) and M. Alewany for their technical assistance. J-F Dion and J. Clark provided valuable field assistance.

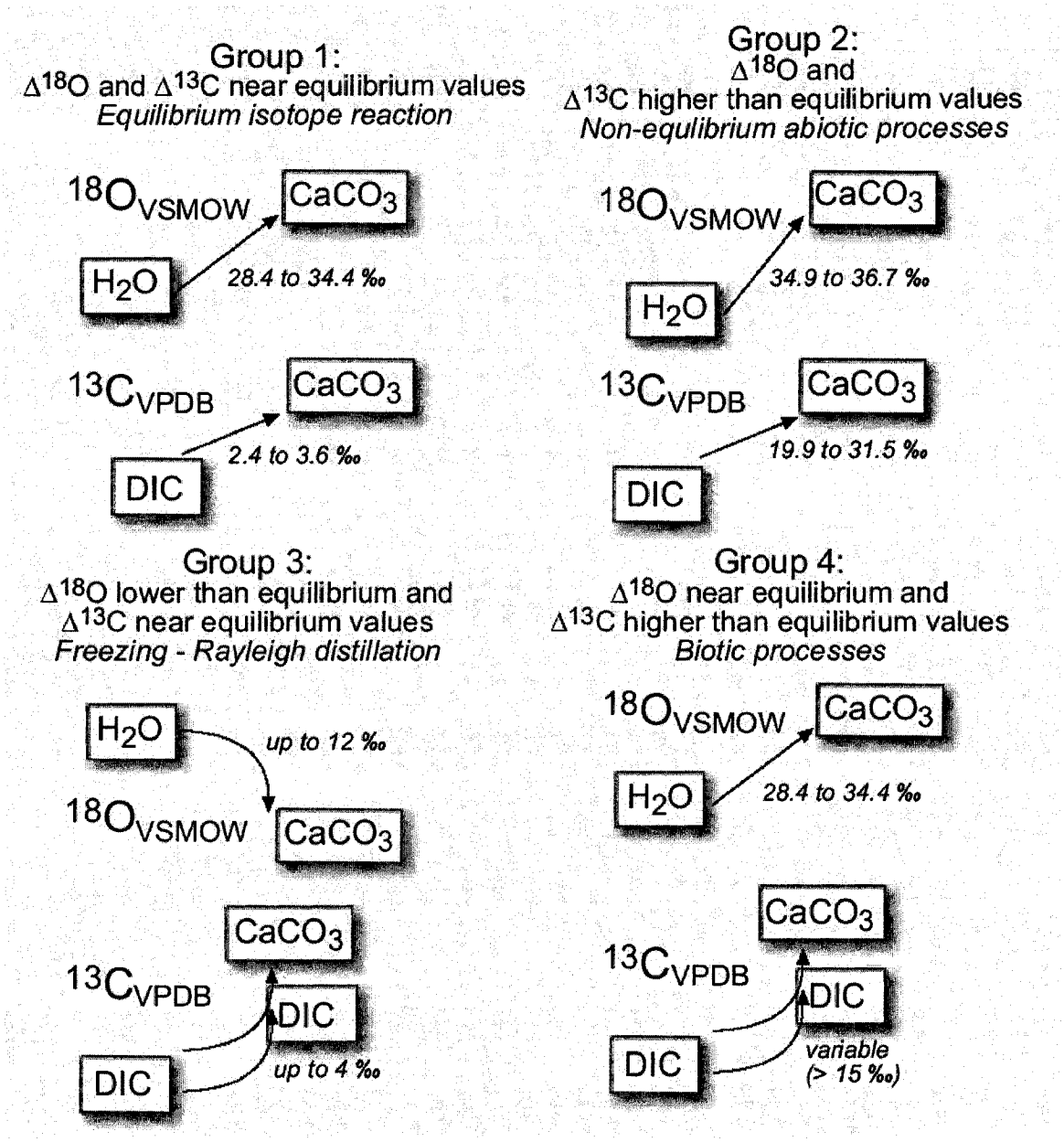

Figure 12. Schematic representation of the mechanisms controls on the stable isotope composition of cold-climate carbonates discussed in the text. Fractionation factors values are valid for the 0 to 25°C temperature range.

References

Adolphe, J.P. 1972. Obtention d'encroûtements carbonates par gel expérimental. Comptes Rendues Académies des Sciences 274, 1139-1142.

Anders, E. 1996. Evaluating the evidence for past life on Mars. Science 274, 2119-2121.

Blake, W. Jr. 2005. Holocene carbonate precipitates on Precambrian bedrock in the High Arctic: age and potential for paleoclimatic information. Geografiska Annaler 87A, 175-192.

Bottinga, I. 1968. Calculation of fractionation factors for carbon and oxygen exchange in the system calcite-CO_2-water. Journal of Physical Chemistry 72, 800-808.

Brook, G.A., Ford, D.C. 1980. Hydrologic and geologic control of carbonate water chemistry in the subarctic Nahanni karst, Canada. Earth Surface Processes and Landscape 7, 1-16.

Bunting, B.T., Christensen L. 1978. Micromorphology of calcareous crusts from the Canadian High Arctic. Geologiska Foreningens Forhandlinger 100, 361-367.

Cailleux, A. 1964. Genèse possible de dépôts chimiques par congélation.Compte Rendus de la Société Géologique de France 1, 11-12.

Carr, R.H., Grady, M.M., Wright, I.P., Pillinger, C.T. 1985. Martian atmospheric carbon dioxide and weathering products in SNC meteorites. Nature 314, 248-250.

Clark, I.D., Lauriol, B. 1992. Kinetic enrichment of stable isotopes in cryogenic calcites. Chemical Geology 102, 217-228.

Clark, I.D., Fritz, P. 1997. Environmental isotopes in hydrogeology. Lewis Publisher, Baco Raton, Florida. 328p.

Clark, I.D., Lauriol, B. 1997. Aufeis of the Firth River basin: insights into permafrost hydrology and karst. Arctic and Alpine Research 29, 240-252.

Clark, I.D., Lauriol, B., Marschner, M., Sabourin, N., Chauret, Y., Desrochers, A. 2004. Endostromatolites from permafrost karst, Yukon Canada: paleoclimatic proxies for the Holocene thermal hypsithermal. Canadian Journal of Earth Sciences 41, 387-399.

Coplen, T.B., Kendall, C., Hopple, J. 1983. Comparison of isotope reference samples. Nature 302, 236.

Courty, M.A., Marlin, C., Dever, L., Tremblay, P., Vachier, P. 1994. The properties, genesis and environmental significance of calcitic pendants from the high Arctic (Spitsbergen). Geoderma 61, 71-102.

Dansgaard, W. 1964. Stable isotopes in precipitation. Tellus 16, 436-468.

Deines, P., Langmur, D., Harmon, R.S. 1974. Stable carbon isotope ratios and the existence of a gas phase in the evolution of carbonate groundwaters. Geochimica et Cosmochimica Acta 38, 1147-1164.

Dijkmans, J.W.A., Koster, E.A., Galloway, J.P., Mook, W.G. 1986. Characteristics and origin of calcretes in a subarctic environment, Great Kobuk sand dunes, northwestern Alaska, U.S.A. Arctic and Alpine Research 18, 377-387.

Drever, J.I. 1997. The geochemistry of natural waters: surface and groundwater environments. 3rd edition. Prentice Hall, Upper Saddle River, New Jersey. 436p.

Epica Community Members. 2004. Eight glacial cycles from an Antarctic ice core. Nature 429, 623–628.

Fairchild, I.J., Bradly, L., Spiro, B. 1993. Carbonate diagenesis in ice. Geology 21, 901-904.

Fairchild, I.J., Bradby, L., Sharp, M., Tison, J.-L. 1994. Hydrochemistry of carbonate terrains in Alpine glacial settings. Earth Surface Processes and Landforms 19, 33-54.

Fairchild, I.J, Smith, C.L., Baker, A., Fuller, L., Spotl, C., Mattey, D., McDermott, F., E.I.M.F. 2006. Modification and preservation of environmental signals in speleothems. Earth Science Reviews 75, 105-153.

Fisher, D.A., Koerner, R.M., Bourgeois, J.C., Zielinski, G., Wake,C., Hammer, C.U., Clausen, H.B., Gundestrup, N., Johnsen, S., Goto-Azuma, K., Hondoh, T., Blake, E., Gerasimoff, M. 1998. Penny Ice Cap cores, Baffin Island, Canada, and the Wisconsinan Foxe dome connection: Two states of Hudson Bay ice cover. Science 279, 692-695.

Ford, D.C., Fuller, P.G. and Drake, J.J. 1970. Calcite precipitates at the sole of temperate glaciers. Nature 226, 441-442.

Ford, D.C. 1976. Evidence of multiple glaciation in southern Nahanni National Park, Mackenzie Mountains, Northwest Territories. Canadian Journal of Earth Sciences 10, 1433-1445.

Forman, S.L., Miller, G. 1984. Time-dependent soil morphologies and pedogenic processes on raised beaches. Broggerhalwoya, Spitsbergen, Svalbard archipelago. Arctic and Alpine Research 16, 381-393.

Ghaleb, B., Hillaire-Marcel, C., Deschamps, P., Lauriol, B., Clark, I.D. 1997. U-Th systematics in high latitude interglacial/interstadial fissure calcretes – examples from Bear Cave Mountain. Proceedings 27th Arctic Workshop, University of Ottawa, 80-83.

Hall, D.K. 1980. Mineral precipitation in North Slope river icings. Arctic 33, 343-348.

Hallet, B. 1976. Deposits formed by subglacial precipitation of CaCO3. Geological Society of America Bulletin 87, 1003-1015.

Hanshaw, B.B., Hallet, B. 1978. Oxygen isotope composition of subglacially precipitated calcite: possible paleoclimatic implications. Science 200, 1267-1270.

Harvey, R.P., McSween, H.Y. 1996. A possible high-temperature origin for the carbonates in the Martian meteorite ALH84001. Nature 382, 49-51.

Heldmann, J.L., Pollard, W.H., McKay, C.P., Andersen, D.T., Toon, O.B. 2005. Annual development cycle of an icing deposit and associated perennial spring activity on Axel Heiberg Island, Canadian High Arctic. Arctic, Antarctic and Alpine Research 37, 127-135.

Hillaire-Marcel, C., Soucy, J.M., Cailleux, A. 1979. Analyse isotopique de concrétions sous-glaciaire de l'inlandsis laurentidiens et teneur en oxygène 18 de la glace. Canadian Journal of Earth Sciences 16, 1494-1498.

Hubbard, B., Hubbard, A. 1998. Bedrock surface roughness and the distribution of subglacially precipitated carbonate deposits: implications for formation at Glacier de Tsansfleuron, Switzerland. Earth Surface and Landforms 23, 261-270.

Killawee, J.A., Fairchild, I.J., Tison, J.L., Janssens, L., Lorrain, R. 1998. Segregation of solutes and gases in experimental freezing of dilute solutions: implication for natural glacier systems. Geochimica Cosmochimica Acta 62, 3637-3655.

Kim, S.T., O'Neil, J.R. 1997. Equilibrium and nonequilibrium oxygen isotope effects in synthetic carbonates. Geochimica et Cosmochimica Acta 61, 3461-3475.

Kuzmin, R.O. 2005. Ground ice in the Martian regolith. In, Water on Mars and Life, T. Tokana (ed.), Advances in Astrobiology and Biogeophysics, pp. 155-189.

Lacelle, D., Lauriol, B., Clark, I.D. 2006. Effect of chemical composition of water on the oxygen-18 and carbon-13 signature preserved in cryogenic carbonates, Artic Canada: implications in paleoclimatic studies. Chemical Geology 234, 1-16.

Lacelle, D., Lauriol, B., Clark, I.D. 2007. Origin, age and paleo-environmental significance of carbonate precipitates in a granitic environment, Akshayuk Pass, Baffin Island, Canada. Canadian Journal of Earth Sciences (In press).

Lauriol, B., Cinq-Mars, J., Clark, I.D. 1991. Localisation, genèse et fonte de quelques naleds du nord Yukon (Canada). Permafrost and Periglacial Processes 2, 225-236.

Lauriol, B., Ford, D.C., Cinq-Mars, J., Morris, W.A. 1997. The chronology of speleothem deposition in northern Yukon and its relationships to permafrost. Canadian Journal of Earth Sciences 34, 902-911.

Lauriol, B., Clark, I.D. 1999. Fissure calcretes in the arctic: a paleohydrologic indicator. Applied Geochemistry 14, 775-785.

Leshin, L.A., McKeegan, K.D., Carpenter, P.K., Harvey, R.P. 1998. Oxygen isotopic constraints on the genesis of carbonates from Martian meteorite ALH84001. Geochimica et Cosmochimica Acta 62, 3-13.

Léveillé, R.J., Longstaffe, F.J., Fyfe, W.S. 2006. An isotopic and geochemical study of carbonate clay mineralization in basaltic caves: abiotic versus microbial processes. Geochimica et Cosmochimica Acta (In Press).

Marlin, C., Dever, L., Vachier, P., Courty, M-A. 1993. Variations chimiques et isotopiques de l'eau du sol lors de la reprise en gel d'une couche active sur pergélisol continu (Presqu'ile de Brogger, Svalbard). Canadian Journal of Earth Sciences 30, 806-813.

Martinez, I., Agrinier, P., Scharer, U., Javoy, M. 1994. A SEM-ATEM and stable isotope study of carbonates from the Haughton impact crater, Canada. Earth and Planetary Science Letters 121, 559-574.

McDermott, F. 2004. Paleo-climate reconstruction from stable isotope variations in speleothems: a review. Quaternary Science Reviews 23, 901-918,

McKay, D.S., Gibson, E.K., Thomas Keprta, K.L., Vali, H., Romanek, C.S., Clement, S.J., Chilier, X.D.F., Maechling, C.R., Zare, R.N. 1996. Search for possible life on Mars: possible relic biogenic activity in Martian meteorite ALH84001. Science 273, 924-930.

Meyers, P.A., Lallier-Vergès, E. 1999. Lacustrine sedimentary organic matter records o fLate Quaternary paleoclimates. Journal of Paleoclimatology 21, 345-372.

Mittlefehldt, D.W. 1994. ALH84001, a cumulate orthopyroxenite member of the Martian meteorite clan. Meteoritics 29, 214-221.

Mook, W.G., Bommerson, J.C., Staverman, W.H. 1974. Carbon isotope fractionation between dissolved bicarbonate and gaseous carbon dioxide. Earth and Planetary Science Letters 22, 169-176.

Nakai, N., Wada, H., Kiyosu, Y., Takimoto, M. 1975. Stable isotope studies on the origin and geological history of water and salts in the Lake Vanda area, Antarctica. Geochemical Journal 9, 7-24.

Niles, P.B., Leshin L.A., Socki, R.A., Guan, Y., Ming, D.W., Gibson, E.K. 2004. Cryogenic calcite – A morphologic and isotopic analog to the ALH84001 carbonates. In, Lunar and Planetary Science XXXV abstract #1459. Lunar and Planetary Institute, Houston, TX.

Niles, P.B., Leshin, L.A., Guan, Y. 2005. Microscale carbon isotope variability in ALH84001 carbonates and a discussion of possible formation environments. Geochimica et Cosmochimica Acta 69, 2931-2944.

Omelon, C.R., Pollard, W.H., Marion, G.M. 2001. Seasonal formation of ikaite ($CaCO_3$ $6H_2O$) in saline spring discharge at Expedition Fjord, Canadian High Arctic: assessing conditional constraint for natural crystal growth. Geochimica et Cosmochimica Acta 65, 1429-1437.

O'Neil, J.R., Clayton, R.N., Mayeda, T.K. 1969. Oxygen isotope fractionation in divalent metal carbonates. Journal of Chemical Physics 51, 5547-5558.

Osinski, G.R., Spray, J.G. 2001. Impact-generated carbonate melts: evidence from the Haughton structure, Canada. Earth and Planetary Science Letters 194, 17-29.

Parkhurst, D.L., Appelo, C.A.J. 1999. User's Guide to PHREEQC (Version 2): A Computer Program for Speciation, Batch-Reaction, One-Dimensional Transport, and Inverse Geochemical Calculations. U.S. Geological Survey Water-Resources Investigations Report 99-4259, 310 p.

Parnell, J., Bowden, S.A., Cockell, C.S., Osinski, G.R., Lee, P. 2006. Surface mineral crusts: a priority target in search for life on Mars. In, Lunar and Planetary Science XXXVII abstract #1049. Lunar and Planetary Institute, Houston, TX.

Pollard, W. 1983. A study of seasonal frost mounds, North Fork Pass, northern interior Yukon Territory. Unpublished PhD Thesis, University of Ottawa.

Pollard, W.H., 2005. Icing processes associated with High Arctic perennial springs, Axel Heiberg Island, Nunavut, Canada. Permafrost and Periglacial Processes 16, 51-68.

Ritchie, J.C., Cwynar, L.C. and Spear, R.W. 1983. Evidence from northwest Canada for an early Holocene Milankovitch thermal maximum. Nature 305, 126-128.

Romanek, C.S., Grady, M.M., Wright, I.P., Mittlefehldt, D.W., Socki, R.A., Pillinger, C.T., Gibson Jr., E.K. 1994. Record of fluid-rock interactions on Mars from the meteorite ALH84001. Nature 372, 655-657.

Sharp, M., Tison, J.L., Fierens, G. 1990. Geochemistry of subglacial calcites: implications for the hydrology of the basal water film. Arctic and Alpine Research 22, 141-152.

Socki, R.A., Romanek, C.S., Gibson Jr., E.K., Golden, D.C. 2001. Terrestrial aufeis formation as martian analog: Clues from laboratory-produced C-13 enriched cryogenic carbonate. In, Lunar and Planetary Science XXXII abstract #2032. Lunar and Planetary Institute, Houston, TX.

Socki, R.A., Gibson Jr., E.K., Golden, D.C., Ming, D.W., McKay, G.A. 2003. Kinetic fractionation of stable isotopes in carbonate on Mars: terrestrial analogs. In, Lunar and Planetary Science XXXII abstract #1938. Lunar and Planetary Institute, Houston, TX.

Socki, R.A., Gibson Jr., E.K., Perry Jr., E.C., Galindo, C., Golden, D.C., Ming, D.M., McKay, G.A. 2004. Stable isotope composition of carbonates formed in low-temperature terrestrial environments as Martian analogs. In, Lunar and Planetary Science XXXII abstract #1841. Lunar and Planetary Institute, Houston, TX.

Sofer, Z., Gat, J.R. 1975. Isotope composition of evaporating brines – Effect of isotopic activity ratio in saline solutions. Earth and Planetary Science Letters 26, 179-186.

Souchez, R.A., Lemmens, M. 1985. Subglacial carbonate deposition – an isotopic study of present-day case. Palaeogeography, Palaeoclimatology and Palaeoecology 51, 357-364.

Stiller, M., Rounick, J.S., Shasha, S. 1985. Extreme carbon isotope enrichments in evaporating brines. Nature 316, 434-435.

Swett, K. 1974. Calcrete crusts in an arctic permafrost environment. American Journal of Science 274, 1059-1063.

Turner, J.V. 1982. Kinetic fractionation of carbon-13 during calcium carbonate precipitation. Geochimica Cosmochica Acta, 46, 1183-1191.

Urey, H.C. 1947. The thermodynamic properties of isotopic substances. Journal of Chemical Society 1947, 562-581.

Vogel, J.C., Grootes, P.M., Mook, W.G. 1970. Isotope fractionation between gaseous and dissolved carbon dioxide. Physics 230, 255-258.

Vogt, T. 1977. Croûtes calcaires quaternaires de période froide en France méditerranéenne. Zeitschrift fur Geomorphologie 21, 26-36.

Vogt, T. 1989. Croûtes calcaires d'orgine cryogénique. Zeitschrift fur Geomorphologie 75, 115-135.

Vogt, T., Del Valle, H.F. 1994. Calcretes and cryogenic structures in the area of Puerto Madryn (Chubut, Patagonia, Argentina). Geografiska Annaler 76A, 57-73.

Vogt, T., Corte, A.E. 1996. Secondary precipitates in Pleistocene and present cryogenic environments (Mendoza Precordillera, Argentina, Transbaikalia, Siberia, and Seymour Island, Antarctica). Sedimentology 43, 53-64.

Waragai, T. 2005. Holocene calcrete crust deposits on the moraine of Batura Glacier, northern Pakistan. The Island Arc 1, 368-377.

Washburn, A.L. 1969. Weathering, frost action, and patterned ground in the Mesters Vig district, Northeast Greenland. Medelelser om Gronland 176, 303p.

Whiticar, M.J., Faber, E., Schoell, M. 1986. Biogenic methane formation in marine and freshwater environments: CO_2 reduction vs. acetate fermentation — Isotopic evidence. Geochimica et Cosmochimica Acta 50, 693–709.

Zak, K., Urban, J., Cilek, V., Hercman, H. 2004. Cryogenic cave calcite from several Central European caves: age, carbon and oxygen isotopes and a genetic model. Chemical Geology 206, 119-136.

Zdanowick, C., Fisher, D., Clark, I.D., Lacelle, D. 2002. An ice-marginal $\delta^{18}O$ record from Barnes Ice Cap, Baffin Island, Canada. Annals of Glaciology 35, 145-149.

Conclusions

1. Conclusions

This thesis examined the origin, age and paleoclimatic implications of secondary carbonate deposits in the Canadian Arctic. Using field observations and stable isotope geochemistry, this thesis (*i*) classified the carbonate deposits encountered in polar regions according to their morphological characteristics; (*ii*) examined the geochemical and isotopic partitioning that occurs prior to and during the precipitation of carbonate deposits in distinct geological setting; (*iii*) examined the effect of the rate of reaction on the stable isotope composition of carbonate deposits; (*iv*) proposed a criteria for identifying the physico-chemical or biological process that led to the precipitation of carbonate deposits; and (*v*) evaluated the use of carbonate deposits as paleoclimatic proxies. Its major findings are summarized below.

1. The carbonate deposits in polar regions were classified into two broad categories: powders and crusts. The cold-climate carbonate precipitates were classified into three broad categories: *powders, crusts* and *speleothems* (e.g. stalagmite, stalactite and flowstone). The carbonate powders include those that precipitated in relation to aufeis aggradation (cryogenic aufeis calcite) and in relation to the growth of various annual and perennial ice formations in caves (cryogenic cave calcite). The carbonate crusts can be further subdivided based on their lithic environment; those that precipitated on the upper surface of bedrock/clasts (i.e. subglacially precipitated calcite and evaporative calcite crusts); those that are located on the underside of clasts (i.e. active layer carbonates); and those that precipitated in rock outcrop fissures (i.e. endostromatolites). Speleothems (e.g. stalagmites, stalactites and flowstones) are classified separately since they are not restricted to periglacial regions and are currently inactive due to the presence of permafrost which impedes groundwater circulation.
2. The geochemical and isotopic partitioning during freezing has a direct effect on the $\delta^{18}O$ composition of the carbonate deposits. Under most circumstances, the $\delta^{18}O$ composition of carbonate is estimated from the $\delta^{18}O$ of the parent water and the temperature at which calcite precipitation occurred. However, an extensive study of the stable isotope composition of cryogenic aufeis calcite collected from a limestone and a granitic terrain revealed that the calcite powders from the granitic terrain had a much lower $\delta^{18}O$ value, even though the $\delta^{18}O$ composition

of the parent water from which they precipitated was very similar to those in the limestone environment. An examination of the geochemical characteristics of the parent water revealed that it is the calcite saturation state of the parent water from which the carbonates precipitation that has influenced the $\delta^{18}O$ composition of the calcite deposits. Given that the waters in the granitic terrain are characterized by a low calcite saturation index, calcite precipitation is expected to occur during the late stage of freezing, which is also when the $\delta^{18}O$ composition of the parent water becomes highly depleted as a result of the progressive removal of heavier isotopes into the ice phase. By contrast, the $\delta^{18}O$ composition of cryogenic calcite in limestone environment will tend to reflect that of the parent water, since the calcite saturation index of the parent water will be near saturation and precipitation will occur during the initial stage of freezing.

3. The effect of the rate of reaction on the stable isotope composition of calcite precipitates was examined under controlled laboratory conditions. A synthetic bicarbonate solution was kinetically evaporated. It was found that kinetic evaporation effectively precludes isotopic equilibrium during the dehydration of bicarbonate, since the precipitation of bicarbonate as calcite is non-fractionating. A $\varepsilon^{13}C_{KIE}$ $CaCO_3$-CO_2 in the 20 to 40‰ range was measured, which is much greater than the equilibrium fractionation factor of 11.1‰ at 20°C. In addition, the measured $\varepsilon^{13}C_{KIE}$ $CaCO_3$-CO_2 value is slightly lower than that obtained by Clark and Lauriol (1992) during freezing of bicarbonate solution, indicating that kinetic isotope fractionation is a thermodynamic reaction.
4. The measurement of the stable isotope composition ($\delta^{18}O$ and $\delta^{13}C$) of the calcite precipitates and of the parent water ($\delta^{18}O$ and $\delta^{13}C_{DIC}$) from which they precipitated is important as it is diagnostic of the process that led to the precipitation of the carbonate deposits. It was found that calcite deposits precipitated under equilibrium physico-chemical conditions will have a $\delta^{13}C$ value that is in equilibrium with that of the parent water, while its $\delta^{18}O$ composition will deviate from that of the parent water, as it is affected by the calcite saturation state of the parent water. By contrast, the $\delta^{18}O$ composition of biogenic

endostromatolites will tend to reflect that of the parent water, while its $\delta^{13}C$ composition will be enriched. In the case of kinetically precipitated carbonate deposits, both their $\delta^{18}O$ and $\delta^{13}C$ values will be enriched over that of the parent water, although slightly less for the $\delta^{18}O$ due to the fact that only one atom in HCO_3^- participates during dehydration of bicarbonate.

Overall, the findings in this thesis have important implications in the use of calcite precipitates in paleoclimatic reconstructions. Unless clear details about the geochemical composition of the parent water are known, care must be taken when interpreting the $\delta^{18}O$ signature in carbonate deposits in polar regions since the $\delta^{18}O$ signature might have been modified by secondary physico-chemical processes, such as freezing or evaporation, prior to calcite being precipitated. However, the $\delta^{13}C$ composition of the carbonate deposits can allow insights into the different water sources contributing to their growth.

2. Future work

This thesis proposes a classification of the cold-climate carbonate precipitates encountered in polar regions according to their morphologies, explores the geochemical and isotopic partitioning that occurs prior to and during the precipitation of carbonate deposits. It also evaluates the use of carbonate deposits as paleoclimatic and paleoenvironmental proxies. Besides its major findings, this thesis suggests a few avenues for future research.

Further research needs to be done to investigate the evolution of pH and partial pressure of CO_2 and their effect on the $\delta^{13}C_{DIC}$ of the solution and the $\delta^{13}C$ of the calcite precipitating from that solution under variable freezing/evaporation rates. This can be accomplished by monitoring under controlled laboratory conditions the unstable parameters (pH and log pCO_2) and collecting samples at regular intervals, thus simulating a static view of a Rayleigh distillation at decreasing water fraction. In addition, a detailed study of the kinetic physico-chemical processes (evaporation and freezing) is required, since it appears that the kinetic isotope effect ($\varepsilon^{13}C_{KIE}$ $CaCO_3$-CO_2) related to rapid precipitation of carbonate is temperature dependent, decreasing from 31.5‰ during freezing, to 22‰ at 20°C and 19.5‰ at 45°C. This could be done by systematically measuring the $\varepsilon^{13}C_{KIE}$ between CO_2 and calcite and HCO_3^- and calcite at increasing temperature.